Title
COPII Specificity and the Regulation of Anterograde Transport for Planar Cell Polarity Proteins in Neural Tube Development

Author
Jensen, Devon Joseph

Publication Date
2010

Peer reviewed|Thesis/dissertation

COPII Specificity and the Regulation of Anterograde Transport for Planar Cell Polarity Proteins in Neural Tube Development

by

Devon Joseph Jensen

A dissertation submitted in partial satisfaction of the

requirements for the degree of

Doctor of Philosophy

in

Molecular and Cell Biology

in the

Graduate Division

of the

University of California, Berkeley

Committee in charge:

Professor Randy W. Schekman, Chair

Professor Nilabh Shastri

Professor Lu Chen

Professor Jay T. Groves

Spring 2010

COPII Specificity and the Regulation of Anterograde Transport for Planar Cell Polarity Proteins in Neural Tube Development

by Devon Joseph Jensen

Abstract

COPII Specificity and the Regulation of Anterograde Transport for Planar Cell Polarity Proteins in Neural Tube Development

by

Devon Joseph Jensen

Doctor of Philosophy in Molecular and Cell Biology

University of California, Berkeley

Professor Randy W. Schekman, Chair

Anterograde transport in eukaryotic cells begins at the endoplasmic reticulum (ER), where cargo proteins that are synthesized at the ER, become packaged into small vesicles for transport to other compartments in the cell. The coat protein complex II (COPII) is a set of proteins responsible for selecting cargo destined to leave the ER, and forming these vesicles from the ER membrane. In mammalian cells, COPII proteins have diversified, as gene duplication events have created multiple paralogs for most of these COPII components. The COPII subunit Sec24 is thought to be the major cargo binding subunit, but the activity and specificity for each of its 4 paralogs in mammalian cells is unknown.

Here I report on the discovery that a mutation in Sec24B leads to a major neural tube defect in mice. Neural tube defects are often the result of deficiencies in a tissue organization pathway called planar cell polarity. Using an *in vitro* reconstitution of COPII vesicle formation, I was able to identify a unique cargo protein that is packaged specifically by Sec24B, the planar cell polarity protein Vangl2. The study of Vangl2 has often centered on mice with specific point mutations called the looptail mutant mice. These mice have phenotypes commonly found associated with defects in planar cell polarity, but the cellular reason for these defects was unclear. I demonstrate that the looptail mutant Vangl2 protein is restricted to the ER and unable to be packaged into COPII vesicles. I further characterized the Vangl2 protein and its looptail mutant forms, identifying many more mutations that result in transport defects. I probed Vangl2 oligomerization, topology, folding status, and binding partners. These results establish a special role for Sec24B in mammalian development, specifically in the transport of Vangl2, and further illustrate the specificity of cargo protein recruitment and transport competence.

Table of Contents

List of Figures

Acknowledgments

Thank you to my wonderful family for all the love and support over the past 6 years. Mom, Dad, Daryl, Jess, and Jonah, Corinne and Patick, Dallin – I miss you but I have really enjoyed our video chats!

Thank you to all the past and present members of the Schekman lab, fellow students, post-docs, and staff, for making this such a pleasant and engaging place to work.

Thank you to my mentor, Randy Schekman, for teaching me how to ask scientific questions, for supporting me on new ideas, for guiding me elsewhere if those ideas didn't work, and for sharing with the lab the location of the Ventana Inn restaurant balcony.

Thank you to my thesis committee for your advice over the years. Thank you to the MCB department staff for always being helpful and making the logistics of graduate school easier. I'm also grateful to Soomin Shim for critical reading of this dissertation.

Chapter One:

An Introduction to Membrane Trafficking and Planar Cell Polarity

Membrane Trafficking and Protein Transport

The central dogma of biology states that gene information in DNA is converted into RNA, which is then converted into protein, but this is just the start of the journey for many proteins in eukaryotic cells. Many proteins must travel to reach one of the multiple separate membrane compartments and surfaces that are specialized to carry out particular functions for the eukaryotic cell, including the nucleus, Golgi apparatus, endoplasmic reticulum, plasma membrane, endosomes, lysosomes, peroxisomes, and mitochondria (Figure 1.1). These compartments and surfaces all depend on having the correct mix of proteins and lipids in order to perform their functions.

The central questions for membrane and protein trafficking are: How do proteins get from point A to point B within the cell? and How can many thousands of proteins get sorted correctly and placed in the correct compartment? The answers to these questions lie within the movement and activity of discrete membrane vesicles, which are sculpted and derived from the original donor membrane and which then travel through the cell to fuse with the target membrane compartment (Jamieson and Palade, 1971; Novick *et al.* 1980; reviewed Pryer *et al.*, 1992). In order to form these membrane vesicles, there exist several different coat protein complexes in the cell. The coat complexes are responsible for not only shaping and forming the vesicle, but also for selecting the "cargo" – that is the proteins which need to be packaged and sent to another location in the cell (Figure 1.1) (reviewed Bonifacino and Lippincott-Schwartz, 2003). In general, it is thought that coat complexes decipher signals in the cargo protein, specific amino acid sequences that determine its trafficking itinerary (Miller et al., 2003). These different coat complexes are generally spatially restricted to particular compartments and only act on certain cargo proteins or membranes. In this way, a protein is able to make its way to the compartment or surface where it is needed. Membrane and luminal proteins are synthesized at the ER, where they start this journey on the secretory pathway.

The Secretory Pathway

The secretory pathway, also called anterograde transport, is one leg of the membrane transport system within a cell that acts as the starting point for the journey of most membrane and luminal proteins. For many compartments, the secretory pathway is the mechanism by which newly synthesized proteins arrive at their designated compartment location. It is also the mechanism by which cells can release proteins and other factors into the external environment.

After being produced at the endoplasmic reticulum (ER), membrane and luminal proteins that are destined for other compartments must first fold correctly and may need to self-associate, or associate with other proteins that enable their folding, called chaperones (Nufer *et al.*, 2003; Rein *et al.*, 1987). Many proteins are also glycosylated within the lumen of the ER, a modification that can contribute to their recognition as

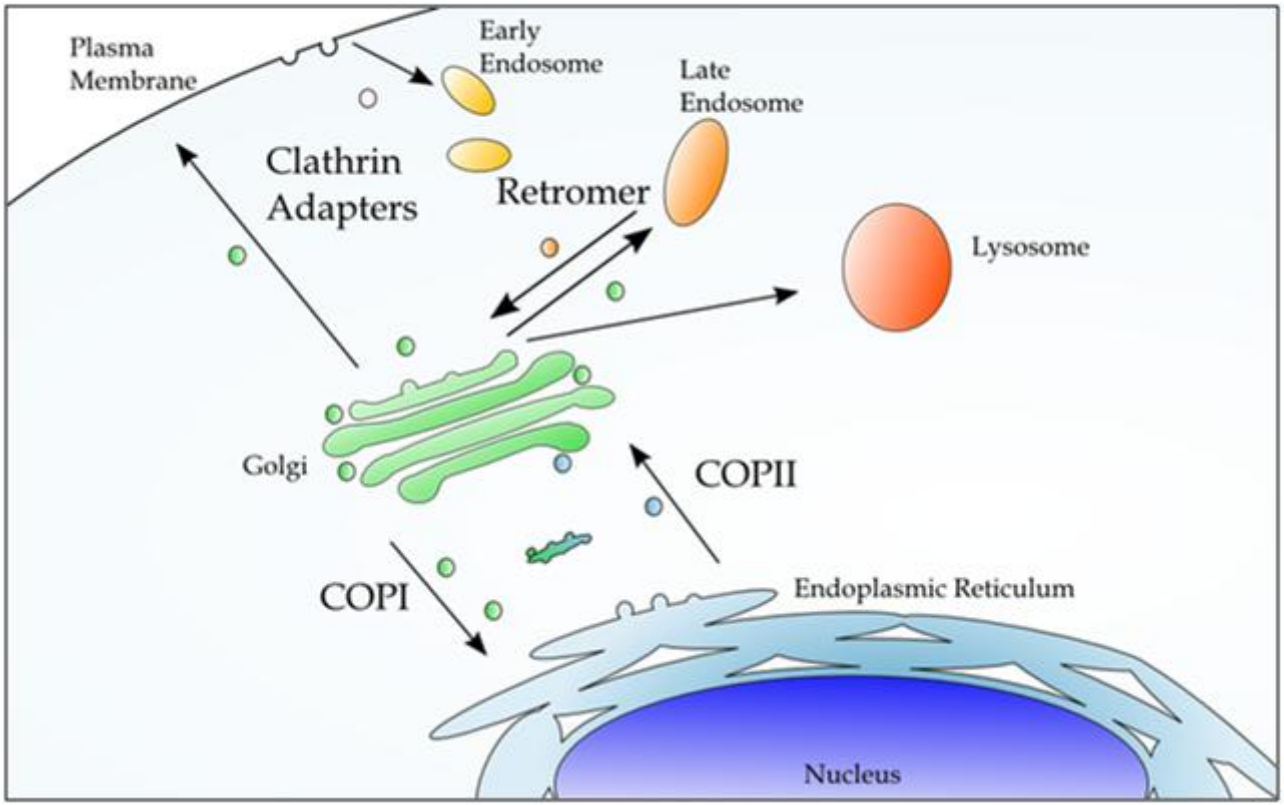

Figure 1.1 – The membrane compartments of a eukaryotic cell. Also includes the coat complexes which enable vesicular traffic between them.

ready for transport (Kornfeld and Kornfeld, 1985). Once transport ready, the protein is brought to or diffuses to particular sites on the ER surface that are hotspots for vesicle formation, called transitional ER or ER exit sites. ER exit sites are defined as an area of high activity for the COPII coat complex (Farquhar and Palade, 1981 ; Orci *et al.*, 1991). Cargo proteins can be brought to these sites by virtue of transport signals in their cytoplasmic sequence that are recognized by members of the COPII coat complex. The five core COPII proteins Sar1, Sec23, Sec24, Sec13, and Sec31 are responsible for forming a membrane vesicle which contains the cargo proteins that need to leave the ER. COPII will be reviewed in greater detail in Chapter 2. This initial step, this exit from the ER, is focus of much of this dissertation.

COPII-derived vesicles will contain a big mixture of proteins that need to go to different places in the cell, for instance, plasma membrane proteins are packaged all together with lysosomal proteins. For this reason, after leaving the ER, proteins in COPII-derived vesicles don't go directly to their final location in the cell, all are thought go to the Golgi complex, a compartment that acts as a sorting station (reviewed Emr *et al*., 2009). In higher organisms, these vesicles can first homotypically fuse and become an ERGIC compartment (ER-Golgi Intermediate Compartment), and then travel on to the Golgi complex (Aridor *et al.*, 1995). At the Golgi complex, proteins can be further modified by glycosylation or be cleaved by peptidases. If the proteins are not Golgi-resident proteins, they make their way through the stacks of Golgi complex until they get to the trans-Golgi where they can again be packaged into vesicles for transit to other places in the cell.

These further packaging steps at the trans-Golgi are mediated by clathrin coats complexes and clathrin adaptors (Friend and Farquhar, 1967; Robinson, 1990). The clathrin adaptors bind to cargo proteins and select them for inclusion into a vesicle that is shaped and formed by the clathrin coat. In this case, the proteins are often segregated into vesicles that are specific for their destination, e.g. plasma membrane proteins are packaged together with other plasma membrane proteins or lysosomal proteins with other lysosomal proteins. Upon traveling to their intended destination, these vesicles fuse with their target membrane (reviewed Südhof and Rothman, 2009). The fusion will place the new membrane proteins on the limiting membrane of the compartment or surface, but the fusion will also dump vesicle luminal proteins into the lumen of the compartment, or in the case of the plasma membrane, will release the vesicle lumen contents into the extracellular space.

These are the basic steps of protein secretion, but there are also many other pathways of protein transport in the cell, for example retrograde transport, endocytosis, and recycling pathways (Figure 1.1). The other pathways are mediated by different clathrin adaptors, or by other coat complexes, such as retromer (Seaman *et al.*, 1998) or COPI (Orci *et al.*, 1986). Additionally, the trafficking itinerary for any one protein can be more complicated than simply travelling from point A to point B. Some proteins constantly cycle in between two compartments (Itin *et al.*, 1995). Other proteins travel along one pathway before reaching their destination along another pathway, for instance a protein that first goes to the plasma membrane before being endocytosed finally

reaching the lysosome (Braun *et al.*, 1989). In the end, proteins reach the proper compartment or surface, where they go about performing their function. One such group of proteins that must reach the plasma membrane are the cell surface receptors involved in planar cell polarity.

Planar Cell Polarity

Planar cell polarity (PCP) directs cells in an epithelium to orient about a plane parallel to the layer of cells. PCP is found in both invertebrate and vertebrate organisms, organizing cell layers that control among other things: the bristle hairs on the wing of a fruitfly, the feather orientation of birds, and the intricate arrangement of the cells of the inner mammalian ear, allowing the sense of hearing. The PCP pathways are also critical during different stages of vertebrate development. Planar cell polarity signaling organizes tissues, allowing sheets of cells to model the shape of critical structures, like the heart and neural tube.

The planar cell polarity pathway was first described in *Drosophila melanogaster*, when classic genetic approaches yielded a group of proteins that were described as "altering orientations of cuticular processes in several regions of the body" (Gubb and García-Bellido, 1982). Further characterization and study lead to the discovery of a number of other critical proteins involved in the process, which have been termed the core set of PCP proteins - those which are required in all cases of known PCP establishment. This core set of proteins include: Frizzled (fz/fzd) (Gubb and Garcia-Bellido, 1982), Van Gogh/Strabismus(vang) (Taylor *et al.*, 1998), Dishevelled (dsh/dvl) (Fahmy and Fahmy, 1959). Celsr/Starry Night/Flamingo/ (stan/fmi) (Chae *et al.*, 1999) , Diego/Diversin (dgo) (Feiguin et al. 2001), and Prickle (Gubb and Garcia-Bellido, 1982). Additional proteins have been found to enable PCP in a tissue specific manner, or are only present in mammals, including: Inturned (Adler *et al.*, 1994), Multiple wing hair (Strutt and Warrington, 2008), Fuzzy (Collier and Gubb, 1997), Scribble 1 (Montcouquiol *et al.*, 2003), and Protein Tyrosine Kinase 7 (Ptk7) (Lu *et al.*, 2004).

Functions of the core planar cell polarity proteins

The core group of PCP proteins consists of several membrane proteins that show a cell surface polarized localization and an assortment of cytosolic signaling factors that interact with the membrane proteins, to transmit signals downstream and help maintain polarity (Figure 1.2). Three are membrane proteins: Frizzled, Vangl, and Celsr, and three are cytosolic: Prickle, Dishevelled and Diego. These membrane proteins and one additional vertebrate specific membrane protein, Ptk7, are of particular interest for the study of protein trafficking since they will need to exit the ER and traverse the secretory pathway before they reach the plasma membrane. As such, any trafficking defects that prevent them from reaching the plasma membrane will lead to phenotypes consistent

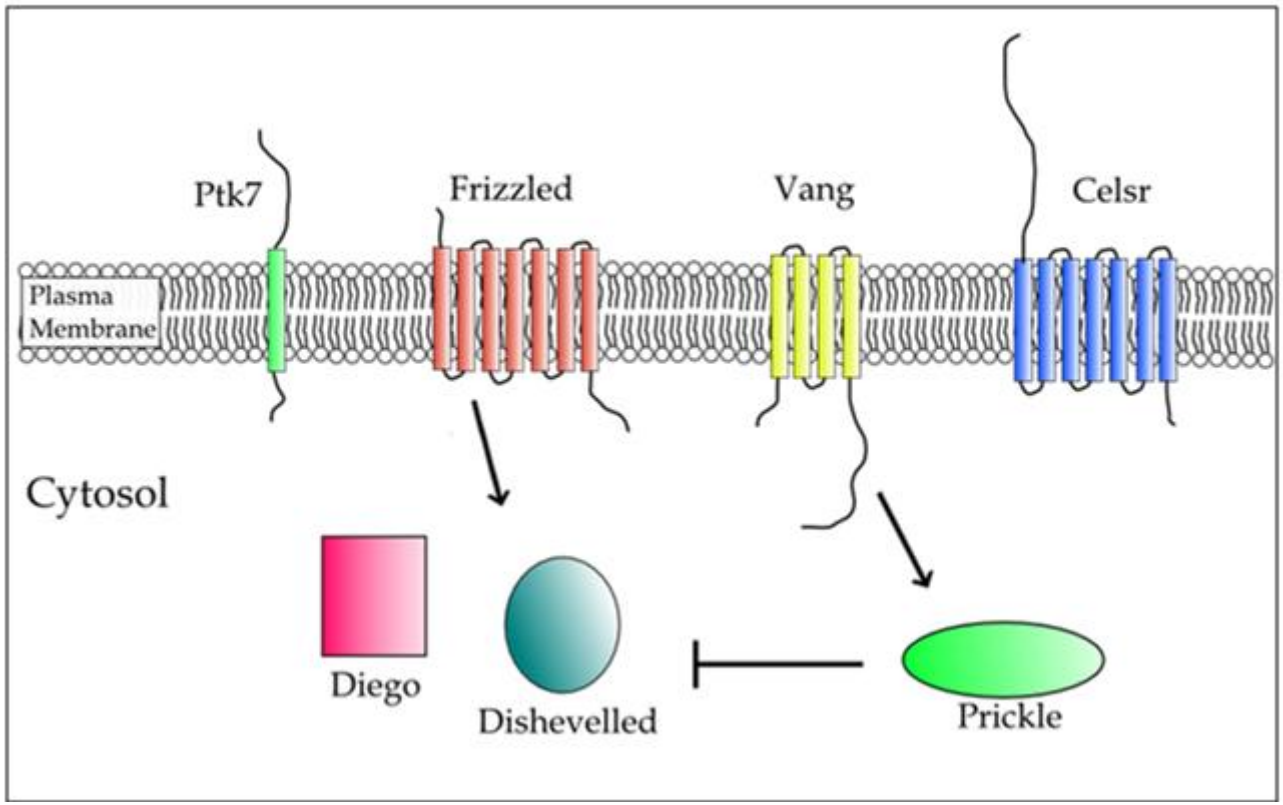

Figure 1.2 – Selected membrane and cytosolic proteins in the planar cell polarity pathway

with defects in the planar cell polarity pathway. Additionally, the cytosolic PCP proteins could be of interest from a trafficking standpoint if they enable the transport of one or more of the membrane proteins by interacting and promoting forward transport or preventing retention.

Frizzled is a 7-pass transmembrane protein that is localized to the distal side of cells with established planar cell polarity. During PCP, Frizzled acts in the non-canonical WNT signaling pathway, but it is also important for canonical WNT/ β-catenin signaling during development (reviewed Wodarz and Nusse, 1998). There are 10 paralogs of Frizzled in the human genome and they are thought to be expressed differentially such that they regulate the polarity in different tissues. For instance, mutations in Frizzled 4 specifically cause familial exudative vitreoretinopathy (FEVR), a disease that is caused by incomplete retinal vascularization, and can lead to scarring and blindness (Robitaille *et al.*, 2002). Additionally, mutations in mouse Frizzled 3 and Frizzled 6 together cause the planar cell polarity defect that results from incomplete convergent extension of the neural tube (Wang *et al.*, 2006). The extracellular amino terminus of Frizzled binds to WNT ligand and the cytoplasmic carboxyl-terminus binds to downstream signaling molecules such as Dishevelled.

Vangl is a 4-pass transmembrane protein found on the opposite side of a planar polarized cell from Frizzled, on the proximal side. There are 2 mammalian paralogs, Vangl1 and Vangl2, which are expressed somewhat differentially, but can partially compensate for one another (Jessen and Solnica-Krezel, 2003). When polarity is established, Vangl along with a cytosolic binding partner, Prickle, is thought to antagonize the activity of Frizzled/Dishevelled and thereby maintain polarity of the cell. Vangl2 will be described and explored in more detail in chapters 3 and 4.

Celsr (Cadherin EGF LAG seven-pass G-type receptor)/Starry Night/Flamingo is a 7-pass transmembrane protein that is thought to associate with both Frizzled and Vangl and is found located on both the proximal and distal sides of a cell with established planar cell polarity (Usui *et al.*, 1999). Cadherins are known to function as cell adhesion molecules, and in this case, Celsr appears to be involved in self-dimerization with another Celsr molecule on a neighboring cell (Usui *et al.*, 1999). This homophilic cell adhesion activity is essential for the establishment of PCP. There are 3 mammalian paralogs of Celsr – Celsr1, 2, and 3 and they are known to have different patterns of expression during mouse development (Formstone and Little, 2001).

Dishevelled is a cytoplasmic signaling protein that is traditionally thought to bind to Frizzled in order to pass Frizzled signaling onto downstream signaling effectors, acting in both canonical WNT/ β-catenin signaling and planar cell polarity (Noordermeer *et al*., 1999). There are three conserved domains found in all Dishevelled proteins: the DIX domain, the PDZ domain and the DEP domain (Boutros and Mlodzik, 1999). The DIX domain mediates self-oligomerization and is important of the canonical WNT signaling (Noordermeer *et al*., 1999). The PDZ domain is a common protein-protein interaction domain that is necessary for binding to Vangl, but the functional implications of this binding are not clear (Park and Moon, 2002). The DEP

domain has been found to be the most important for planar cell polarity signaling (Axelrod *et al.*, 1998). In mammals, there are 3 Dishevelled paralogs which are somewhat redundant as determined by mouse knockout studies (Etheridge *et al.*, 2008).

Prickle and Diego are two additional cytoplasmic signaling proteins active in the planar cell polarity pathway. Prickle is localized on the same proximal side of the cell as Vang and is known to bind Vang (Bastock *et al.*, 2003). It is thought that Prickle can antagonize the activity of Frizzled-mediated Dishevelled activation, by binding Dishevelled and preventing it's localization with Frizzled (Tree et al., 2002). Rounding out the core set of planar cell polarity genes, Diego interacts with Celsr/Flamingo/Stan and seems to mediate the clustering of this protein (Feiguin *et al.*, 2001).

Finally, Ptk7 is a vertebrate specific planar cell polarity gene, shown to function in mice and frogs. A mouse gene trap line for Ptk7 showed classic mammalian planar cell polarity defects, such as an unclosed neural tube and mis-aligned cells of the cochlea (Lu *et al.*, 2004). The protein is arranged as a single pass transmembrane protein, with 7 extracellular immunoglobulin domains, and a cytoplasmic domain with a non-functional yet conserved tyrosine kinase domain. Beyond this, little is known about what role it may be playing to help establish planar cell polarity.

The expansion of multiple paralogs for most of these core PCP genes in mammalian organisms points toward the versatility of this pathway. The planar cell polarity pathway is a remarkable example of how a conserved set of proteins can be adapted over time to function in similar and new ways. As touched on earlier, a multitude of different phenotypes are found in mammalian organisms with defects in members of the PCP pathway. These include: neural tube closure disorders, cochlea defects, congenital heart problems, eye vascularization defects, skin hair patterning changes, polycystic kidney disease, and incorrect axon guidance of the central nervous system (Figure 1.3) (reviewed Simons and Mlodzik, 2008). Also, a recent report indicates that down-regulation of Vangl2 can lead to cancer metastasis, underscoring the role of planar cell polarity in establishing and maintaining an epithelial cell layer (Cantrell and Jessen, 2010).

About this Dissertation

This dissertation concerns the way that membrane proteins of the planar cell polarity pathway are able to traffic to the cell surface, focusing mostly on Vangl2 and its initial step out of the ER. This initial step is mediated by the COPII protein coat, which is reviewed in detail in chapter 2. Besides an overview of all the core COPII proteins that enable this step in transport, chapter 2 also discusses how the multiple paralogs of COPII proteins and several newly identified proteins play specific roles in the transport of the more complex repertoire of cargo proteins found in mammalian cells.

Figure 1.3 – Selected phenotypes of *Drosophila melanogaster* and *Mus musculus* with planar cell polarity defects

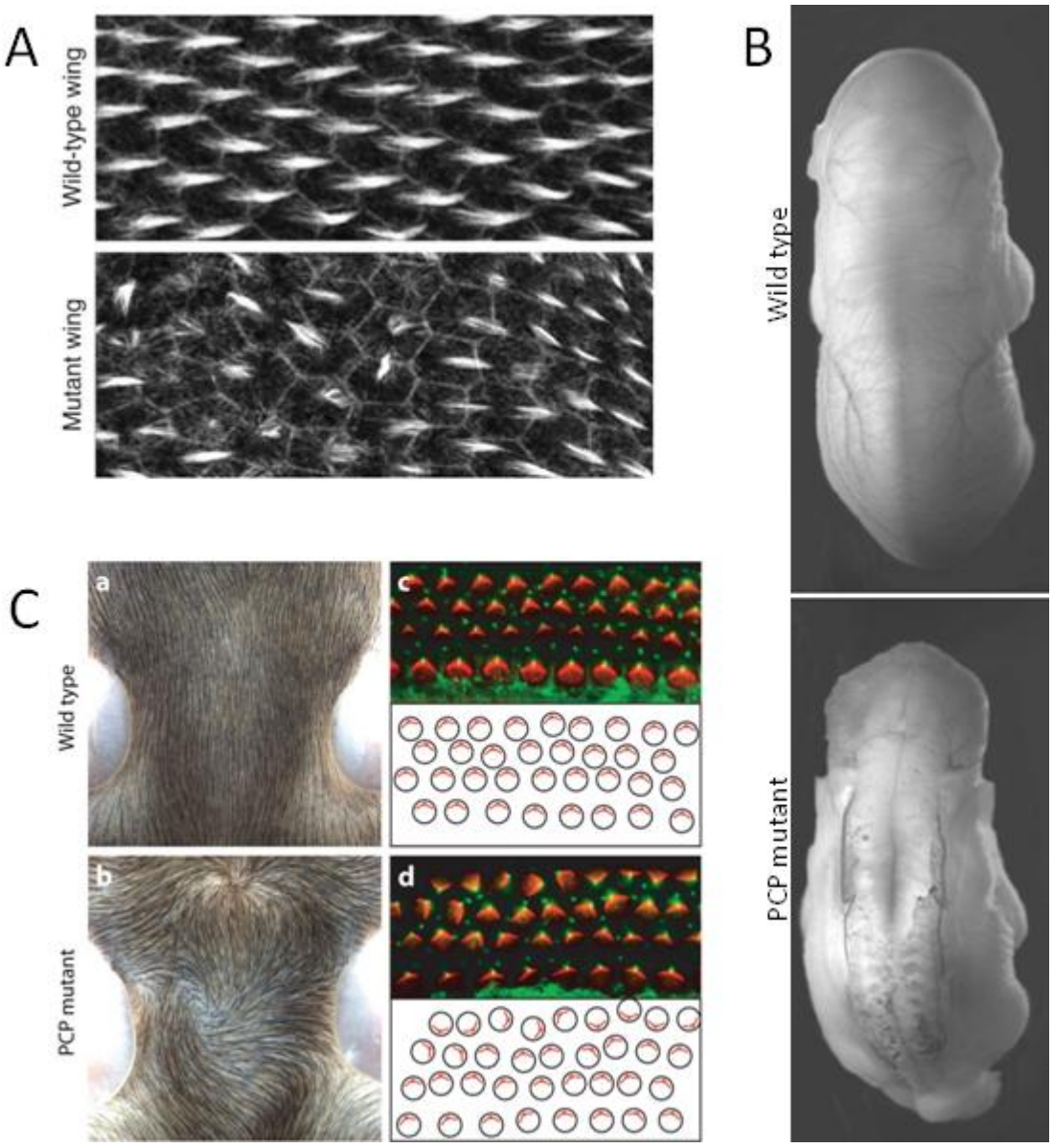

(A) Wild type and PCP mutant *Drosophila* wing epithelium, labeled with phalloidin to stain actin (Vladar *et al.*, 2009). (B) Wild type mouse embryo compared to a PCP mutant mouse embryo with a severe neural tube defect (Wang *et al.*, 2006). (C) More mouse phenotypes. [a-b] PCP mouse hair shows a whirled appearance. [c-d] Cochlea cells are not aligned properly in PCP mutant (Simons and Mlodzik, 2006).

One specific member of this expanded group of mammalian COPII paralogs is the focus of chapter 3, where in published work it is shown that a mutation in Sec24B is responsible for strong neural tube defects in mice. These defects arise from the dysfunctional transport of a specific member of the planar cell polarity pathway, Vangl2.

The study of planar cell polarity and the proteins involved has been traditionally the domain of developmental biologists whose main tool is genetics. The field can benefit from a more rigorous application of biochemical studies for some of the proteins involved. This is a task I have begun in my work on the molecular and functional analysis of Vangl2, found in chapter 4. My main concern was the effect of mutations on Vangl2 on trafficking, but incorrect trafficking will prevent functioning of the protein, so these mutants will be applicable to the study of PCP in a more *in vivo* setting.

Finally, chapter 5 contains a summary and discussion of what my findings mean for these two specific areas of biology – COPII transport and planar cell polarity. Included is preliminary data on the trafficking of other planar cell polarity proteins and proinsulin, a further preliminary analysis of Sec24B, a brief study of COPII expression in developing neural cells, and information on the *in vitro* translation and budding technique development.

References

Adler PN, Charlton J, Park WJ. (1994). The Drosophila tissue polarity gene inturned functions prior to wing hair morphogenesis in the regulation of hair polarity and number. *Genetics*. 137(3):829-36.

Aridor M, Bannykh SI, Rowe T, Balch WE. (1995). Sequential coupling between COPII and COPI vesicle coats in endoplasmic reticulum to Golgi transport. *J Cell Biol*. 131(4):875-93.

Axelrod JD, Miller JR, Shulman JM, Moon RT, Perrimon N. (1998). Differential recruitment of Dishevelled provides signaling specificity in the planar cell polarity and Wingless signaling pathways. *Genes Dev*. 12(16):2610-22.

Bastock R, Strutt H, Strutt D. (2003). Strabismus is asymmetrically localised and binds to Prickle and Dishevelled during Drosophila planar polarity patterning. *Development*. 130(13):3007-14.

Bonifacino JS, Lippincott-Schwartz J. (2003). Coat proteins: shaping membrane transport. *Nat Rev Mol Cell Biol*. 4(5):409-14.

Boutros M, Mlodzik M. (1999). Dishevelled: at the crossroads of divergent intracellular signaling pathways. *Mech Dev*. 83(1-2):27-37.

Braun M, Waheed A, von Figura K. (1989). Lysosomal acid phosphatase is transported to lysosomes via the cell surface. *EMBO J*. 8(12):3633-40.

Cantrell VA, Jessen JR. (2010). The planar cell polarity protein Van Gogh-Like 2 regulates tumor cell migration and matrix metalloproteinase-dependent invasion. *Cancer Lett*. 287(1):54-61.

Chae J, Kim MJ, Goo JH, Collier S, Gubb D, Charlton J, Adler PN, Park WJ. (1999). The Drosophila tissue polarity gene starry night encodes a member of the protocadherin family. *Development*. 126(23):5421-9.

Collier S, Gubb D. (1997). Drosophila tissue polarity requires the cell-autonomous activity of the fuzzy gene, which encodes a novel transmembrane protein. *Development*. 124(20):4029-37.

Emr S, Glick BS, Linstedt AD, Lippincott-Schwartz J, Luini A, Malhotra V, Marsh BJ, Nakano A, Pfeffer SR, Rabouille C, Rothman JE, Warren G, Wieland FT. (2009). Journeys through the Golgi--taking stock in a new era. *J Cell Biol*. 187(4):449-53.

Etheridge SL, Ray S, Li S, Hamblet NS, Lijam N, Tsang M, Greer J, Kardos N, Wang J, Sussman DJ, Chen P, Wynshaw-Boris A. (2008). Murine dishevelled 3 functions in redundant pathways with dishevelled 1 and 2 in normal cardiac

outflow tract, cochlea, and neural tube development. *PLoS Genet*. 4(11):e1000259.

Fahmy OG, Fahmy M. (1959). New mutants report. *Dros Inf Serv* 33:82–94.

Farquhar MG, Palade GE. (1981). The Golgi apparatus (complex)-(1954-1981)-from artifact to center stage. *J Cell Biol*. 91(3 Pt 2):77s–103s.

Feiguin F, Hannus M, Mlodzik M, Eaton S. (2001). The ankyrin repeat protein Diego mediates Frizzled-dependent planar polarization. *Dev Cell*. 1(1):93-101.

Formstone CJ, Little PF. (2001). The flamingo-related mouse Celsr family (Celsr1-3) genes exhibit distinct patterns of expression during embryonic development. *Mech Dev*. 109(1):91-4.

Friend DS and Farquhar MG. (1967). Functions of coated vesicles during protein absorbtion in the rat vas deferens. *J Cell Biol.* 35:357-376.

Gubb D, García-Bellido A. (1982). A genetic analysis of the determination of cuticular polarity during development in Drosophila melanogaster. *J Embryol Exp Morphol*. 68:37-57.

Itin C, Schindler R, Hauri HP. (1995). Targeting of protein ERGIC-53 to the ER/ERGIC/cis-Golgi recycling pathway. *J Cell Biol*. 131(1):57-67.

Jamieson JD, Palade GE. (1971). Synthesis, intracellular transport, and discharge of secretory proteins in stimulated pancreatic exocrine cells. *J Cell Biol.* 50:135–158.

Jessen JR and Solnica-Krezel L. (2004). Identification and developmental expression pattern of van gogh-like 1, a second zebrafish strabismus homologue. *Gene Expr Patterns*. 4(3):339-44.

Kornfeld R, Kornfeld S. (1985). Assembly of asparagine-linked oligosaccharides. *Annu Rev Biochem*. 54:631-64.

Lu X, Borchers AG, Jolicoeur C, Rayburn H, Baker JC, Tessier-Lavigne M. (2004). PTK7/CCK-4 is a novel regulator of planar cell polarity in vertebrates. *Nature*. 430(6995):93-8.

Miller EA, Beilharz TH, Malkus PN, Lee MC, Hamamoto S, Orci L, Schekman R. (2003). Multiple cargo binding sites on the COPII subunit Sec24p ensure capture of diverse membrane proteins into transport vesicles. *Cell.* 114:497–509.

Montcouquiol M, Rachel RA, Lanford PJ, Copeland NG, Jenkins NA, Kelley MW. (2003). Identification of Vangl2 and Scrb1 as planar polarity genes in mammals. *Nature*. 423(6936):173-7.

Noordermeer J, Klingensmith J, Perrimon N, Nusse R. (1994). Dishevelled and armadillo act in the wingless signalling pathway in Drosophila. *Nature*. 367(6458):80-3.

Novick P, Field C, Schekman R. (1980). Identification of 23 complementation groups required for post-translational events in the yeast secretory pathway. Cell. 21(1):205-15.

Nufer O, Kappeler F, Guldbrandsen S, Hauri HP. (2003). ER export of ERGIC-53 is controlled by cooperation of targeting determinants in all three of its domains. *J Cell Sci*. 116(Pt 21):4429-40.

Orci L, Glick BS, Rothman JE. (1986). A new type of coated vesicular carrier that appears not to contain clathrin: its possible role in protein transport within the Golgi stack. *Cell*. 46(2):171-84.

Orci L, Ravazzola M, Meda P, Holcomb C, Moore HP, Hicke L, Schekman R. (1991). Mammalian Sec23p homologue is restricted to the endoplasmic reticulum transitional cytoplasm. *Proc Natl Acad Sci U S A*. 88(19):8611-5.

Park M, Moon RT. (2002). The planar cell-polarity gene stbm regulates cell behaviour and cell fate in vertebrate embryos. *Nat Cell Biol*. 4(1):20-5.

Pryer NK, Wuestehube LJ, and Schekman R. (1992). Vesicle mediated protein sorting. *Annu. Rev. Biochem*. 67, 471-516.

Rein RS, Seemann GH, Neefjes JJ, Hochstenbach FM, Stam NJ, Ploegh HL. (1987). Association with beta 2-microglobulin controls the expression of transfected human class I genes. *J Immunol*. 138(4):1178-83.

Robinson MS. (1990). Cloning and expression of gamma-adaptin, a component of clathrin-coated vesicles associated with the Golgi apparatus. *J Cell Biol*. 111(6 Pt 1):2319-26.

Robitaille J, MacDonald ML, Kaykas A, Sheldahl LC, Zeisler J, Dubé MP, Zhang LH, Singaraja RR, Guernsey DL, Zheng B, Siebert LF, Hoskin-Mott A, Trese MT, Pimstone SN, Shastry BS, Moon RT, Hayden MR, Goldberg YP, Samuels ME. (2002). Mutant frizzled-4 disrupts retinal angiogenesis in familial exudative vitreoretinopathy. *Nat Genet*. 32(2):326-30.

Seaman MN, McCaffery JM, Emr SD. (1998). A membrane coat complex essential for endosome-to-Golgi retrograde transport in yeast. *J Cell Biol*. 142(3):665-81.

Simons M, Mlodzik M. (2008). Planar cell polarity signaling: from fly development to human disease. *Annu Rev Genet*.42:517-40.

Strutt D, Warrington SJ. (2008). Planar polarity genes in the Drosophila wing regulate the localisation of the FH3-domain protein Multiple Wing Hairs to control the site of hair production. *Development*. 135(18):3103-11.

Südhof TC, Rothman JE. (2009). Membrane fusion: grappling with SNARE and SM proteins. *Science*. 323(5913):474-7.

Taylor J, Abramova N, Charlton J, Adler PN. (1998). Van Gogh: a new Drosophila tissue polarity gene. *Genetics*. 150(1):199-210.

Tree DR, Shulman JM, Rousset R, Scott MP, Gubb D, Axelrod JD. (2002). Prickle mediates feedback amplification to generate asymmetric planar cell polarity signaling. *Cell*. 109(3):371-81.

Usui T, Shima Y, Shimada Y, Hirano S, Burgess RW, Schwarz TL, Takeichi M, Uemura T. (1999). Flamingo, a seven-pass transmembrane cadherin, regulates planar cell polarity under the control of Frizzled. *Cell*. 98(5):585-95.

Vladar EK, Antic D, Axelrod JD. (2009). Planar Cell Polarity Signaling: The Developing Cell's Compass. *Cold Spring Harb Perspect Biol*. 1(3):a002964.

Wang Y, Guo N, Nathans J. (2006). The role of Frizzled3 and Frizzled6 in neural tube closure and in the planar polarity of inner-ear sensory hair cells. *J Neurosci*. 26(8):2147-56.

Wodarz A, Nusse R. (1998). Mechanisms of Wnt signaling in development. *Annu Rev Cell Dev Biol*. 14:59-88.

Chapter Two:

COPII at a Glance

This chapter is an article in preparation for the “At a glance” series of review articles from Journal of Cell Science.

Introduction

Eukaryotic cells contain a number of different membrane compartments with specialized roles. Each compartment depends on a specific mixture of proteins for their identity and function. For many compartments, proteins arrive via small membrane vesicles that travel through the cell from an originating compartment (Bonifacino and Glick, 2004; Gürkan et al., 2007). Small membrane vesicles are created by the action of coat proteins that deform membranes into the shape of vesicles and simultaneously select "cargo" proteins for inclusion into those vesicles (Kirchhausen, 2000; Bonifacino and Lippincott-Schwartz, 2003). Coat protein complex II (COPII) is a set of highly conserved proteins that are responsible for creating small membrane vesicles that originate from the endoplasmic reticulum (ER) (Lee et al., 2004; Barlowe et al., 1994). The formation and movement of these COPII-derived vesicles is a critical first step in the cellular secretion pathway. This pathway is the way in which membrane and luminal cargo proteins are transported from their site of synthesis at the ER, onward to other membrane compartments in the cell.

In this article, we first consider the 5 proteins that constitute the conserved core of the COPII vesicle creation machinery and take a look at how they are able to shape membranes, select cargo proteins that need to be transported, and form a polymeric coat that results in a vesicle. Then, we examine more recent discoveries that show how deficiencies in COPII can lead to disease. Finally, we quickly explore how additional factors can work with the COPII proteins to enhance transport efficiency in particular cases. We hope that this brief overview will be useful and encourage readers to consider how efficient or deficient forward transport can affect the activity of the proteins they study.

The five core COPII proteins and vesicle formation

The COPII coat machinery consists of 5 cytosolic proteins: Sar1, Sec23, Sec24, Sec13, and Sec31. In cells, Sec23 and Sec24 form a tight heterodimer, called the "inner" COPII coat and Sec13 and Sec31 are found in a stable heterotetramer with two subunits of each, called the "outer" COPII coat (Barlowe et al., 1994). Sar1 and these two stable complexes are sequentially recruited to the ER membrane and work together to create a complete COPII vesicle (Figure 2.1). In most eukaryotic organisms, this recruitment to the membrane does not occur spontaneously across the entire surface of the ER. Instead, COPII proteins from the cytosol and cargo proteins on the membrane are recruited to discrete regions of the ER membrane called ER exit sites or transitional ER (tER) (Budnik and Stephens, 2009; Bannykh et al., 1996). These exit sites are microdomains of high COPII activity and they label brightly with COPII proteins when visualized by immunofluorescence (Figure 2.2). Localizing COPII activity into these microdomains likely helps to maintain a critical concentration of COPII proteins and enable the efficient recycling of these coat proteins as they are recruited back to the membrane for use in subsequent rounds of COPII budding (Orci et al., 1991).

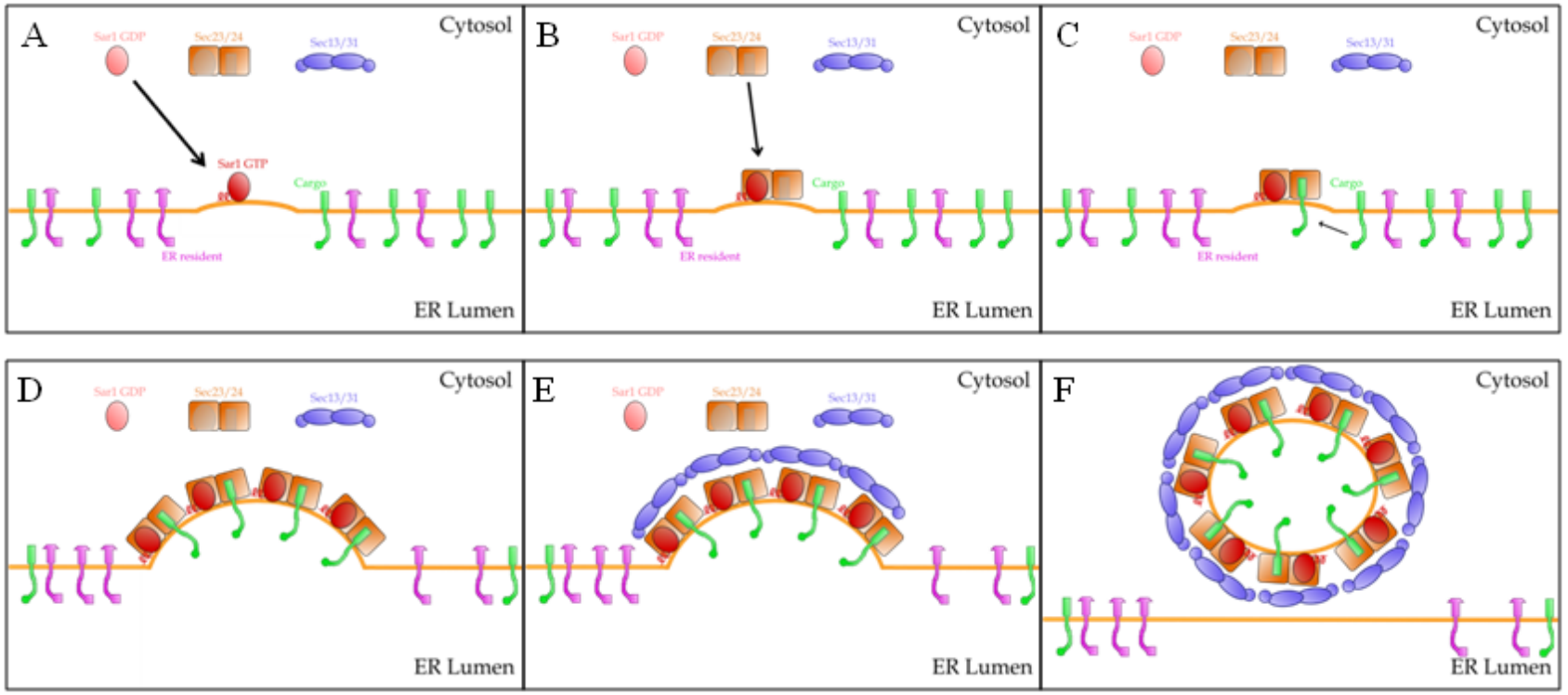

Figure 2.1 - Formation of a COPII vesicle requires sequential recruitment of 5 proteins: Sar1, Sec23/24 and Sec13/31. A – Sar1 is recruited to the ER membrane where it exchanges for GTP. B – Sec23/24 is recruited to the membrane by Sar1. C – Sec24 binds to transmembrane cargo proteins and the group becomes a prebudding complex. D – Several prebudding complexes are at an ER exit site. E – Sec13/31 is recruited and crosslinks many prebudding complexes together. F – The full vesicle completes and pinches off the donor ER membrane.

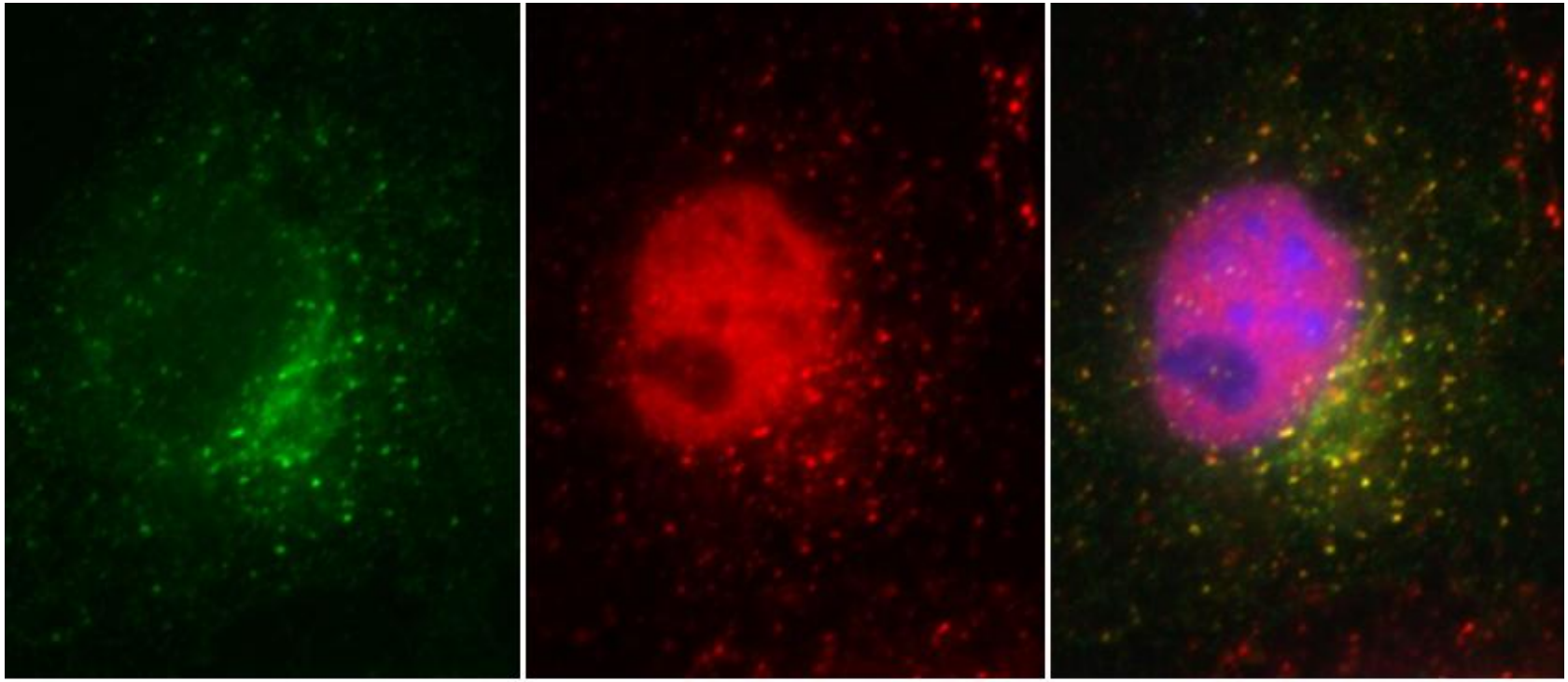

Figure 2.2 – Immunofluorescence of ER exit sites. COPII proteins of both the inner (Sec24B) and outer (Sec13) coat are localized to discrete microdomains of the ER membrane called ER exit sites. (Devon Jensen, unpublished)

Green – Myc-Sec24B (FITC) Red – Endogenous Sec13 (TRITC) Blue – Dapi

Sar1is the first COPII component recruited to the ER membrane and it begins the process of vesicle formation. Sar1 is a small GTPase whose activity, like that of other small G-proteins, is controlled by the state of nucleotide to which it is bound (Pucadyil and Schmid, 2009). In its GDP bound state, Sar1 is cytosolic and dormant, but when bound to GTP, Sar1 activates by exposing an amphipathic amino-terminal α-helix which embeds into the ER membrane (Lee and Miller, 2007, Bielli et al., 2005). This activity is restricted to the ER membrane because Sec12, the guanine nucleotide exchange factor (GEF) that activates Sar1, is only found at the ER (Gillingham and Munro, 2007). By embedding this α-helix, Sar1 anchors the forming coat complex on the membrane, but it also initiates membrane budding. In fact, activated Sar1 can, by itself, form long thin tubules when added to synthetic liposomes (Lee et al., 2005). Acting as a membrane bound anchor for the other COPII components, activated Sar1 directly binds and recruits the next COPII sub-complex to arrive at the site of the forming vesicle, the Sec23/24 heterodimer.

The Sec23/Sec24 sub-complex arrives at the scene by virtue of the direct interaction between Sar1 and Sec23 (Bi et al., 2002). This interaction serves not only a structural role in assembling the inner coat complex on the membrane, but it also serves a catalytic role. Sec23 is a GTPase activating protein (GAP) for Sar1, accelerating the meager intrinsic GTPase activity possessed by Sar1 itself; although full GTPase activity is not realized until the complete COPII coat is assembled upon the arrival of the Sec13/31 outer coat (Yoshihisa et al., 1993; Antonny et al., 2001). This catalytic activity is thought to provide a built-in timing mechanism that causes Sar1 to revert to its inactive form, leading to the disassembly of the coat from the membrane of a completed COPII vesicle (Lee and Miller, 2007).

Sec24 is considered to be the primary subunit responsible for binding to membrane cargo proteins at the ER and concentrating them into the forming vesicle (Miller et al., 2002). Many cargo proteins have specific export signal sequences in their cytoplasmic domains to mark them for COPII transport. Types of COPII signal sequences include di-hydrophobic, di-acidic, C-terminal hydrophobic and aromatic motifs (Wendeler et al., 2007; Barlowe, 2003). A number of cargo binding pockets and the corresponding signal sequences they bind have been identified on the surface of Sec24 and have been termed the A-, B- and C- sites (Miller et al., 2003). Not all proteins that need to leave the ER contain a signal for direct binding to Sec24. Some proteins may interact with a transport adaptor, and thus be included in the COPII vesicle via an indirect interaction (Baines and Zhang, 2007). Still other proteins may passively enter COPII vesicles by simple diffusion – a process called bulk flow (Thor et al., 2009). Of those tested, many cargo proteins are found in COPII vesicles at concentrations higher than a bulk flow model would suggest, indicating that concentrative sorting by Sec24 may be the rule (Malkus et al., 2002). Sec24 is brought to sites of COPII vesicle formation through its interaction with Sec23. Altogether, the set of proteins consisting of a membrane bound Sar1 along with a cargo-loaded Sec23/Sec24 dimer has been termed a "prebudding complex," a complex ready for the activity of Sec13/31 to complete the formation of the vesicle.

The Sec13/31 heterotetramer is the last set of COPII proteins recruited to the ER membrane as a vesicle is forming. This outer layer of the coat collects prebudding complexes and shapes the membrane to form a bud enriched in cargo molecules. To accomplish this task, Sec31 directly interacts with Sec23 and Sar1 (Bi et al., 2007). Under certain *in vitro* conditions, the elongated Sec13/31 molecules can polymerize at vertices to form the edges of round "empty cages", illustrating their potential to provide a structural framework for the shape of the vesicle as it buds off the donor ER membrane (Stagg *et al.*, 2006). With the full complement of COPII proteins assembled into a polymerized coat, the extruded membrane is separated from the donor ER membrane by fission to form an intact vesicle. Unlike some other vesicle coats, COPII does not require a specialized GTPase, such as dynamin, to constrict the neck of the forming vesicle and release it from the membrane. Purified COPII components alone are able to form small vesicles from synthetic liposome membrane (Matsuoka et al., 1998). The end result of this process is a spherical membrane vesicle roughly 60-70nm in size that contains cargo proteins en route to the ER-Golgi intermediate compartment, or in yeast possibly directly to the cis-Golgi membrane. This process works well for the wide variety of cargo proteins trafficked from the ER, but what could go wrong if one of these 5 core COPII proteins was missing or mutated?

COPII proteins linked to disease

COPII transport in the mammalian system has diversified, as gene duplication events have created multiple paralogs for 4 out of the 5 COPII proteins (Figure 2.3). The mammalian repertoire consists of: two Sar1 paralogs, Sar1A and Sar1B; two Sec23 paralogs, Sec23A and Sec23B; four Sec24 paralogs, Sec24A, Sec24B, Sec24C, and Sec24D; a single Sec13; and two Sec31 paralogs, Sec31A and Sec31B. In recent years, one of the challenges for the field has been to elucidate the reason that these multiple paralogs have been conserved among higher organisms. Are these COPII paralogs functionally redundant but expressed in different tissues? Or have some of these paralogs become specialized to transport different cargo? Examples of developmental disorders and human diseases caused by mutations in Sar1B, Sec23A, Sec23B, and Sec24B have begun to shed light on these questions.

Several different mutations in Sar1B have been associated with two related fat malabsorption diseases – chylomicron retention disease and anderson disease (Jones et al., 2003). Affected individuals are deficient in fat-soluble vitamins, have low blood cholesterol levels, and show a lack of chylomicrons in their blood. Chylomicrons, one of the major types of circulating lipoprotein, are produced in the ER of intestine cells and secreted by those cells into the bloodstream. More interesting still is the fact that chylomicrons range in size from 75-450nm in diameter (Hussain, 2000). So how can COPII vesicles, which are typically only 60-70nm, accommodate such a large cargo molecule? Is Sar1B specialized for enabling the transport of chylomicrons and perhaps other largo cargo molecules like pro-collagen? These issues remain unresolved (Fromme and Schekman, 2005).

Figure 2.3 – Core COPII proteins compared between yeast and mammalian organisms

Yeast COPII	Mammalian COPII	Associated Diseases
Sar1p	Sar1A	
	Sar1B	Chylomicron Retention Disease Anderson Disease
Sec23p	Sec23A	Cranio-lenticulo-sutural dysplasia
	Sec23B	Congenital dyserythropoietic anemia type II
Sec24p (Iss1)* (Lst1)*	Sec24A	
	Sec24B	Craniorachischisis and other planar cell polarity phenotypes
	Sec24C	
	Sec24D	
Sec13p	Sec13	
Sec31p	Sec31A	
	Sec31B	

In mammals, gene duplication events in have created multiple paralogs for most of the COPII proteins that are found in yeast. Genetic diseases caused by mutations in COPII proteins have been identified for Sar1B, Sec23A, Sec23B, and Sec24B.
* Yeast homologs of Sec24p

A single missense mutation in Sec23A (F382L) has been found to lead to an autosomal recessive disease called cranio-lenticulo-sutural dysplasia (CLSD) (Boyadjiev et al., 2006). The disease is marked by skeletal defects, cataracts, and facial dysmorphisms. The molecular nature of this amino acid change has been studied in detail and it was found that the mutation is near the part of Sec23A that binds and recruits Sec31 (Bi et al., 2007). Failure to recruit Sec31 leads to a large reduction in the packaging of cargo proteins *in vitro* and leads to a distended ER full of untransported cargo *in vivo* (Fromme et al., 2007). Additionally, the tissues that are most affected by the disease appear to express low levels of the paralog Sec23B, suggesting that these tissues may not have enough fully functional Sec23 overall.

Many separate mutations in Sec23B were found in patients with a disease called congenital dyserythropoietic anemia type II (CDAII) (Schwarz et al., 2009; Bianchi et al., 2009). The symptoms of the disease appear to be largely due to defective erythropoiesis, in which red blood cell progenitors are often multinucleate and circulating red blood cells are morphologically abnormal. Various proteins in these red blood cells show immature glycosylation, indicating transport defects, but how this might be related to the cytokinesis defect in the multinucleate progenitor cells is unclear. Analysis of gene expression during wild type erythroid differentiation detected an increase in Sec23B RNA expression of 5-7 fold over that of Sec23A RNA expression (Schwarz et al., 2009). As with the Sec23A mutation, it seems that the Sec23B mutations only affect a very specific tissue. It may be that Sec23A and Sec23B are functionally redundant, and able to largely compensate for one another in unaffected tissues where they are normally both expressed.

Recent reports demonstrate that two distinct premature stop codons in Sec24B lead to major neural tube defects in mice (Merte et al., 2010; Wansleeben et al., 2010). Homozygous mutant mice developed craniorachischisis and several other phenotypes indicative of defects within the tissue-organizing planar cell polarity pathway. A candidate based approach looking at cargo proteins involved in establishing planar cell polarity, revealed that Vangl2 appears to be specifically packaged by Sec24B. The entry of Vangl2 into COPII vesicles *in vitro* showed that the packaging was specifically enhanced in the presence of recombinant Sec24B and not the other Sec24 paralogs (Merte et al., 2010). *In vivo* analysis of mutant primary fibroblasts also showed a selective defect in the transport of Vangl2 (Wansleeben et al., 2010). Sec24 is a very versatile protein, but in this case, Sec24B appears to have specific binding activity for at least one important cargo protein that cannot be compensated by the presence of other Sec24 paralogs.

Additional proteins that enable transport in mammalian cells

The core COPII proteins accommodate many different cargo proteins, but given the complex range of cargo molecules, additional adaptors appear to play cargo-selective roles. Here we provide a brief digest of the recent progress on this topic:

Tango1 is found at ER exit sites and helps to load Collagen VII, and perhaps other bulky cargo, into COPII vesicles (Saito et al. 2009). PDZ proteins Grasp65 and Syntenin enable the efficient ER export of proteins with carboxyl-terminal PDZ binding motifs (D'Angelo et al., 2009; Fernández-Larrea et al., 1999). Erv26p/Svp26 acts as a transport adaptor for some type II membrane proteins in yeast (Bue et al., 2006; Noda and Yoda, 2010). Stam1 and Stam2 interact with COPII proteins and affect traffic, though the mechanism is not clear (Rismanchi et al., 2009). Knockdown of Sec23IP (Sec23 interacting protein) in *Xenopus* embryos resulted in defective neural crest cell migration patterns (McGary et al., 2010). ALG-2 stablilzes Sec31 at ER exit sites and may regulate the timing of COPII vesicle homotypic fusion (Bentley et al., 2010).

Perspectives

Recent developments have made this an opportune time to review the study of COPII-mediated vesicle transport. The past couple years have seen a transition in the field, from the original understanding of the basic mechanisms of COPII in simpler organisms, to establishing the roles of the multiple COPII paralogs and associated factors that drive COPII transport in the more complex mammalian system. This new knowledge comes with examples of deficiencies in COPII that cause developmental disorders and human disease. In the future, we expect selected mouse knock-out studies to supply information about the specific roles of other COPII paralogs. Additionally, insight into the mechanism for packaging of large cargos and additional factors that enable efficient COPII transport will surely be found.

References

Antonny, B., Madden, D., Hamamoto, S., Orci, L. and Schekman, R. (2001). Dynamics of the COPII coat with GTP and stable analogues. *Nat. Cell Biol.* **3,** 531-537.

Baines, A. C. and Zhang, B. (2007). Receptor-mediated protein transport in the early secretory pathway. *Trends Biochem. Sci.* **32,** 381-388.

Bannykh, S. I., Rowe, T. and Balch, W. E. (1996). The organization of endoplasmic reticulum export complexes. *J. Cell Biol.* **135,** 19-35.

Barlowe, C. (2003). Signals for COPII-dependent export from the ER: What's the ticket out? *Trends Cell Biol.* **13,** 295-300.

Barlowe, C., Orci, L., Yeung, T., Hosobuchi, M., Hamamoto, S., Salama, N., Rexach, M. F., Ravazzola, M., Amherdt, M. and Schekman, R. (1994). COPII: A membrane coat formed by sec proteins that drive vesicle budding from the endoplasmic reticulum. *Cell* **77,** 895-907.

Bentley, M., Nycz, D. C., Joglekar, A., Fertschai, I., Malli, R., Graier, W. F. and Hay, J. C. (2010). Vesicular calcium regulates coat retention, fusogenicity, and size of pre-golgi intermediates. *Mol. Biol. Cell* **21,** 1033-1046.

Bi, X., Corpina, R. A. and Goldberg, J. (2002). Structure of the Sec23/24-Sar1 pre-budding complex of the COPII vesicle coat. *Nature* **419,** 271-277.

Bi, X., Mancias, J. D. and Goldberg, J. (2007). Insights into COPII coat nucleation from the structure of Sec23.Sar1 complexed with the active fragment of Sec31. *Dev. Cell.* **13,** 635-645.

Bianchi, P., Fermo, E., Vercellati, C., Boschetti, C., Barcellini, W., Iurlo, A., Marcello, A. P., Righetti, P. G. and Zanella, A. (2009). Congenital dyserythropoietic anemia type II (CDAII) is caused by mutations in the SEC23B gene. *Hum. Mutat.* **30,** 1292-1298.

Bielli, A., Haney, C. J., Gabreski, G., Watkins, S. C., Bannykh, S. I. and Aridor, M. (2005). Regulation of Sar1 NH2 terminus by GTP binding and hydrolysis promotes membrane deformation to control COPII vesicle fission. *J. Cell Biol.* **171,** 919-924.

Bonifacino, J. S. and Glick, B. S. (2004). The mechanisms of vesicle budding and fusion *Cell* **116,** 153-166.

Bonifacino, J. S. and Lippincott-Schwartz, J. (2003). Coat proteins: Shaping membrane transport. *Nat. Rev. Mol. Cell Biol.* **4,** 409-414.

Boyadjiev, S. A., Fromme, J. C., Ben, J., Chong, S. S., Nauta, C., Hur, D. J., Zhang, G., Hamamoto, S., Schekman, R., Ravazzola, M. et al. (2006). Cranio-lenticulo-sutural dysplasia is caused by a SEC23A mutation leading to abnormal endoplasmic-reticulum-to-golgi trafficking. *Nat. Genet.* **38,** 1192-1197.

Budnik, A. and Stephens, D. J. (2009). ER exit sites--localization and control of COPII vesicle formation. *FEBS Lett.* **583,** 3796-3803.

Bue, C. A., Bentivoglio, C. M. and Barlowe, C. (2006). Erv26p directs pro-alkaline phosphatase into endoplasmic reticulum-derived coat protein complex II transport vesicles. *Mol. Biol. Cell* **17,** 4780-4789.

D'Angelo, G., Prencipe, L., Iodice, L., Beznoussenko, G., Savarese, M., Marra, P., Di Tullio, G., Martire, G., De Matteis, M. A. and Bonatti, S. (2009). GRASP65 and GRASP55 sequentially promote the transport of C-terminal valine-bearing cargos to and through the golgi complex. *J. Biol. Chem.* **284,** 34849-34860.

Fernandez-Larrea, J., Merlos-Suarez, A., Urena, J. M., Baselga, J. and Arribas, J. (1999). A role for a PDZ protein in the early secretory pathway for the targeting of proTGF-alpha to the cell surface. *Mol. Cell* **3,** 423-433.

Fromme, J. C., Ravazzola, M., Hamamoto, S., Al-Balwi, M., Eyaid, W., Boyadjiev, S. A., Cosson, P., Schekman, R. and Orci, L. (2007). The genetic basis of a craniofacial disease provides insight into COPII coat assembly. *Dev. Cell.* **13,** 623-634.

Fromme, J. C. and Schekman, R. (2005). COPII-coated vesicles: Flexible enough for large cargo? *Curr. Opin. Cell Biol.* **17,** 345-352.

Gillingham, A. K. and Munro, S. (2007). The small G proteins of the arf family and their regulators. *Annu. Rev. Cell Dev. Biol.* **23,** 579-611.

Gurkan, C., Koulov, A. V. and Balch, W. E. (2007). An evolutionary perspective on eukaryotic membrane trafficking *Adv. Exp. Med. Biol.* **607,** 73-83.

Hussain, M. M. (2000). A proposed model for the assembly of chylomicrons. *Atherosclerosis* **148,** 1-15.

Jones, B., Jones, E. L., Bonney, S. A., Patel, H. N., Mensenkamp, A. R., Eichenbaum-Voline, S., Rudling, M., Myrdal, U., Annesi, G., Naik, S. et al. (2003). Mutations in a Sar1 GTPase of COPII vesicles are associated with lipid absorption disorders. *Nat. Genet.* **34,** 29-31.

Kirchhausen, T. (2000). Three ways to make a vesicle. *Nat. Rev. Mol. Cell Biol.* **1,** 187-198.

Lee, M. C. and Miller, E. A. (2007). Molecular mechanisms of COPII vesicle formation. *Semin. Cell Dev. Biol.* **18,** 424-434.

Lee, M. C., Miller, E. A., Goldberg, J., Orci, L. and Schekman, R. (2004). Bi-directional protein transport between the ER and golgi. *Annu. Rev. Cell Dev. Biol.* **20,** 87-123.

Lee, M. C., Orci, L., Hamamoto, S., Futai, E., Ravazzola, M. and Schekman, R. (2005). Sar1p N-terminal helix initiates membrane curvature and completes the fission of a COPII vesicle. *Cell* **122,** 605-617.

Malkus, P., Jiang, F. and Schekman, R. (2002). Concentrative sorting of secretory cargo proteins into COPII-coated vesicles. *J. Cell Biol.* **159,** 915-921.

Matsuoka, K., Orci, L., Amherdt, M., Bednarek, S. Y., Hamamoto, S., Schekman, R. and Yeung, T. (1998). COPII-coated vesicle formation reconstituted with purified coat proteins and chemically defined liposomes. *Cell* **93,** 263-275.

McGary, K. L., Park, T. J., Woods, J. O., Cha, H. J., Wallingford, J. B. and Marcotte, E. M. (2010). Systematic discovery of nonobvious human disease models through orthologous phenotypes. *Proc. Natl. Acad. Sci. U. S. A.*

Merte, J., Jensen, D., Wright, K., Sarsfield, S., Wang, Y., Schekman, R. and Ginty, D. D. (2010). Sec24b selectively sorts Vangl2 to regulate planar cell polarity during neural tube closure. *Nat. Cell Biol.* **12,** 41-6; sup pp 1-8.

Miller, E., Antonny, B., Hamamoto, S. and Schekman, R. (2002). Cargo selection into COPII vesicles is driven by the Sec24p subunit. *EMBO J.* **21,** 6105-6113.

Miller, E. A., Beilharz, T. H., Malkus, P. N., Lee, M. C., Hamamoto, S., Orci, L. and Schekman, R. (2003). Multiple cargo binding sites on the COPII subunit Sec24p ensure capture of diverse membrane proteins into transport vesicles. *Cell* **114,** 497-509.

Noda, Y. and Yoda, K. (2010). Svp26 facilitates endoplasmic reticulum-to-golgi transport of a set of mannosyltransferases in saccharomyces cerevisiae. *J. Biol. Chem.*

Orci, L., Ravazzola, M., Meda, P., Holcomb, C., Moore, H. P., Hicke, L. and Schekman, R. (1991). Mammalian Sec23p homologue is restricted to the endoplasmic reticulum transitional cytoplasm. *Proc. Natl. Acad. Sci. U. S. A.* **88,** 8611-8615.

Pucadyil, T. J. and Schmid, S. L. (2009). Conserved functions of membrane active GTPases in coated vesicle formation. *Science* **325,** 1217-1220.

Rismanchi, N., Puertollano, R. and Blackstone, C. (2009). STAM adaptor proteins interact with COPII complexes and function in ER-to-golgi trafficking. *Traffic* **10,** 201-217.

Saito, K., Chen, M., Bard, F., Chen, S., Zhou, H., Woodley, D., Polischuk, R., Schekman, R. and Malhotra, V. (2009). TANGO1 facilitates cargo loading at endoplasmic reticulum exit sites. *Cell* **136,** 891-902.

Schwarz, K., Iolascon, A., Verissimo, F., Trede, N. S., Horsley, W., Chen, W., Paw, B. H., Hopfner, K. P., Holzmann, K., Russo, R. et al. (2009). Mutations affecting the secretory COPII coat component SEC23B cause congenital dyserythropoietic anemia type II. *Nat. Genet.* **41,** 936-940.

Stagg, S. M., Gurkan, C., Fowler, D. M., LaPointe, P., Foss, T. R., Potter, C. S., Carragher, B. and Balch, W. E. (2006). Structure of the Sec13/31 COPII coat cage. *Nature* **439,** 234-238.

Thor, F., Gautschi, M., Geiger, R. and Helenius, A. (2009). Bulk flow revisited: Transport of a soluble protein in the secretory pathway. *Traffic* **10,** 1819-1830.

Wansleeben, C., Feitsma, H., Montcouquiol, M., Kroon, C., Cuppen, E. and Meijlink, F. (2010). Planar cell polarity defects and defective Vangl2 trafficking in mutants for the COPII gene Sec24b. *Development* **137,** 1067-1073.

Wendeler, M. W., Paccaud, J. P. and Hauri, H. P. (2007). Role of Sec24 isoforms in selective export of membrane proteins from the endoplasmic reticulum. *EMBO Rep.* **8,** 258-264.

Yoshihisa, T., Barlowe, C. and Schekman, R. (1993). Requirement for a GTPase-activating protein in vesicle budding from the endoplasmic reticulum. *Science* **259,** 1466-1468.

Chapter Three:

Sec24b selectively sorts Vangl2 to regulate planar cell polarity during neural tube closure

Acknowledgements

This work is the result of a fruitful collaboration between our lab and David Ginty's lab from Johns Hopkins University. The work is previously published as:

Janna Merte*, Devon Jensen*, Kevin Wright, Sarah Sarsfield, Yanshu Wang, Randy Schekman & David D. Ginty

Sec24b selectively sorts Vangl2 to regulate planar cell polarity during neural tube closure

Nature Cell Biology 12, 41 - 46 (2010).
Published online: 6 December 2009

*These authors contributed equally to this work

The article is reprinted here with permission.

Results and Discussion

Neural tube closure defects result from fundamental failures of developmental processes during neurulation. Most common among these disorders is spina bifida, a failure of caudal tube closure, and anencephaly, a failure of rostral neural tube closure. A rare disorder, craniorachischisis, is a closure failure along the entire anterior-posterior axis from the midbrain-hindbrain boundary to the most caudal end of the neural tube. During neurulation in the mouse, the neural plate undergoes several morphological changes: neural folds are created, migrate toward the midline, and eventually fuse. As migratory cells intercalate with each other, the embryo is lengthened at the expense of the width within the medial-lateral plane in a process called convergent extension (CE). The first neural tube closure event (closure 1) begins at the boundary between the hindbrain and the cervical region and spreads both rostrally and caudally into the hindbrain and developing spinal cord, respectively. Thus, when closure 1 fails, the entire neural tube from the midbrain to the caudal neural tube remains open resulting in craniorachischisis[1, 2].

Currently, all known mutations that result in craniorachischisis in the mouse have been mapped to the vertebrate orthologs of components of the planar cell polarity (PCP) pathway, first identified for its role in tissue patterning of the fly[1,2]. Loss-of-function mutations in *Vangl2*[3,4], *Fzd*, (*Fzd3;Fzd6* double mutants[5]), *Celsr1*[6], *Dvl* (*Dvl1;Dvl2* double mutants[7, 8]) as well as *Ptk7*[9] and *Scribble*[10, 11] all cause craniorachischisis in the mouse, indicating that the non-canonical Wnt signaling pathway is critical for developmental events underlying the initiation of closure 1 during neurulation. Craniorachischisis in these mutants results from deficits in CE during the migratory movements required to initiate closure 1[12-14].

Using a three-generation, forward-genetic screen for recessive mutations affecting neural development[15] (Figure 3.S1) we identified mouse line 811. Mutant 811 mice were easily distinguished from their littermates, as homozygous mutants within this allelic group developed craniorachischisis (Figure 3.1A). This mutant allele was found to segregate with Mendelian ratios with 48% (129/267) of parents carrying the allele and 12% (1/4 effected x 1/2 females are carriers) of embryos (232/1984) displaying the fully open neural tube (Figure 3.S2). By embryonic day 18.5 (E18.5), approximately 33% of the mutants isolated were dead or dying but could still be scored and genotyped.

The genetic lesion underlying the craniorachischisis observed in line 811 was mapped to a 1.8 Mb region of chromosome 3 between rs13477397 and rs1347704 that contained 17 open reading frames. We sequenced the exons containing 5'UTR and coding sequence for the 14 loci without existing mouse models (Methods; Figure 3.1B). This sequence analysis revealed a single base pair substitution within all of the sequences analyzed. This point mutation was a T>A transversion in exon 9 of *Sec24b*. Two different transcript variants can be processed from the *Sec24b* locus of the mouse: *ENMUST00000001079/NCBI (1079)* and *ENMUST00000098616 (98616)* (Figure 3.1C, exon 9 highlighted in red). The T>A transversion is 2078T>A in *1079* and 1834T>A in *98616* (Figure 3.1D). The nucleotide substitution results in truncated proteins, Sec24b

Figure 3.1 – The mutation in mouse line 811 is Sec24b Y613

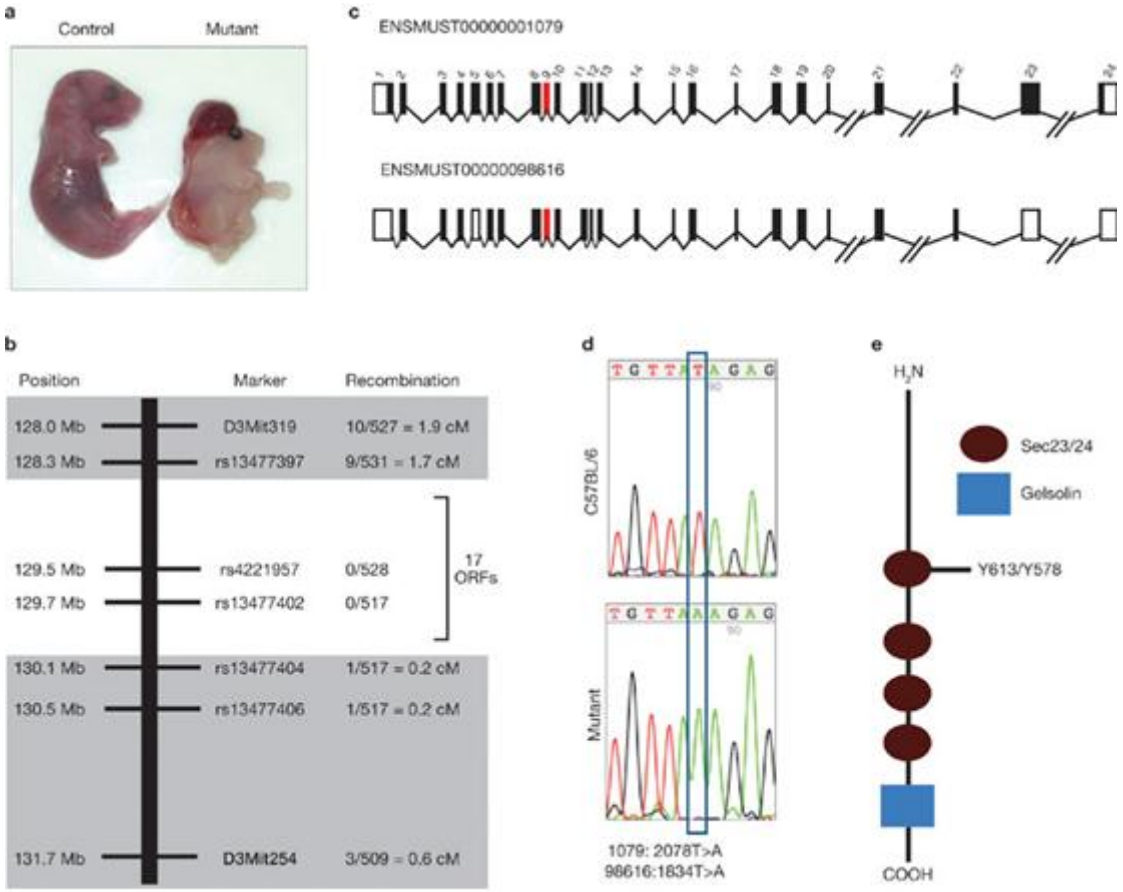

(A) Wholemount image of E18.5 811 mutant and control littermate showing the reduced size and craniorachischisis phenotype. (B) Schematic diagram of the region of chromosome 3 found to contain the 811 mutation, the markers used to diagnose linkage, and the frequency of recombination events observed at these markers. (C) Schematic diagram of the *Sec24b* genomic locus highlighting exon 9 (red) in which a single base pair substitution was observed. Shown in black are the coding exons from the two predicted transcripts, designated 1079 and 98616 generated from the mouse *Sec24b* locus (D) Sequence data highlighting the mutation *Sec24b* 1079: 2078T>A, 98616: 1834T>A observed in 811 mutants compared to C57BL/6 wildtype DNA. (E) Schematic diagram of Sec24b. The 811 point mutation introduces a stop codon within a Sec23/24 domain of Sec24b.

Y613 and Sec24b Y578 in 1079 and 98616, respectively (Figure 3.1E). The neural tube closure phenotype associated with line 811 is caused by the mutation in *Sec24b* (*Sec24b*^{Y613}) because a second mouse mutant harboring a distinct loss-of-function mutation in *Sec24b* (*Sec24b*^{S135X}) and exhibiting chraniorachischisis was independently identified (Frits Meijlink, Hubrecht Institute, Netherlands, personal communication). Sec24b is one of four mammalian orthologs of the yeast Sec24, and the first vertebrate Sec24 to be characterized *in vivo*.

Sec24b functions as a cargo-binding component of the COPII vesicle coat[16-19]. These COPII vesicles are the primary pathway for active transport of secretory proteins from the ER to the Golgi. Thus, as an initial step in the forward secretion of nearly all non-ER-resident membrane and luminal proteins, COPII-mediated vesicle transport plays a key role in enabling the proper cellular localization of thousands of proteins. Sec23, the GTPase activating member of the complex, and Sec24 components form tight heterodimers in the cytosol, and this complex is then recruited to sites of active COPII budding – termed ER exit sites. Once recruited to the ER membrane, Sec24 proteins package cargo into the vesicle at sites of active budding. Based on co-crystal structural studies[20], it appears that Sec24b Y613 is truncated prior to the putative Sec23 binding site. Therefore, we predicted that Sec24b Y613 would lose its ability to associate with its Sec23 binding partners, rendering it functionally inactive. Indeed, we found that in contrast to wildtype Sec24b, mutant Sec24b Y613 failed to co-immunoprecipatate with either Sec23a or Sec23b in heterologous cells and was not concentrated at ER exit sites marked by another COPII component, Sec13 (Figure 3.S3). Thus, *Sec24b*^{Y613} functions as a loss-of-function allele encoding a protein that is incapable of associating with other components of the COPII complex and is not recruited to ER exit sites.

Given that other mouse mutants with craniorachischisis have deficits in CE[12, 14, 21], we analyzed the embryonic morphology of *Sec24b* mutants during neurulation prior to neural tube closure. To do this, we examined *Sec24b*$^{Y613/Y613}$ mutants and control littermates at E8.5 for deficits in the length: width ratio. A decrease in this ratio reflects a developmental failure in the migratory movements required to lengthen the embryo and facilitate midline fusion[14]. At the 6-, 7-, 8-, and 10-somite stages, *Sec24b*$^{Y613/Y613}$ mutants were shorter and wider than littermates, confirming a deficit in the morphogenic movements of CE (Figure 3.2A). These finding indicate that the developmental events underlying craniorachischisis in *Sec24b*^{Y613} mutants are shared with other mouse mutants in the PCP-signaling pathway.

CE-deficient craniorachischisis is common to mouse mutants with deficits in the PCP-signaling pathway; thus, we sought to determine if other PCP-dependent phenotypes were also found in *Sec24b*$^{Y613/Y613}$ embryos. First, all mutants isolated at E18.5 were scored for omphalocele, a congenital birth defect in which the intestines, liver, and occasionally other organs develop outside of the abdomen because the tissues of the abdominal wall fail to fuse at the midline. We observed omphalocele in 45% (n=38) of the late gestation mutant embryos but in fewer than 1% (n=166) of littermate controls. Second, we examined the fusion of the eyelids in all of the E18.5

Figure 3.2 – *Sec24b*$^{Y613/Y613}$ embryos have deficits in cochlear hair cell development and convergent extension

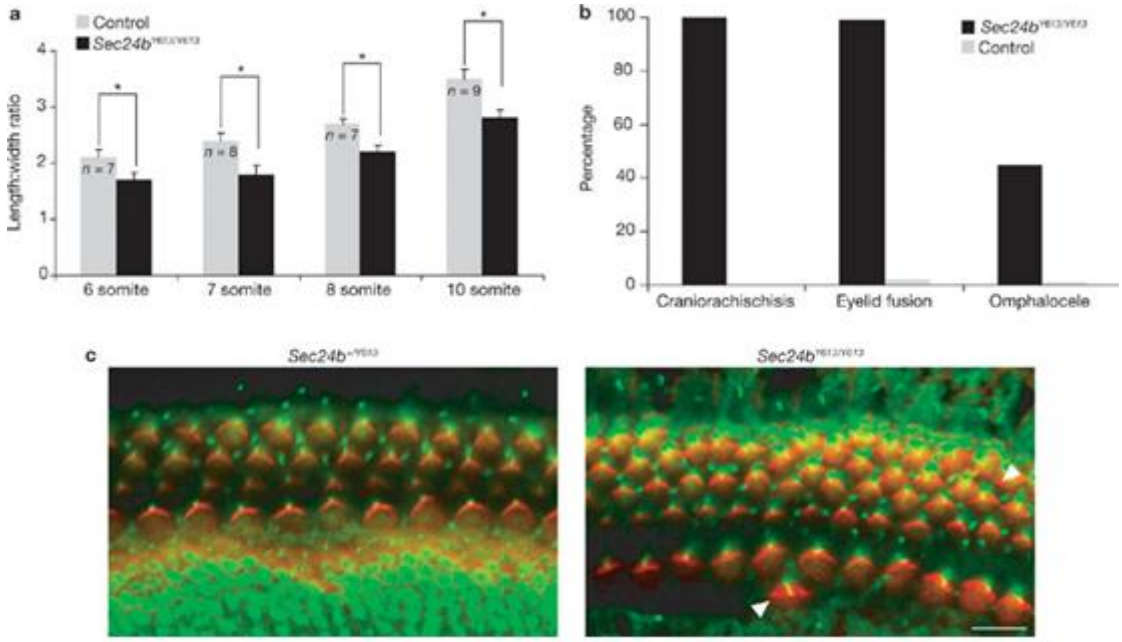

(A) *Sec24b* $^{Y613/Y613}$ mutants have deficits in convergent extension compared to *Sec24b* $^{+/Y613}$ and *Sec24b* $^{+/+}$ controls as assessed by the length:width ratio measured in 6-, 7-, 8-, and 10-somite staged E8.5 mutants. Mutants and controls from E8.5 litters were isolated and then binned based on somite number. The length and width of each embryo was then quantified, the length:width ratio calculated, the embryos were then genotyped and the length:width ratio compared between mutants and controls. n=7, 8, 7, 9 mutants and n=20, 18, 24, 28 controls at the 6-, 7-, 8-, and 10-somite stages, respectively (ANOVA, followed by Student Newman-Keuls, post hoc analysis *=p<0.01). (B) Frequency of craniorachischisis, eyelid fusion, and omphalocele observed in *Sec24b* $^{Y613/Y613}$ (n=38) mutants compared to littermate controls (n=166). (C) Wholemount immunohistochemistry using acetylated-tubulin (green) and phalloidin (red) staining of E18.5 cochlea from *Sec24b* $^{Y613/Y613}$ mutants (n=10) and *Sec24b* $^{+/Y613}$ (n=10) controls. Arrowheads point to cells that have fallen out of phase.

Sec24b$^{Y613/Y613}$ embryos. In nearly all of these mutants (99%, n=38), the upper and lower eyelids failed to fuse. In contrast, eyelid fusion failure was observed in only 2% (n=166) of littermate controls (Figure 3.2B).

Defects in the orientation of sensory hair cells of the cochlea and the vestibular system are also frequently observed in mice lacking core PCP components[22]. Using immunological techniques to label the cilia of hair cells within these tissues, we examined the orientation of hair cells of the cochlea and vestibular system. In the cochlea, *Sec24b*$^{Y613/Y613}$ embryos exhibited deficits in the orientation of both the outer and inner hair cells. In addition, the alignment of both the outer and inner hair cells of the cochlea was abnormal in *Sec24b*$^{Y613/Y613}$ embryos with hair cells periodically falling out of phase from the row (Figure 3.2C). This defect was present across the entire organ of Corti. However, no differences between the *Sec24b*$^{Y613/Y613}$ mutants and littermate controls with respect to the orientation of hair cells in the vestibular system were observed. In addition, we examined the orientation of hair follicles of the back skin in *Sec24b*$^{Y613/Y613}$ embryos and their littermate controls. Hair follicle orientation of the mutants at this stage appeared relatively normal (data not shown). Therefore, in addition to craniorachischisis, *Sec24b*$^{Y613/Y613}$ mutants share most of the phenotypic characteristics of mice harboring mutations within components of the core PCP-signaling complex indicating that Sec24b might function by interacting with a component of the PCP pathway.

The role of Sec24b in the formation of COPII vesicles destined to transit between the ER and Golgi and the PCP-signaling dependent phenotypes found in *Sec24b*$^{Y613/Y613}$ mutants indicate that Sec24b Y613 might fail to properly sort and traffic a known member of the core PCP complex. Of the mouse mutants displaying craniorachischisis, five alleles code for proteins that are trafficked through the secretory pathway: Vangl2, Celsr1, Ptk7, Fzd6, and Fzd3. Of these genes, *Vangl2* is the only dosage sensitive allele. Loss-of-function *Vangl2* (*Vangl2*^{LP}) heterozygotes have partial deficits with respect to neural tube closure that result in the looped-tail phenotype[23]. Moreover, the *Vangl2*^{LP} allele genetically interacts with other members of the PCP signaling complex[9, 10, 24].

Given the functional centrality of Vangl2 in PCP signaling as well as the dosage sensitivity of *Vangl2*^{LP} mice[23], we tested for a genetic interaction between *Sec24b* and *Vangl2* by crossing *Vangl2*$^{+/LP}$ mice with *Sec24b*$^{+/Y613}$ mice to create *Vangl2*$^{+/LP}$ *; Sec24b*$^{+/Y613}$ embryos. In litters collected between E13.5 and E18.5, approximately 5% (n=40) of the *Vangl2*$^{+/LP}$ *; Sec24b*$^{+/+}$ embryos had a caudal neural tube closure defect. In striking contrast, 68% (n=18) of *Vangl2*$^{+/LP}$*; Sec24b*$^{+/Y613}$ embryos exhibited spina bifida. No littermates of other genotypes displayed this defect (Figure 3.3). In addition, between late embryogenesis and four weeks of age, over 50% of the *Vangl2*$^{+/LP}$ *; Sec24b*$^{+/Y613}$ mice died. The strong genetic interaction between *Sec24b* and *Vangl2* suggests that Sec24b might directly regulate the trafficking and cell surface expression of Vangl2 during development.

Many transmembrane proteins are likely sorted into COPII vesicles via cargo binding sites common among all Sec24 proteins[19]. However, the conservation of four

Figure 3.3 – *Sec24b* and *Vangl2* genetically interact

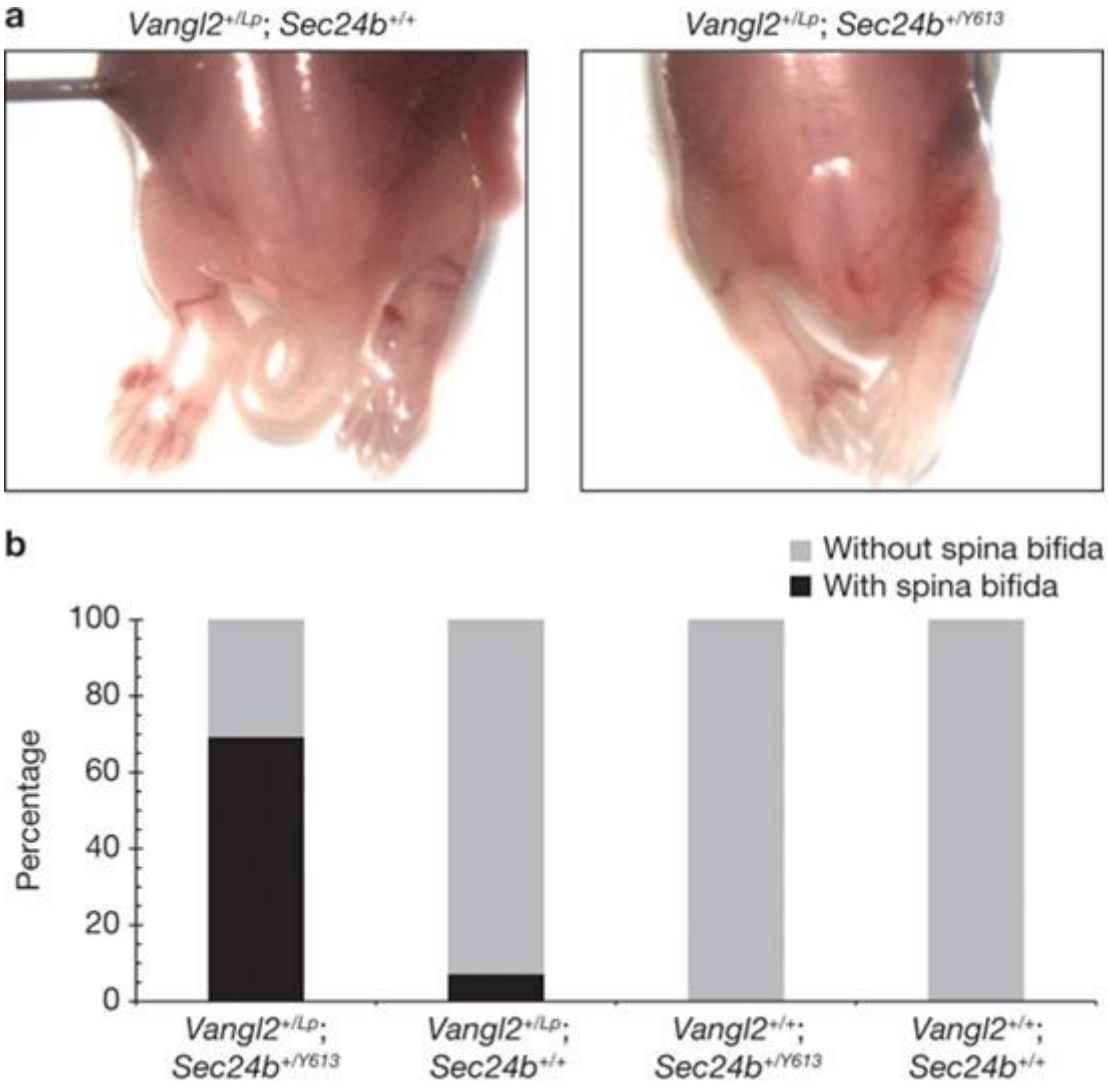

(A) Posterior half of dorsal side up E16.5 embryos: *Vangl2*$^{+/LP}$*; Sec24b*$^{+/+}$ embryo (n=40) with proper neural tube closure and *Vangl2*$^{+/LP}$*; Sec24b*$^{+/Y613}$ transheterozygous embryo (n=18) with a posterior neural tube closure phenotype resembling spina bifida. (B) Quantification of the spina bifida phenotype penetrance in *Vangl2*$^{+/LP}$*; Sec24b*$^{+/Y613}$, *Vangl2*$^{+/LP}$*; Sec24b*$^{+/+}$, *Vangl2*$^{+/+}$*; Sec24b*$^{+/Y613}$, *and Vangl2*$^{+/+}$*; Sec24b*$^{+/+}$ embryos.

distinct vertebrate paralogs suggests that each Sec24 may have evolved the ability to transport specific and essential cargos. To establish a direct measure of the ER export of Vangl2 and to assess the role of Sec24b in the trafficking of Vangl2, we used an *in vitro* vesicle budding reaction[25]. Using this assay, Vangl2-containing vesicles were formed in a COPII-dependent manner. More importantly, reactions supplemented with recombinant Sec24b, but not with the other Sec24 paralogs, substantially increased the amount of Vangl2 packaged into COPII vesicles. In contrast, another known COPII cargo protein Amyloid Precursor Protein (APP), which is packaged and transported in a COPII dependent manner, showed no specificity for any of the Sec24 paralogs (Figure 3.4A). Thus, Vangl2 is preferentially sorted by Sec24b during COPII vesicle formation from the ER.

Two semi-dominant, loss-of-function alleles of Vangl2 have been mapped and isolated using classical genetics: *Vangl2*^{LP} (S464N)[10] and *Vangl2*$^{Lp\text{-}m1Jus}$ (D255E)[3]. Heterozygotes of both alleles exhibit a looped-tail phenotype whereas homozygous mutants exhibit craniorachischisis. Both point mutations map to the cytosolic C-terminal domain of Vangl2 and could inhibit the ability of Vangl2 to interact with COPII or other cytosolic chaperones. Therefore, we assessed the ability of Vangl2 looptail mutant proteins to be packaged into COPII vesicles using the *in vitro* vesicle budding assay. As before, Vangl2 was packaged into vesicles in a COPII dependent manner, but strikingly, neither Vangl2 S464N nor D255E was capable of entering COPII vesicles (Figure 3.4B). This effect was especially surprising given the conservative D255E substitution found in the *Vangl2*$^{Lp\text{-}m1Jus}$ allele. Neither mutation depressed COPII budding, as other cargo proteins were still packaged normally (Figure 3.S4). Correspondingly, Vangl2 D255E and S464N co-localize with Protein Disulfide Isomerase (PDI), an ER marker, and fail to reach the plasma membrane (Figure 3.4C).

Our findings suggest that the loss-of function phenotypes observed in *Sec24b*$^{Y613/Y613}$, *Vangl2*^{LP} and *Vangl2*$^{Lp\text{-}m1Jus}$ mice result from trafficking defects in which the Vangl2 protein fails to package into COPII vesicles and exit the ER and are consistent with other studies showing a lack of Vangl2 plasma membrane localization in Vangl2^{LP} mutants[26]. To further test this idea, we used immunohistochemistry to analyze the subcellular localization of Vangl2 in the developing neural tube of both *Sec24b*$^{Y613/Y613}$ and *Vangl2*^{LP} mutant mice. As a control, the subcellular localization of Beta-catenin, a membrane bound protein not associated with the PCP pathway, was assessed in the same tissue. Vangl2 protein was mislocalized to puncta within the cytoplasm of *Sec24b*$^{Y613/Y613}$ mutants while Vangl2 co-localized with Beta-catenin at the plasma membrane in wildtype embryos (Figure 3.5). As previously reported[26], Vangl2 trafficking to the plasma membrane in *Vangl2*^{LP} mutants was aberrant (Figure 3.5). In contrast, Fzd3, like Beta-Catenin, was associated with the plasma membrane in *Sec24b*$^{Y613/Y613}$ and *Vangl2*^{LP} mutant neural tube sections (Figure 3.S5). These results are consistent with our *in vitro* findings showing that Vangl2 is selectively sorted by Sec24b during COPII vesicle formation. Most fundamentally, these data indicate that Sec24b is essential for proper membrane localization of Vangl2 *in vivo*.

Figure 3.4 – Sec24b strongly enhances the ER export of Vangl2 but not Vangl2 looptail mutants

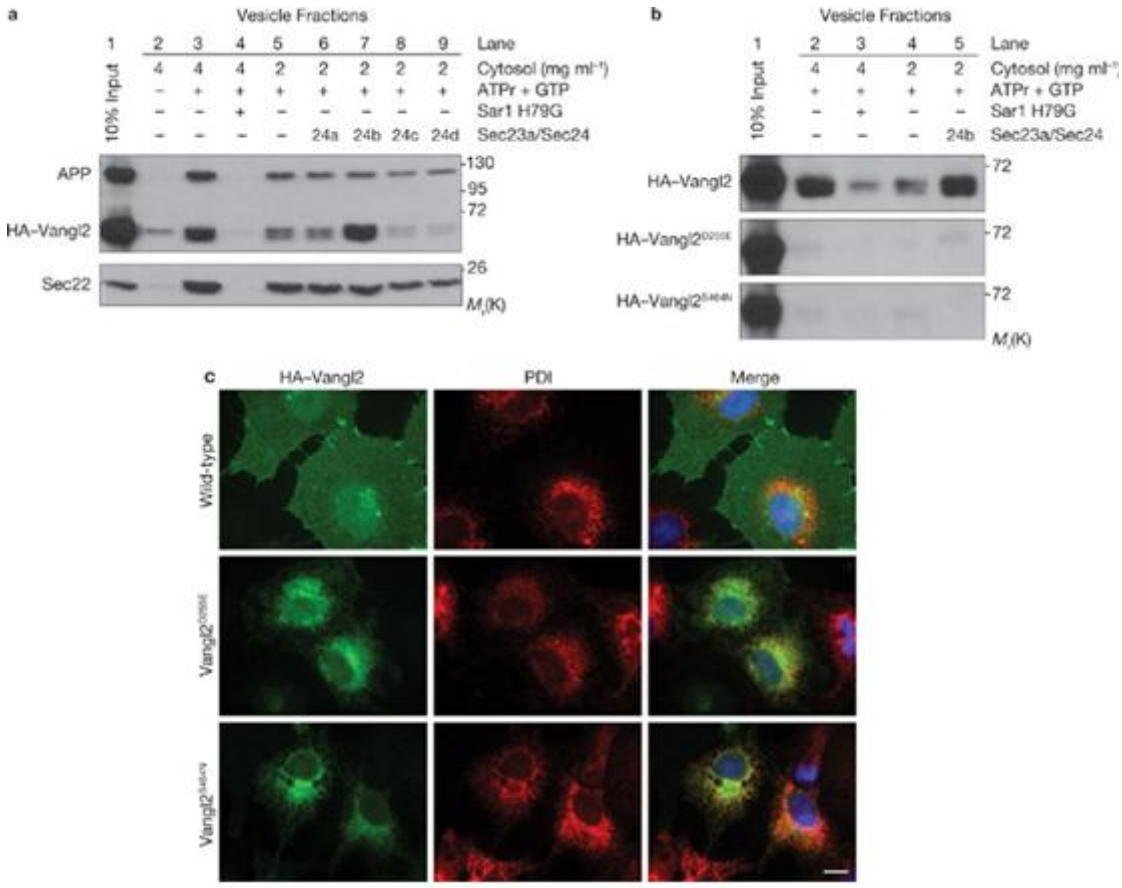

(A) *In vitro* formation of COPII vesicles containing Vangl2. Donor (10% input, lane 1) membranes were incubated with rat liver cytosol. Strong productive budding of HA-Vangl2, APP, and Sec22 cargo proteins was detected at a cytosol concentration of 4mg/ml (lane 3) and reduced at 2mg/ml (lane 5). Excluding ATPr +GTP (lane 2) or addition of the dominant negative inhibitor of COPII budding, Sar1 H79G (lane 4), inhibited all three cargos from entering the vesicle fraction. Supplementing the lower concentration of cytosol with 10nM recombinant Sec23a/Sec24b (lane 7) strongly increased the degree to which HA-Vangl2 entered the COPII vesicles, but did not significantly affect the budding of APP or Sec22. Addition of the other recombinant Sec23a/Sec24 paralog combinations at the same 10nM concentration did not enhance the ability of HA-Vangl2 to enter vesicles (lanes 6, 8, and 9). (B) The ability of wildtype HA-Vangl2 to be packaged into COPII vesicles was compared to that of both Vangl2 mutant proteins, D255E and S464N. Wildtype Vangl2 entered the vesicle fraction in a COPII dependent manner and budding was enhanced by recombinant Sec23a/Sec24b (lanes 2-5). However, the single point mutations D255E or S464N completely blocked Vangl2 from entering COPII vesicles and leaving the ER. Positive control cargo proteins were packaged normally into COPII vesicles (Supplemental

(Figure 3.4 cont.)

Figure 4) (C) Immunofluorescence staining of anti-HA (green) and anti-PDI (red) in COS7 cells. Transiently transfected wildtype HA-Vangl2 (WT) reached the cell surface, while both Vangl2 mutants D255E and S464N remain in the ER where they co-localize with the PDI ER marker. PDI=Protein Disulfide Isomerase, APP=Amyloid Precursor Protein, ATPr=ATP regenerating system. Images are representative of at least three independent experiments.

Figure 3.5 – *Sec24b*$^{Y613/Y613}$ embryos show aberrant subcellular localization of Vangl2 in the developing spinal cord *in vivo*

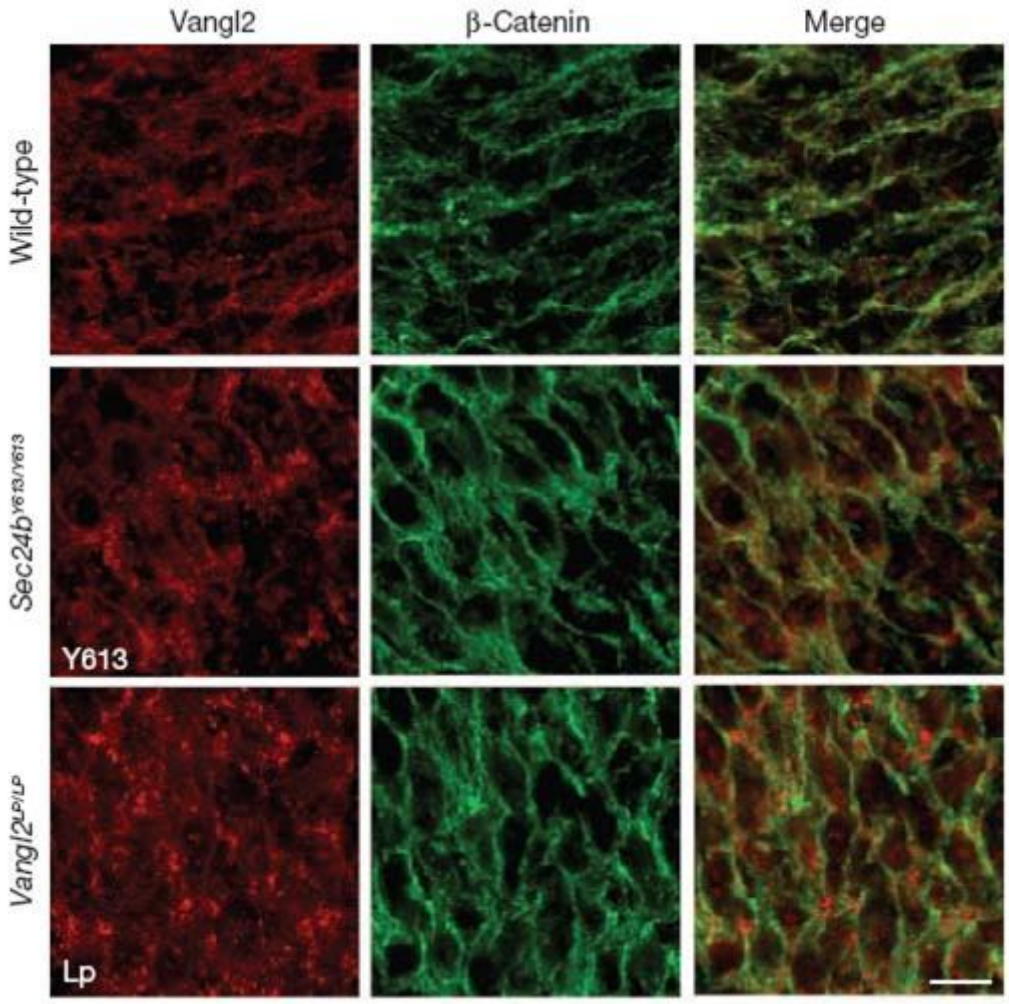

Immunofluorescence staining shows co-localization of Vangl2 (red) and membrane bound Beta-Catenin (green) in the developing spinal cord of wildtype embryos. In contrast, developing spinal neuroepithelium of both Sec24$^{Y613/Y613}$ and *Vangl*$^{LP/LP}$ mutant embryos showed decreasedVangl2 membrane localization and increased intracellular puncta, while Beta-Catenin retained its membrane localization. Images are representative of three independent experiments.

Here, we have identified Sec24b as a critical regulator of planar cell polarity signaling. In addition to the severe craniorachischisis phenotype, *Sec24b*^{Y613} mutants have several other phenotypic abnormalities common to mouse mutants in components of the core PCP complex. Sec24b regulates cell surface expression of the dosage-dependent, core PCP protein Vangl2 by preferentially sorting this cargo into COPII vesicles. Additionally, Vangl2 looptail mutations prevent Vangl2 from being packaged into COPII vesicles and exiting the ER. Thus, it is likely that insufficient Vangl2 is brought to the cell surface during neurulation in *Sec24b* or *Vangl2* mutants. This

mislocalization of Vangl2 disrupts the entire PCP signaling cascade, resulting in a neural tube closure deficit similar to that observed in null alleles of other components of the core PCP complex. It is noteworthy that mice that are heterozygous for both *Sec24b*^{Y613} and *Vangl2*^{LP} have a propensity to develop spina bifida. Given that most human genetic diseases are not recessive but rather arise from the interactions of multiple loci, human mutations in *Sec24b* are likely to contribute to spina bifida.

Our analysis of Sec24b Y613 identifies a novel mechanism of protein regulation during development. Sec24b is one of four paralogs that function in the trafficking of secretory proteins between the ER and Golgi. Thus, loss of Sec24b function would be predicted to lead to deficits in the cell surface expression of some transmembrane proteins. *Sec24b* mutants, though clearly developmentally abnormal for neural tube closure, are relatively spared with respect to many other developmental processes. Vangl2 may be one of a small set of COPII cargo proteins whose expression is strictly dependent on Sec24b. Nonetheless, our findings indicate that cargo specificity has evolved between the four Sec24 paralogs with Sec24b being specifically required for trafficking of a core PCP component, Vangl2, and the establishment of planar cell polarity, convergent extension and neural tube closure.

Figure 3.S1 – Schematic diagram of the recessive screen for novel alleles affecting neural development

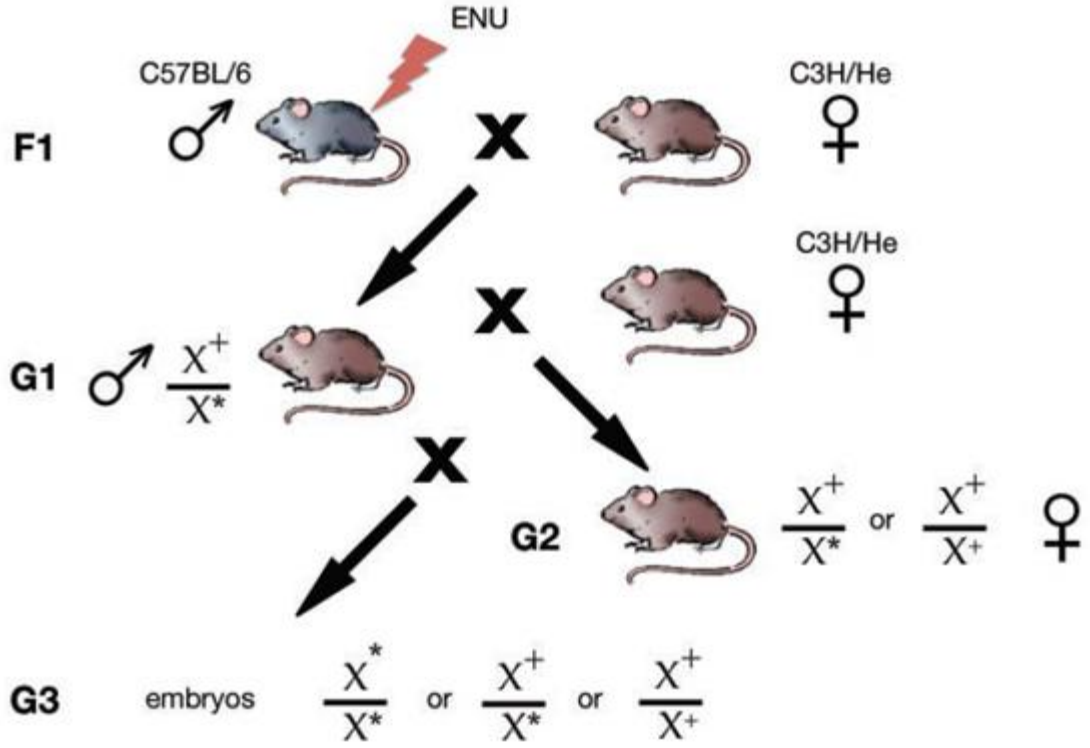

C57BL/6 male mice (8-10 weeks old) were injected with 3X100mg/kg body weight N-ethylnitrosourea (ENU). F1 males that regained fertility were mated to C3H/He females to produce G1 male mice (lines). Each of these G1 males was in turn mated to C3H/He females to produce G2 daughters, some of which are presumed heterozygous for a given mutation. After crossing the G2 females to their G1 fathers, recessive mutations were produced and scored for developmental anomalies.

Figure 3.S2 – Line 811 represents an allelic group with craniorachischisis

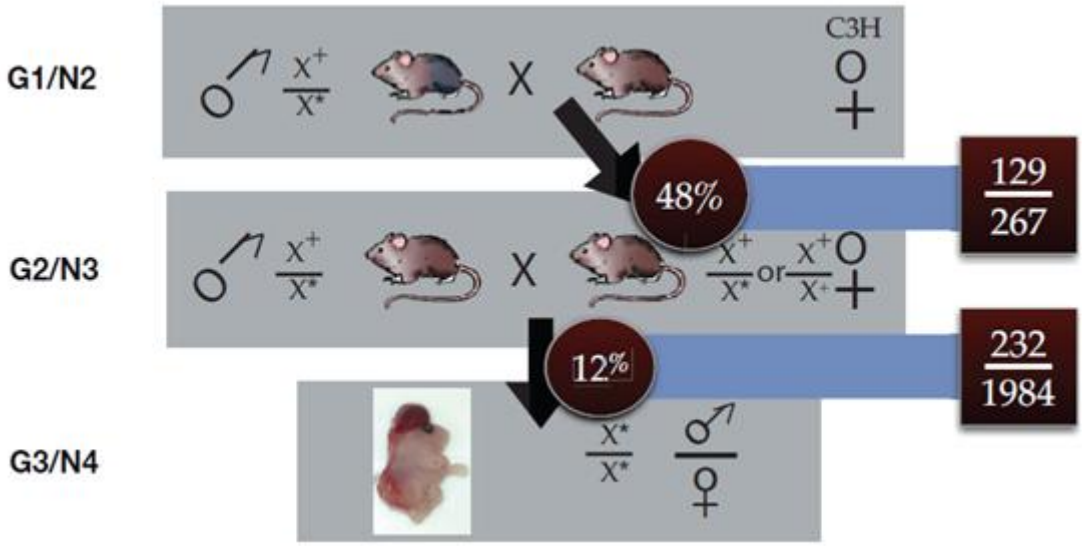

Evidence suggesting that the 811 phenotype is caused by a recessive Medelian mutation. Shown are the frequencies at which transmission of the allele between heterozygotes and of the mutation in presumed heterozygote intercrosses were observed.

Figure 3.S3 – The Sec24b Y613 mutation abrogates interaction with Sec23 and thereby eliminates its localization to sites of productive COPII activity

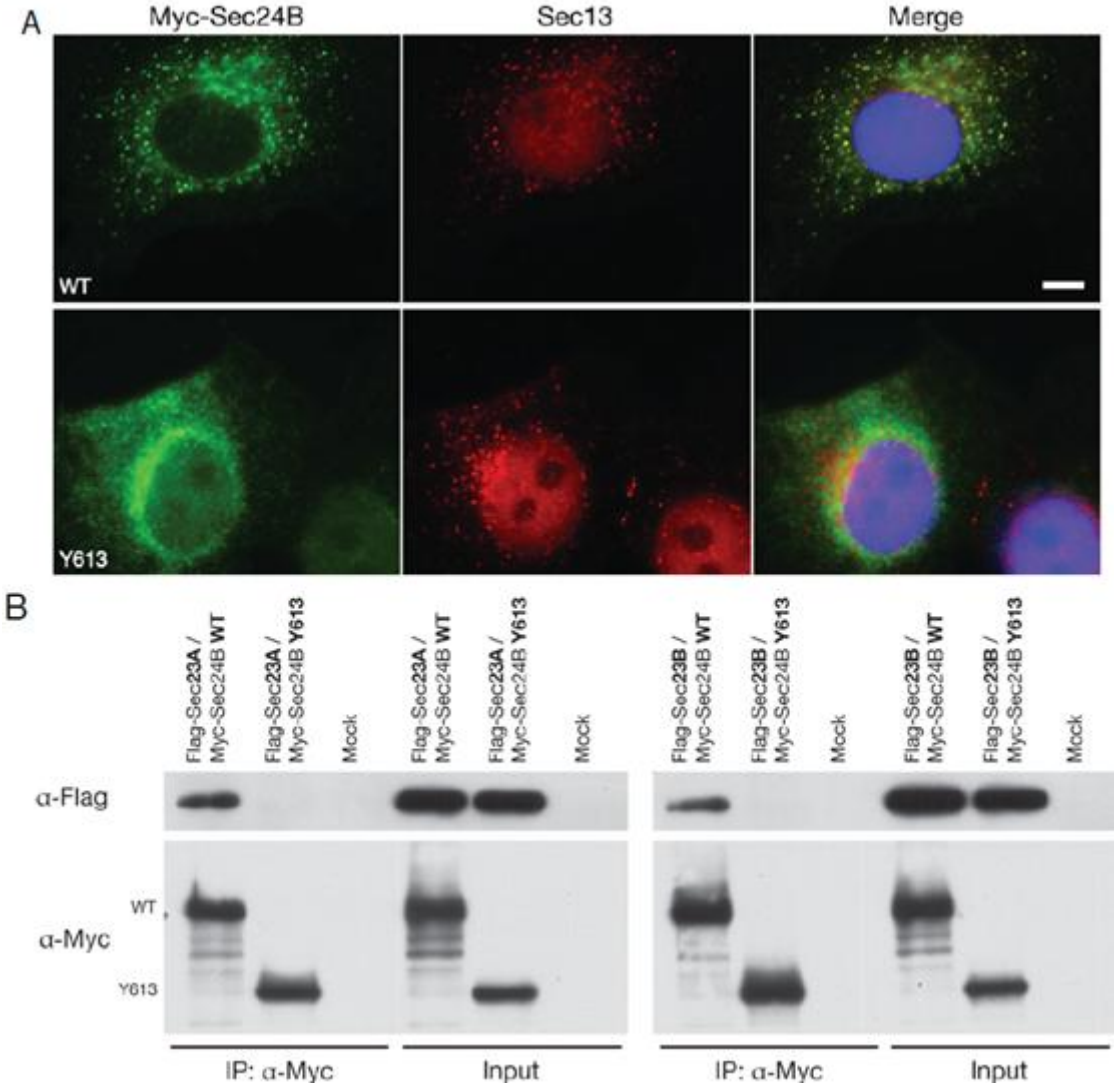

(A) Immunofluorescence staining of anti-Myc (green) and anti-Sec13 (red) in COS7 cells. Transiently transfected Myc-Sec24b was found highly co-localized with the endogenous COPII protein Sec13 at ER exit site punctae. Mutant Sec24b Y613 did not co-localize with Sec13 and was not found concentrated at ER exit site punctae. (B) Immunoprecipatation of transiently transfected Flag-Sec23a and Flag-Sec23b with Myc-Sec24b vs. Sec24b Y613 in COS7 cells. Both Flag-Sec23a and Flag-Sec23b coimmunoprecipatated with Myc-Sec24b WT (lane 1 of each image) but did not co-immunoprecipatate with Myc-Sec24b Y613 (lane 2 of each image). Scale bar in panel (A) is 10μM.

Figure 3.S4 – Positive control COPII cargo proteins enter COPII vesicles in the presence of mutant HA-Vangl2

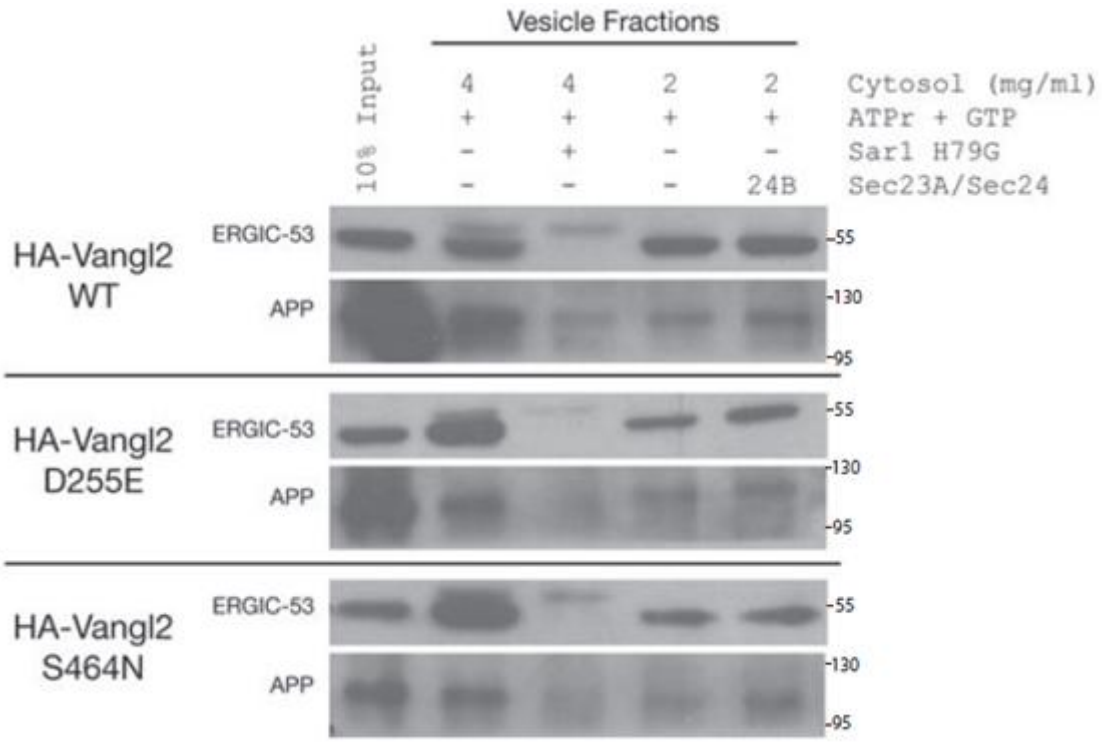

(**A**) *In vitro* formation of COPII vesicles, as described in Figure 4B. Positive control endogenous cargo proteins ERGIC-53 and APP entered COPII vesicles normally in the presence of the HA-Vangl2 D255E and S464N mutants indicating that the mutations did not cause a general depression in all COPII vesicle formation. Both ERGIC-53 and APP are inhibited as expected by the dominant negative Sar1 H79G. Neither one showed enhanced vesicle budding in the presence of recombinant Sec23a/Sec24b. APP=Amyloid Precursor Protein.

Figure 3.S5 – Fzd3 retains membrane localization in the developing spinal cord of *Sec24bY613/Y613* and *VanglLP/LP* mutants *in vivo*

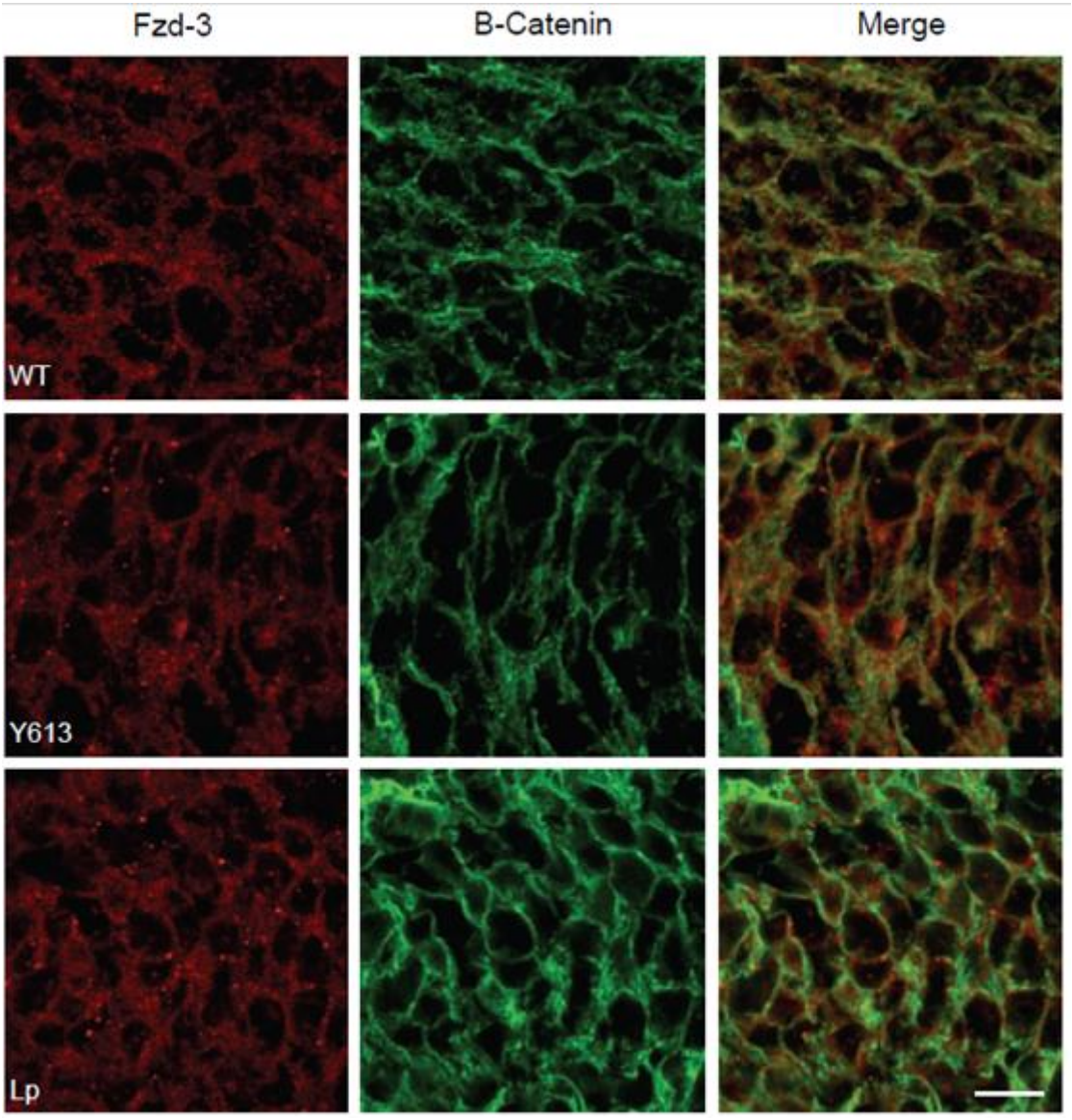

Immunofluorescence staining shows co-localization of Fzd3 (red) and Beta-Catenin (green) in the developing spinal cord of wildtype, Sec24*Y613/Y613* mutants and *VanglLP/LP* mutants. All three genotypes show similar Fzd3 and Beta-Catenin membrane localization. Images are representative of two independent experiments. Scale bar is 10μM.

Materials and Methods

Mutagenesis. C57BL/6 (BL6) mice were injected with ENU as described [27-29]. Briefly, BL6 male mice were injected with 3X100mg/kg body weight ENU to induce random mutations throughout the genome. Using a three-generation forward-genetic screen, we outbred and isolated the mutations in C3H/He mice to facilitate mapping by polymorphism. Resulting G1 fathers were mated to their G2 daughters and embryos were screened for developmental anomalies (Figure 3.S1).

Mapping. The genetic lesion responsible for craniorachischisis in line 811 was mapped via backcross (Figure 3.S3) using standard linkage analysis with a panel of PCR polymorphisms between C57BL/6 (BL6) and C3H/He C3H) mice to the distal end of chromosome 3. Analyses at several other polymorphisms placed 811 within a 3.7Mb region between D3MIT319 and D3MIT254. We analyzed the D3MIT319 recombinants (10/527) at rs13477397, rs4231957, and rs13477402 and found recombination at rs13477397 (9/531) but not at rs4231957 or rs13477402. Likewise, we analyzed the recombinants at D3MIT254 (3/509) at rs13477404 and rs13477406 as well as rs4231957 and rs13477402 and identified a single recombination event that spanned D3MIT254 through rs13477404. Thus, 811 was determined to be in the 1.8 Mb region between rs13477397 and rs1347704 (although significantly closer to rs1347704) containing 17 open reading frames. Of these 17 predicted genes, 3 had mouse models that did not exhibit craniorachischisis and could be eliminated. We sequenced the exons containing 5'UTR and coding sequence for all of the 14 remaining loci (*ENSMUSG00000074236, Elov6, ENSMUSG00000080139, ENSMUSG00000068627, Rrh, Nola1, Cfi, Pla2g12a, 9030408N13Rik (Ccdc109b), Sec24b, Rpl12, Col25a1, ENSMUSG00000065788*) using DNA isolated from two mutants and one BL6 control mouse. Several of these genes were sequenced by the Harvard University Partners Genomics Facility.

Genotyping. S*ec24b*^{Y613} creates a restriction enzyme-sensitive polymorphism. This line is genotyped by amplification of an approximately 200 bp fragment with TCAAACACCATCGTGAGGTGCC and ACCCGAAACTCACCATCAATAACT, followed by subsequent digestion with MseI.

Convergent extension. Mutants and controls from E8.5 litters were isolated and then binned based on somite number. The length and width of each embryo was then quantified, the length:width ratio calculated, the embryos were then genotyped and the length:width ratio compared between mutants and controls by ANOVA followed by Student Newman-Keuls post hoc. n=7, 8, 7, 9 mutants at the 6-, 7-, 8-, and 10-somite stages, respectively.

Immunohistochemisty. E18.5 mouse cochlea staining was performed as described[5]. Staining of E10.5 spinal cords was performed as described with minor modifications[26]**.** Embryos were fixed in 2% paraformaldehyde, washed twice in PBS, embedded in OCT and frozen. 10µM sections were collected on slides and antigen retrieval was performed by incubating the slides in Sodium Citrate Buffer (10 mM Sodium Citrate, 0.05% Tween-20, pH 6.0) for 30 minutes at 95° C. Slides were washed three times in PBS and incubated overnight at 4°C with PBS containing anti-Vangl2 (1:150), anti-B-Catenin (1:250), and/or anti-Fzd-3 (1:50), 10% normal goat serum and 0.4% Triton-X100. The following day, slides were washed and incubated with the appropriate fluorescent secondary antibodies (1:400) for 4 hours at room temperature.

In Vitro COPII vesicle budding assay. Procedure for making cell free mRNA, semi-intact cells, and subsequent *in vitro* translation was preformed as described[25,30] with some modifications. The vesicle formation reaction and vesicle purification procedure was essentially as described[31], with some modifications. In detail, COS7 cells grown in 3x100mM plates were washed in PBS, removed from plates with trypsin, and washed again in PBS containing 10µg/ml soybean trypsin inhibitor. Then, cells were permeablized with 40µg/ml digitonin for 5 minutes in ice-cold KHM buffer (110 mM KOAc, 20 mM Hepes, pH 7.2, and 2 mM $Mg(OAC)_2$) and washed and resuspended in 100µl KHM. Endogenous RNA was degraded after addition of 1mM $CaCl_2$ and 10µg/ml micrococcal nuclease and incubation at room temperature for 12 minutes. After incubation, the nuclease reaction was stopped by addition of 4mM EGTA, and cells were pelleted and washed. Semi-intact RNA-free cells were resuspended in KHM buffer such that the measurement of absorbance (600 nm) for 5µl of cells in 500µl KHM was 0.08. These cells were added to an *in vitro* translation reaction with rabbit reticulocyte lysate (Promega, Flexi®) and RNA encoding HA-Vangl2, which was incubated for 60 minutes at 30°C. Then, these donor membranes were washed to remove non-translocated protein products and resuspended in KHM.

To form vesicles, donor membranes with newly synthesized HA-Vangl2 were combined where indicated with rat liver cytosol, ATP regenerating system (40 mM creatine phosphate, 0.2 mg/ml creatine phosphokinase, and 1 mM ATP), 0.2 mM GTP and/or recombinant COPII proteins, followed by incubation at 30°C for 1 hour. Newly formed vesicles were separated from the more rapidly sedimenting donor membranes by centrifugation at 13000*xg* for 12 minutes. Vesicles were collected by centrifugation at 115000*xg* for 25 minutes. Vesicle pellets were resuspended and washed in 100µl cold KHM, centrifuged again, and finally solubilized in 16 µl of Buffer C (10 mM Tris-HCl (pH 7.6), 100 mM NaCl, 1% Triton X-100 plus protease inhibitor mixture) and Laemmli sample buffer. Vesicle fractions and original donor membranes were resolved on SDS-PAGE, transferred onto PVDF membranes, and subjected to immunoblot to detect HA-Vangl2 and the positive control endogenous cargo proteins, Amyloid Precursor Protein, ERGIC-53 and Sec22.

Antibodies. Anti-Sec13 antiserum was raised in rabbits injected with a purified recombinant His-tagged human full length Sec13 produced in baculovirus-infected SF9 cells. Anti-Sec22 antiserum was raised in rabbits injected with the peptide (CG)-HSEFDEQHGKKVPTVSRPYSFIEFDT (residues 91-116) conjugated to rabbit serum albumin. Anti-HA was purchased from Covance (16B12). Anti-Myc was purchased from Cell Signaling Technologies (2276). Anti-Flag and Anti-Amyloid Precursor Protein were purchased from Sigma (F3165 and A8717, respectively). Monoclonal anti-Protein Disulfide Isomerase was a gift from S. Fuller (EMBL-Heidelberg). Anti-ERGIC-53/LMAN-1/p58 antiserum was generated as described[32]. Anti-Vangl2 was a gift from P. Gros and anti-Fzd-3 was a gift from J. Nathans. Anti-Beta-Catenin was purchased from Cell Signaling Technologies (2677). Anti-mouse and Anti-rabbit HRP conjugates were purchased from GE Healthcare UK (NXA931 and NA934V, respectively). Anti-mouse FITC conjugate and Anti-rabbit TRITC conjugate were both purchased from Jackson ImmunoResearch (715-095-151 and 711-025-152, respectively).

Immunofluorescence. COS7 cells grown on coverslips were transiently transfected with plasmids encoding 3xHA-Vangl2 WT, Lp255, or Lp464 or 6xMyc-Sec24b WT or Y613 using Lipofectamine 2000 and the manufacturer's recommended protocol. Twenty hours later, cells were processed by immunofluorescence. All subsequent steps were at room temperature and all washing steps used 3 changes of 2ml PBS. Cells on coverslips were fixed in 2.5% paraformaldehyde for 15 minutes and washed. Next, they were permeablized in 0.1% Trition X-100 in PBS for 1 minute and washed. The cells were then blocked with 1% BSA in PBS for 30 minutes. Next, cells on coverslips were incubated with the indicated primary antibodies diluted in 1% BSA for 1 hour and washed. Then, they were incubated in secondary anti-rabbit or anti-mouse fluorescent conjugates diluted in 1% BSA for 1 hour and washed. Finally, coverslips were briefly incubated in 1ug/ml DAPI and were mounted on glass slides in mowiol mounting medium. Cells were imaged using a Zeiss AxioObserver Z1 fluorescent microscope and images were captured and merged with Metamorph software from Molecular Devices.

Immunoprecipatations. COS7 cells grown in wells of a 6-well plate were transiently transfected with 6xMyc-Sec24b WT or Y613, and with Flag-Sec23a or Flag-Sec23b, using Lipofectamine 2000 and the manufacturer's recommended protocol. Twenty-four hours later, cells were washed 2 times in PBS. Then, cells were solubilized in 200µl of RIPA buffer (1% Triton X-100, 1% sodium deoxycholate, 0.1% SDS, 0.15 M NaCl, 0.01 M Na_2PO_4, protease inhibitor mixture, pH 7.2). Cell lysates were cleared by centrifugation at 15000*xg* for 10 minutes and the supernatant was transferred to a new tube. A 20µl sample of input lysate was reserved in a separate tube and mixed with Buffer C and Laemmli sample buffer. Primary anti-Myc antibody was added to a concentration of 1:300 and rotated at 4°C for 3 hours. Then, 40µl of 50% slurry washed

Protein A-sepharose beads was added and the lysate was again rotated at 4°C for 2 hours. Beads were pelleted at 2000*xg* and washed 4 times in RIPA buffer. The beads were resuspended in 80 µl of Buffer C and 2x Laemmli sample buffer. Finally, samples were resolved on SDS-PAGE, transferred onto PVDF membranes, and subjected to immunoblot to detect Myc-Sec24b and Flag-Sec23.

Recombinant protein purification. Recombinant human Sar1 H79G was overexpressed in E. Coli and purified as previously described[31]. Human Flag-Sec23a/His-Sec24a, Flag-Sec23a/His-Sec24b, Flag-Sec23a/His-Sec24c, and Flag-Sec23a/His-Sec24d were expressed in SF9 cells using a baculovirus system and purified as previously described[31].

Materials. Rabbit muscle creatine phosphokinase, creatine phosphate, ATP, GTP and protease inhibitor mixture tablets were purchased from Roche Applied Science. Protein A-sepharose was purchased from BioVision. Rat liver cytosol was prepared as previously described[31]. Trypsin 0.05% with EDTA was purchased from Invitrogen. Soybean trypsin inhibitor was purchased from Fluka Biochemika. Micrococcal nuclease from Staphylococcus aureus was purchased from USB-Affymetrix, dissolved in 50mM glycine, 5mM $CaCl_2$ pH 9.2 and stored in 1mg/ml aliquots. Digitonin was purchased from Sigma and dissolved in DMSO at 40mg/ml.

Plasmids. 3xHA-Vangl2 Lp255 and Lp464 were created using site-directed mutagenesis on the pCS2 3xHA-Vangl2 WT plasmid according to the QuikChange protocol from Stratagene, using respective primers: 5'-GTCGTGCGATCCACAGAAGGGGCCAGC-3' + 5'-GCTGGCCCCTTCTGTGGATCGCACGAC-3' or 5'-AAACAGTGGACCTTGGTGAACGAGGAGCCG-3' + 5'-CGGCTCCTCGTTCACCAAGGTCCACTGTTT-3'. Flag-Sec23a and Flag-Sec23b mammalian expression vectors were created by amplifying the tagged ORF from separate baculovirus plasmids, pFastBac-Flag-Sec23a and pFastBac-Flag–Sec23b (9), using primers: 5'-GCGCGGATCCATGGACTACAA-3' (both forward) and 5'-TCTCGGCGCGCCTCAAGCAGCACTGGACACAGC-3' or 5'-TCTCGGCGCGCCTTAACAGGCACTGGAGACAGCC-3' (reverse, respectively). Then, the tagged ORFs were inserted into BamHI and AscI restriction sites of the mammalian expression plasmid pCS2.

References

1. Kibar, Z., Capra, V. & Gros, P. Toward understanding the genetic basis of neural tube defects. Clin Genet 71, 295-310 (2007).

2. De Marco, P., Merello, E., Mascelli, S. & Capra, V. Current perspectives on the genetic causes of neural tube defects. Neurogenetics 7, 201-221 (2006).

3. Kibar, Z. Identification of a New Chemically Induced Allele (Lpm1Jus) at the Loop-Tail Locus: Morphology, Histology, and Genetic Mapping. Genomics 72, 331-337 (2001).

4. Montcouquiol, M. et al. Identification of Vangl2 and Scrb1 as planar polarity genes in mammals. Nature 423, 173-177 (2003).

5. Wang, Y., N., G. & Nathans, J. The Role of Frizzled3 and Frizzled6 in Neural Tube Closure and in the Planar Polarity of Inner-Ear Sensory Hair Cells. J Neurosci 26, 2147-2156 (2006).

6. Curtin, J.A. et al. Mutation of Celsr1 disrupts planar polarity of inner ear hair cells and causes severe neural tube defects in the mouse. Curr Biol 13, 1129-1133 (2003).

7. Hamblet, N. et al. Dishevelled 2 is essential for cardiac outflow tract development, somite segmentation and neural tube closure. Development 129, 5827-5838 (2002).

8. Etheridge, S.L. et al. Murine dishevelled 3 functions in redundant pathways with dishevelled 1 and 2 in normal cardiac outflow tract, cochlea, and neural tube development. PLoS Genet 4, e1000259 (2008).

9. Lu, X. et al. PTK7/CCK-4 is a novel regulator of planar cell polarity in vertebrates. Nature 430, 93-98 (2004).

10. Murdoch, J. et al. Circletail, a New Mouse Mutant with Severe Neural Tube Defects: Chromosomal Localization and Interaction with the Loop-Tail Mutation. Genomics 78, 55-63 (2001).

11. Murdoch, J. et al. Disruption of scribble (Scrb1) causes severe neural tube defects in the circletail mouse. Human Molecular Genetics 12, 87-98 (2003).

12. Ybot-Gonzalez, P. et al. Convergent extension, planar-cell-polarity signalling and initiation of mouse neural tube closure. Development 134, 789-799 (2007).

13. Mlodzik, M. Planar cell polarization: do the same mechanisms regulate Drosophila tissue polarity and vertebrate gastrulation? Trends Genet 18, 564-571 (2002).

14. Wallingford, J., Fraser, S.E. & Harland, R.M. Convergent extension: the molecular control of polarized cell movement during embryonic development. Developmental Cell 2, 695-706 (2002).

15. Kasarskis, A., Manova, K. & Anderson, K.V. A phenotype-based screen for embryonic lethal mutations in the mouse. Proc Natl Acad Sci U S A 95, 7485-7490 (1998).

16. Wendeler, M., Paccaud, J. & Hauri, H. Role of Sec24 isoforms in selective export of membrane proteins from the endoplasmic reticulum. EMBO Rep 8, 258-264 (2007).

17. Shimoni, Y. et al. Lst1p and Sec24p cooperate in sorting of the plasma membrane ATPase into COPII vesicles in Saccharomyces cerevisiae. J Cell Biol 151, 973-984 (2000).

18. Miller, E., Antonny, B., Hamamoto, S. & Schekman, R. Cargo selection into COPII vesicles is driven by the Sec24p subunit. EMBO J 21, 6105-6113 (2002).

19. Miller, E.A. et al. Multiple cargo binding sites on the COPII subunit Sec24p ensure capture of diverse membrane proteins into transport vesicles. Cell 114, 497-509 (2003).

20. Bi, X., Corpina, R.A. & Goldberg, J. Structure of the Sec23/24-Sar1 pre-budding complex of the COPII vesicle coat. Nature 419, 271-277 (2002).

21. Wallingford, J. & Harland, R. Neural tube closure requires Dishevelled-dependent convergent extension of the midline. Development 129, 5815-5825 (2002).

22. Jones, C. & Chen, P. in Bioessays, Vol. 29 120-132 (2007).

23. Copp, A.J., Checiu, I. & Henson, J.N. Developmental basis of severe neural tube defects in the loop-tail (Lp) mutant mouse: use of microsatellite DNA markers to identify embryonic genotype. Dev Biol 165, 20-29 (1994).

24. Qian, D. et al. Wnt5a functions in planar cell polarity regulation in mice. Dev Biol 306, 121-133 (2007).

25. Kim, J. et al. Biogenesis of gamma-secretase early in the secretory pathway. J Cell Biol 179, 951-963 (2007).

26. Torban, E. et al. in Gene Expression Patterns, Vol. 7 346-354 (2007).

27. Justice, M. et al. in Mamm Genome, Vol. 11 484-4882000).

28. Justice, M.J., Noveroske, J.K., Weber, J.S., Zheng, B. & Bradley, A. in Human Molecular Genetics, Vol. 8 1955-19631999).

29. Weber, J.S., Salinger, A. & Justice, M.J. in Genesis, Vol. 26 230-2332000).

30. R. Wilson et al., Biochem. J. 307, 679 (1995).

31. J. Kim, S. Hamamoto, M. Ravazzola, L. Orci, and R. Schekman, J. Biol. Chem. 280, 7758 (2005).

32. J.C. Fromme et al., Dev. Cell 13, 623 (2007).

Chapter Four:

A Molecular and Functional Analysis of Vangl2

Introduction

Vang- Like 2 (Vangl2) is a mammalian homolog of a protein originally discovered in *Drosphila melanogaster* called Strabismus/Van Gogh. Strabismus was noted and named for its effect on the proper formation and orientation of the *Drosphila* eye (Wolff and Rubin, 1998). In addition to the eye, at the time of its discovery, it was also seen to play a role in the orientation of other cells, including the legs and the hair bristles in many locations on the fly exterior. Although, in this original paper it was observed that there were mouse and human homologs of strabismus, the broad role of Strabismus/Vangl for establishing tissue polarity in many animals was not fully appreciated until two independent groups identified mutations in the Vangl2 gene as the causative defect in mice with the looptail phenotype (Kibar *et al.*, 2001; Murdoch *et al.*, 2001).

The mouse looptail phenotype, originally described over 60 years ago, is one in which mice heterozygous for the mutation are phenotypically normal except for a looped tail, while mice homozygous for the mutation develop a severe neural tube disorder called craniorachischisis (Strong and Hollander, 1949). As previously discussed, these neural tube defects are indicative of problems in a process called convergent extension. Convergent extension requires cells able to establish planar cell polarity (Reviewed Wallingford *et al.*, 2002). This inability to establish cell polarity links the defects seen in the Strabismus mutated flies with the looptail mice, showing that some aspects of establishing cell polarity have been conserved and function through the activity of the Strabismus/Vangl2 homologs.

The original looptail mutation was identified as a missense mutation, which changes a serine at position 464 to asparagine (Hereafter Vangl2 S464N or Lp464) (Kibar *et al.*, 2001). In a separate paper, the lab of Phillipe Gros also created a chemically induced allele in the same gene, presenting the same mouse phenotype. This new allele was found to be a separate missense mutation, one in which the aspartic acid at position 255 was changed into a glutamic acid. (Hereafter Vangl2 D255E or Lp255) (Kibar *et al.*, 2001).

Mouse and human Vangl2 are 521 amino acid long integral membrane proteins with 4 predicted trans-membrane segments oriented such that both the amino- and carboxyl- termini face the cytoplasm, comprising the bulk of the protein, with only small loops oriented to the luminal/extracellular side of the membrane (Figure 4.1A). Both looptail mutations map to the cytosolic carboxyl-terminus, representing regions of the protein that could potentially interact with transport coat complexes or other cytosolic proteins.

Vangl2 is very well conserved, showing high sequence identity even when compared with the *Drosphila* homolog, Strabismus (Figure 4.1B). There is a paralog of Vangl2 called Vangl1 found in both mice and humans. Much of the conserved sequence found among Vangl2 homologs is also conserved in Vangl1, suggesting that they may share the same function. Indeed, Vangl1 mutations have been observed in several human patients with neural tube defects (Kibar *et al.*, 2007; Kibar *et al.*, 2009).

Figure 4.1 – Vangl2 membrane topology, looptail mutations and sequence conservation

A

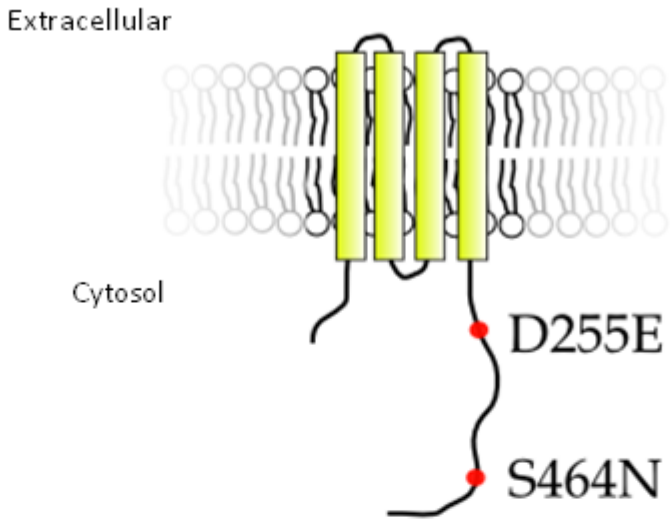

B

% Identity	*Homo Sapiens*	*Mus Musculus*	*Danio Rerio*	*Drosophila Melanogaster*
Homo Sapiens	-	99%	77%	48%
Mus Musculus	99%	-	78%	48%
Danio Rerio	77%	78%	-	48%
Drosophila Melanogaster	48%	48%	48%	-

(A) Model of the predicted topology of Vangl2 showing the approximate locations of the looptail point mutations, D255E and S464N.

(B) Percent identity matrix for Vangl2/Strabismus proteins among 4 species: *Homo sapiens, Mus musculus, Danio rerio, and Drosophila melanogaster*

Additionally, in zebrafish, ectopic expression of Vangl1 was able to partially suppress developmental defects seen in Vangl2 mutant embryos (Jessen and Solnica-Krezel, 2003).

Despite the discovery of the looptail mouse and the causative gene, no one had characterized the defects found in the Vangl2 protein containing either the Lp255 or Lp464 mutation at the cellular level. After I had established that the looptail mutations prevent Vangl2 from exiting the ER (published as described in the preceding chapter), I set out to further characterize the regions of the Vangl2 protein that contain these looptail mutations, and also to determine why these separate mutations led to ER retention. I have considered several alternative explanations for the failure of the looptail mutant Vangl2 to exit the ER and have tested a few possibilities. Along with the looptail regions, I have examined other regions of the protein that may be involved in ER export.

Results

Point mutation analysis of the cytoplasmic carboxyl-terminus of Vangl2

The cytoplasmic carboxyl-terminus of Vangl2 extends from the fourth and last transmembrane domain, and is 283 amino acids long. Despite many regions of strong conservation, this carboxyl-terminus does not belong to any known protein family and has just 1 small protein motif, a small PDZ binding motif (ETxV) comprising the last 4 amino acids at the extreme carboxyl-terminus. PDZ binding motifs are known to bind to PDZ domains, a common domain found in 436 human proteins, but the identity of a potential binding partner for Vangl2 is unknown (Kay and Kehoe, 2004). In addition, a carboxyl-terminal valine residue as found on Vangl2 has been described as a sufficient ER export motif, but to my knowledge it has only been tested on shorter cytoplasmic domains (~10-40aa) (Nufer *et al.*, 2002). Since the carboxyl-terminal valine and PDZ binding motif is highly conserved among Vangl1 and Vangl2, I wanted to determine if it had a role in the ER export of Vangl2.

To test the role of the extreme carboxyl-terminus on the ability of Vangl2 to exit the ER, I used scanning mutagenesis, making a series of point mutations among the conserved resides found there. In all, I mutated each amino acid from 514-521 and then tested each mutant Vangl2 protein in the ability to reach the cell surface (Figure 4.2). Each amino acid was mutated to alanine except for residue 521, which was mutated to glycine. A valine to glycine mutation had already been found in a similar extreme carboxyl-terminal context, to lead a long delay in ER export of a protein called proTGF-alpha (Fernández-Larrea *et al.*, 1999). The mutations were made in the plasmid pCS2 3xHA-mouse Vangl2 and were introduced using the Stratagene QuikChange© site-directed mutagenesis protocol. Then, as a first test for Vangl2 transport, each mutant 3xHA-Vangl2 was transfected into Cos7 cells and processed for immunofluorescence with an antibody against the HA tag. Looking at the cells for the presence of Vangl2

Figure 4.2 – List of all the Vangl2 mutants produced in this study, and their relative effects on Vangl2 ER export

	Vangl2 Construct	Surface staining by immunofluroescence	Packaging in COPII Budding Reaction
	Vangl2 WT	++++	++++
Looptail 255 region	V251A	+++	nt
	R252A	-	-
	S253A	+++	nt
	T254A	++++	nt
	Looptail D255E	-	-
	D255A	-	-
	G256R	-	nt
	G256V	-	-
	G256N	++++	nt
	S258A	++++	nt
	R259A	++++	nt
	F260A	++	nt
	Y261A	-	-
Looptail 464 region	K458A	+++	nt
	Q459A	++++	nt
	W460A	-	-
	T461A	++	++
	L462A	-	-
	V463A	++++	+++
	Looptail S464N	-	-
	S464A	++	++
	E465A	++++	nt
	E465A+E466A	++++	nt
	P467A	++++	nt
	V468A	+++	nt
	T469A	++++	nt
Carboxyl-terminus	R514A	++/-	nt
	L515A	++/-	nt
	Q516A	++++	nt
	S517A	++++	nt
	E518A	+++	nt
	T519A	++++	nt
	S520A	++++	nt
	V521G	+	-

Surface immunofluorescence and *in vitro* COPII vesicle budding are estimated using a scale relative to wild type level of surface staining or COPII packaging equal to (++++) and down to looptail level of surface staining or COPII packaging (-). Nt – not tested.

fluorescence on the cell surface allowed me to quickly determine if Vangl2 transport was affected.

Immunofluorescence images showed that many of the single point mutant Vangl2 proteins traffic normally and reached the cell surface, including Q516A, S517A, T519A, and S520A (Figure 4.3). Other point mutations affected trafficking to various degrees, including R514A, L515A, E518A, and V521G. The mutations at positions 514 and 515 are odd in that the cells had very heterogeneous staining – some showed clear indication of surface Vangl2, while other cells on the same coverslip showed strong ER "reticular" staining. This could be due to different clonal populations of cells within the Cos7 cells that are somehow more or less competent for transporting Vangl2. The mutation at position 518 looked intermediate between wild type and the strong ER retention of the looptail mutations. This could be interesting because this glutamic acid is part of the predicted PDZ binding motif. The V521G mutation showed a more consistent defect in trafficking. In cells expressing this construct, there was a little surface Vangl2 evident, but in most cells a large portion of the Vangl2 is delayed or stuck in the ER (Figure 4.3).

To confirm the aberrant ER export of the Vangl2 V521G mutant, I set up budding reactions in a manner similar to the Vangl2 looptail budding reactions performed in the preceding chapter. This involved synthesis of mRNA from the Vangl2 V521G mutant plasmid, and *in vitro* translation and translocation of the newly formed protein into permeabilized cultured cells. COPII budding reactions showed the trafficking defect of Vangl2 V521G. Compared to wild type Vangl2, V521G was poorly packaged into COPII vesicles (Figure 4.4A). In each test of this mutant Vangl2, other positive control proteins known to be active COPII cargos were packaged normally (Figure 4.4B).

Point mutation analysis of the looptail regions of Vangl2

The looptail mutations are single point mutations more than 200 amino acids apart but they cause the same mouse phenotype, and they show the same defect in Vangl2 trafficking (Kibar *et al.*, 2001; Merte *et al.*, 2010). The conservative looptail 255 mutation, where a glutamic acid is substituted for an aspartic acid (D255E), is surprisingly restrictive. This mutation preserves the negative charge of the amino acid but adds an additional carbon atom in the side chain. Such a conservative mutation is often tolerated in other contexts. I set out to determine if there were other amino acid residues nearby the looptail mutations which when mutated would also lead to the same trafficking defect in Vangl2. A cluster of close by amino acids could define a binding site for another protein, or have structural implications for the folding of Vangl2.

In order to characterize the looptail regions, I again employed scanning mutagenesis, making point mutations upstream and downstream of both of the original looptail mutations. In most cases I made alanine point mutants, but in some cases I wanted to see the affect of more bulky residues. I mutated each amino acid from

Figure 4.3 – Immunofluorescence of carboxyl-terminal Vangl2 point mutants demonstrates some transport defects

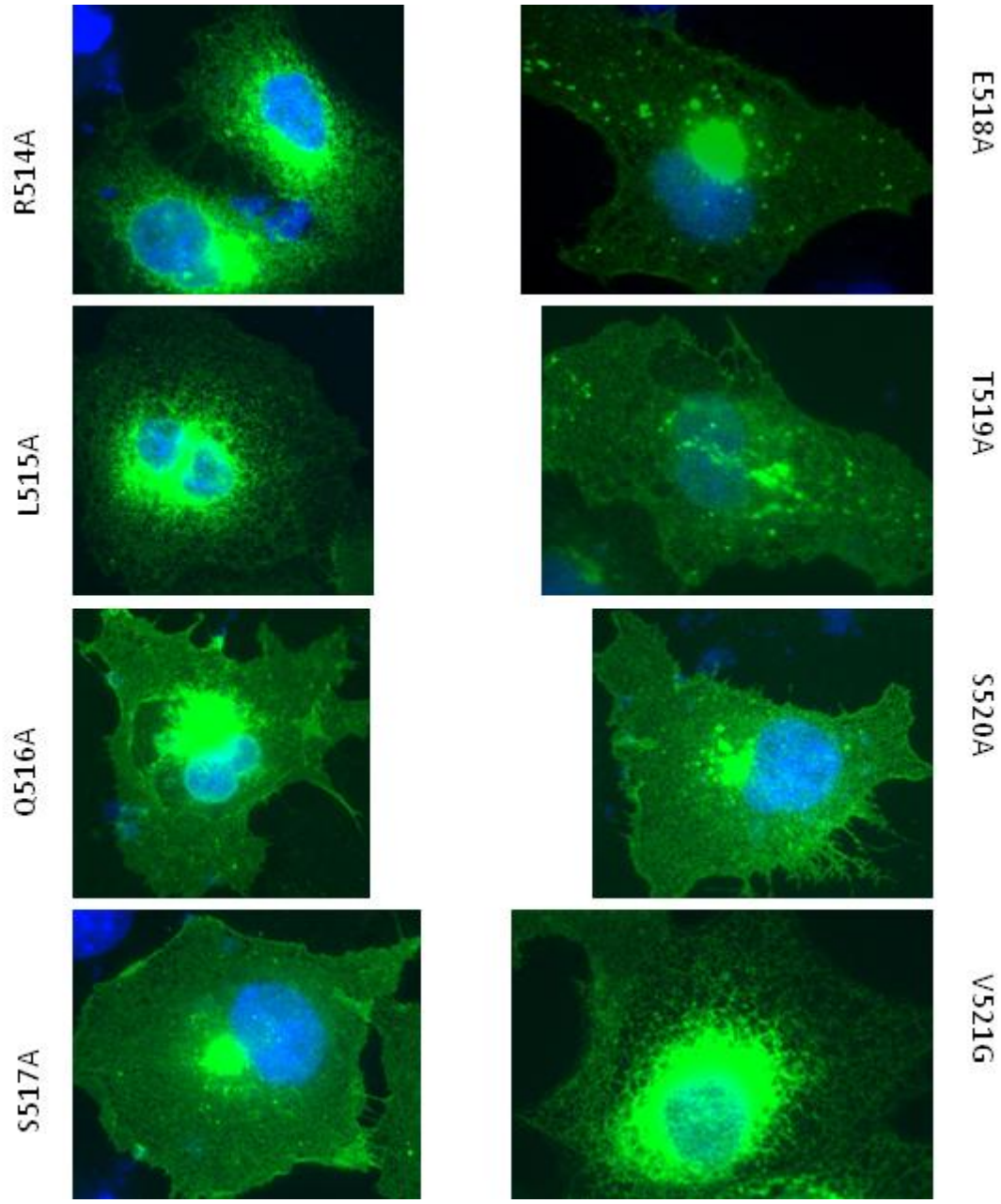

Immunofluorescence images of each carboxyl-terminal point mutation. HA-tagged Vangl2 plasmid (4µg) was transfected into COS7 cells. Twenty four hours later, the cells were fixed in paraformaldehyde and processed for immunofluorescence. Mutants at position 514, 515, 518, and 521 showed various levels of altered trafficking.

Figure 4.4 – *In vitro* COPII budding reaction confirms the aberrant trafficking of the Vangl2 mutant V521G

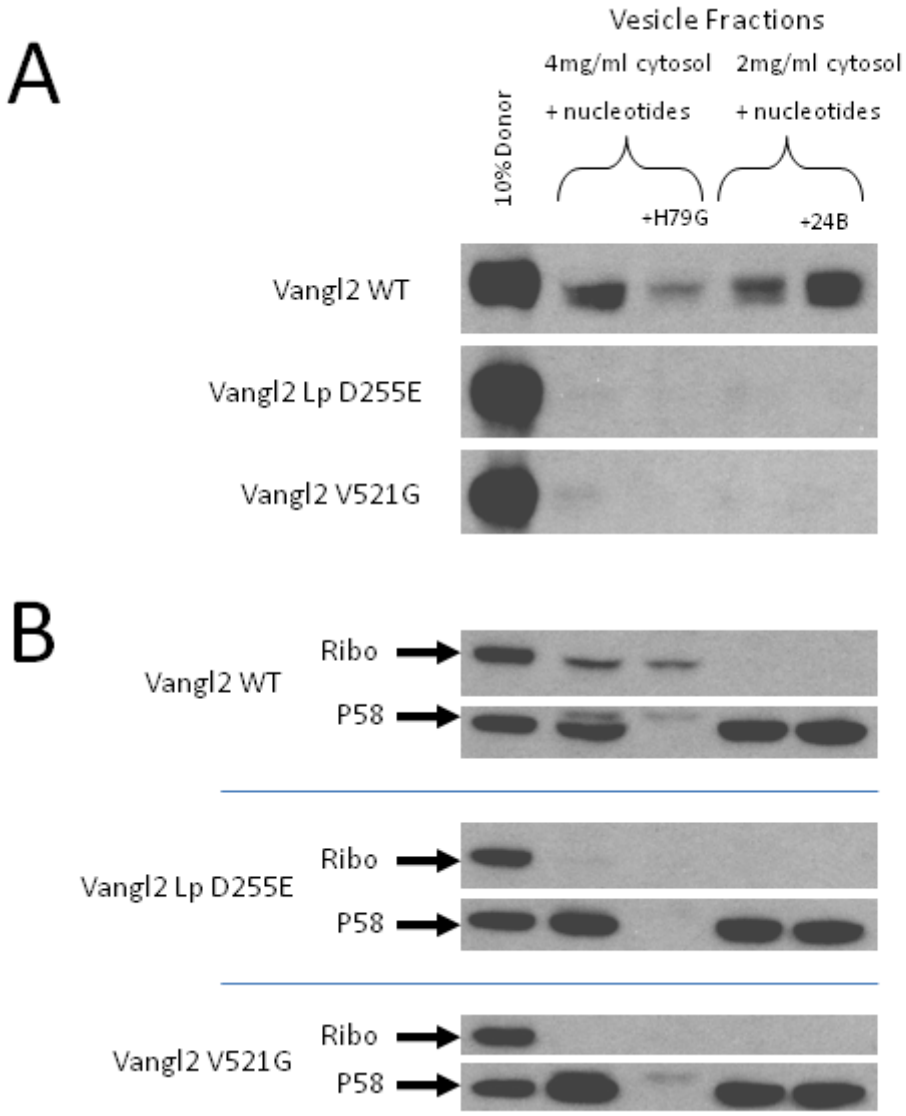

(A) *In vitro* COPII budding reaction to compare the packaging of Vangl2 wild type, Lp D255E, and V521G. Vangl2 wild type was incorporated into COPII vesicles, but Vangl2 mutant V521G was not packaged.

(B) Positive and negative control proteins from the same reactions as in (A). Known COPII cargo, P58 was readily packaged, while ER resident Ribophorin was not.

position 251-261 near the looptail 255 site and each amino acid from position 458-469 near the looptail 464 site (Figure 4.2). Several positions showed a looptail-like severe defect in Vangl2 localization by immunofluorescence, e.g., R252A, D255A, G256R, G256V, Y261A, W460A, and L462A (Figure 4.5). Other positions showed intermediate defects, e.g., T461A and S464A (Figure 4.6). Interestingly, some substitutions at a particular amino acid position were tolerated while others were not – for instance, G256R and G256V mutant proteins remained in the ER, but G256N was found at the cell surface.

To confirm the aberrant trafficking of these new looptail region mutants, I again utilized the *in vitro* COPII budding reaction. I tested all of the defective and intermediate mutants, along with a few of the normally trafficked mutant proteins. After creating the mutant mRNA for these mutants, I used *in vitro* translation of the RNA and translocated the newly formed protein into permeabilized cells. After separate COPII budding reactions for each mutant, along with positive and negative controls, I found that the results correlated with the immunofluorescence data (Figure 4.7). When a mutant appeared to remain in the ER as visualized by immunofluorescence, it also failed to enter into COPII vesicles in the budding reaction. Additionally, mutants that showed an intermediate localization by immunofluorescence, likewise showed an intermediate ability to enter COPII vesicles (Figure 4.6).

The substitution of residues surrounding the original looptail mutations reveal additional features required for sorting into COPII vesicles. The amino acid sequences RxxDGxxxxY and WxLxS for the looptail sites 255 and 464 respectively constitute novel signals. To my knowledge, these motifs do not correspond to any known trafficking motifs previously found in other proteins or even a motif involved in another process. There are a number of different things that these two regions could be doing that when mutated would lead to Vangl2's defective trafficking. Some possibilities for these looptail regions include:

1. They constitute a binding site for a COPII protein, perhaps specifically Sec24B.
2. They are a binding site for a different protein that acts as a chaperone or adaptor for Vangl2, enabling it to leave the ER. This protein could itself be recognized by COPII, or it may mask ER retention signals found in the Vangl2 protein.
3. They are a site of oligomerization – many proteins need to oligomerize before leaving the ER.
4. They are important for the structural folding of the cytosolic carboxyl-terminus of Vangl2. Mis-folded proteins are often retained in the ER by quality control machinery.

It seems likely that the two regions are working in concert on the same process since the phenotypes and trafficking defects mirror each other so closely. I will explore these ideas further in this chapter.

Figure 4.5 – Immunofluorescence of Vangl2 looptail region mutants with strong export defects

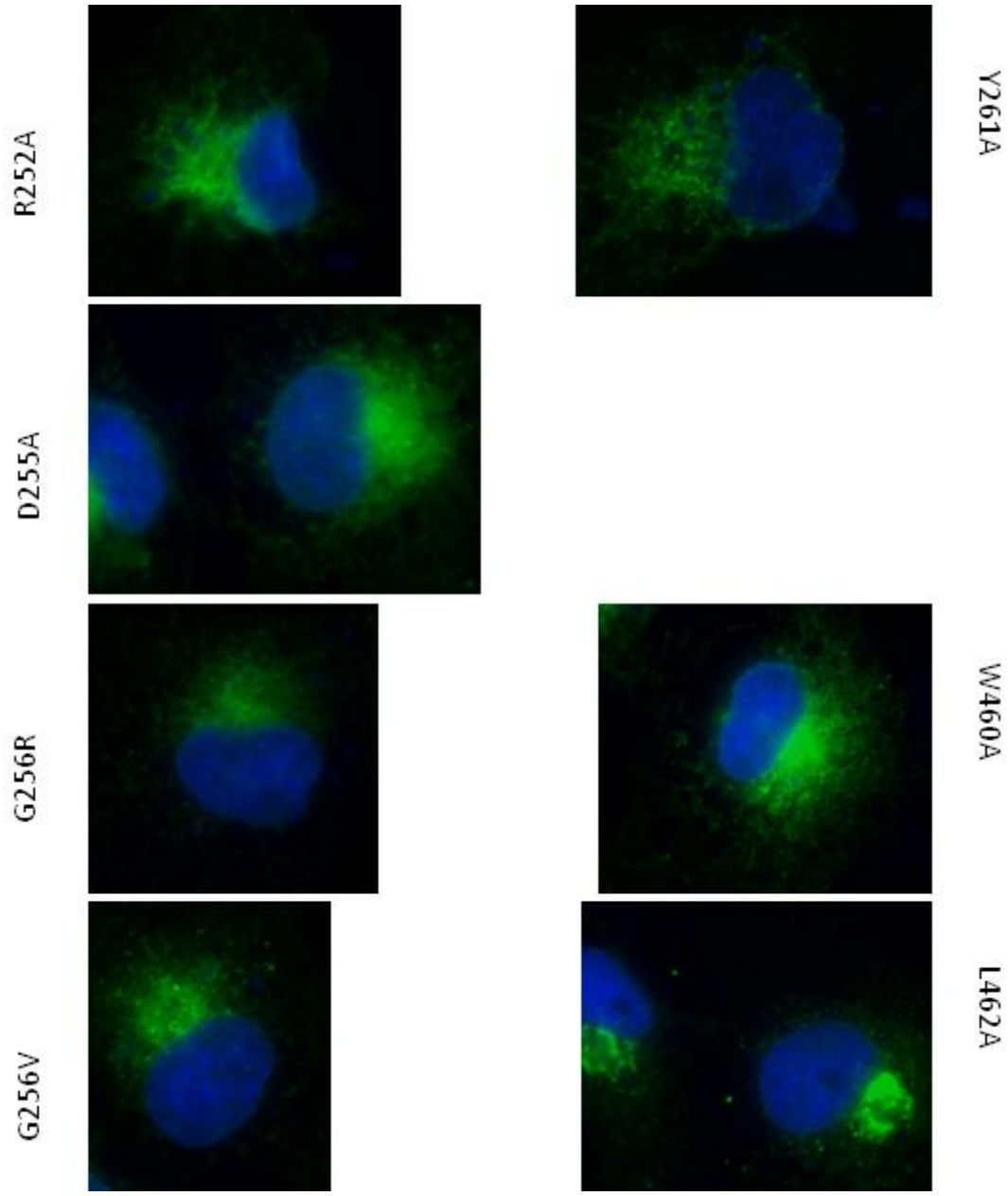

Immunofluorescence images of the Vangl2 looptail region mutants that showed strong ER retention. HA-Vangl2 plasmid (1µg) was transfected into COS7 cells for 18h. Then, the cells were fixed in paraformaldehyde and processed for immunofluorescence. In all experiments, control wild type Vangl2 was found at the cell surface (not shown).

Figure 4.6 – Intermediate defects in localization and *in vitro* COPII budding for Vangl2 mutants T461A and S464A

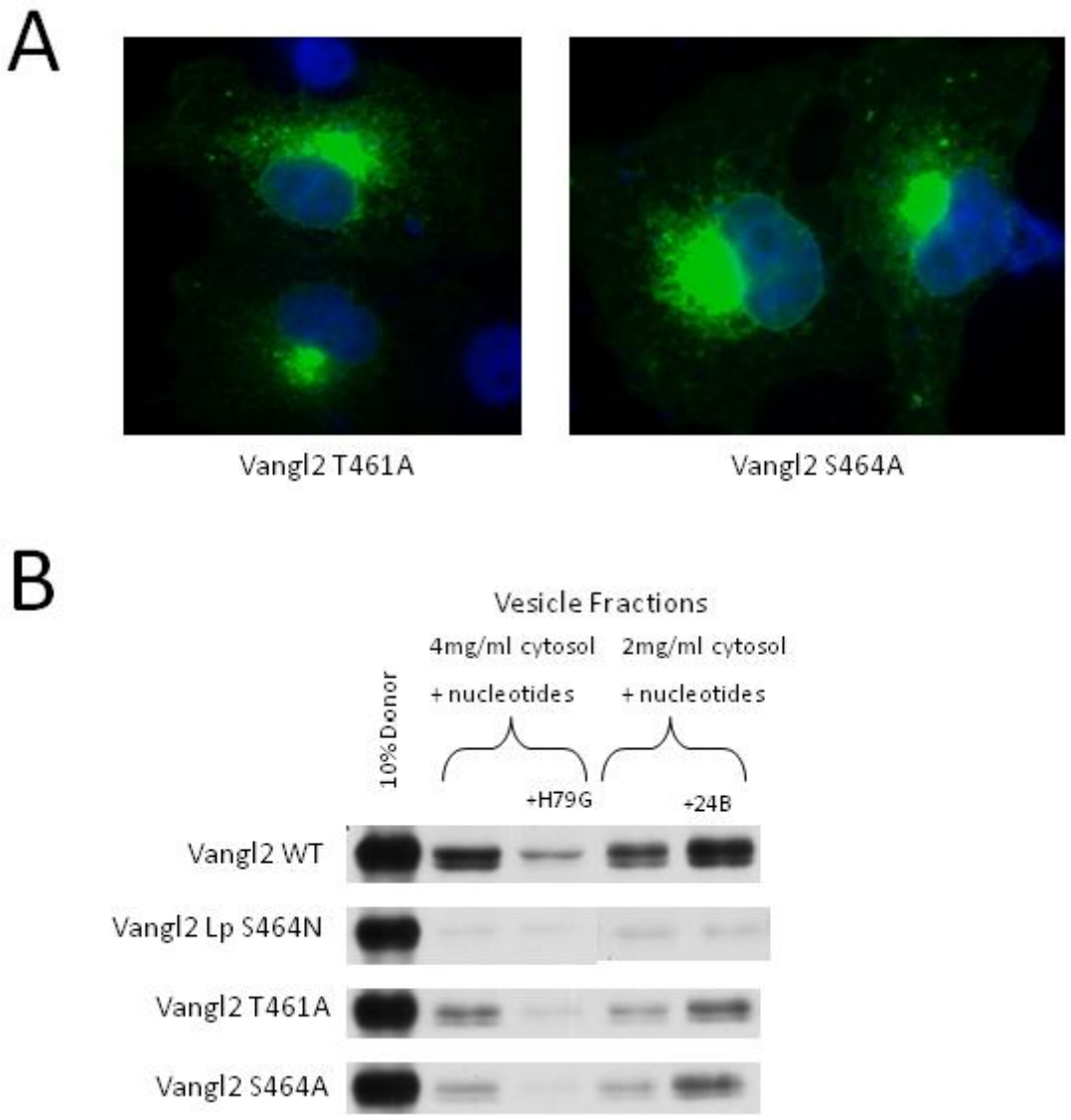

(A) Immunofluorescence images of the Vangl2 mutants T461A and S464A showed an intermediate localization. ER staining was seen, but surface staining also was evident.

(B) *In vitro* COPII budding reactions to compare the packaging of Vangl2 wild type, Lp S464N, T461A, and S464A. The Vangl2 mutants T461A and S464A were packaged into vesicles but not as efficiently at wild type Vangl2, suggesting a partial defect.

Figure 4.7 – *In vitro* COPII budding reactions confirm the trafficking defects of the looptail region mutants

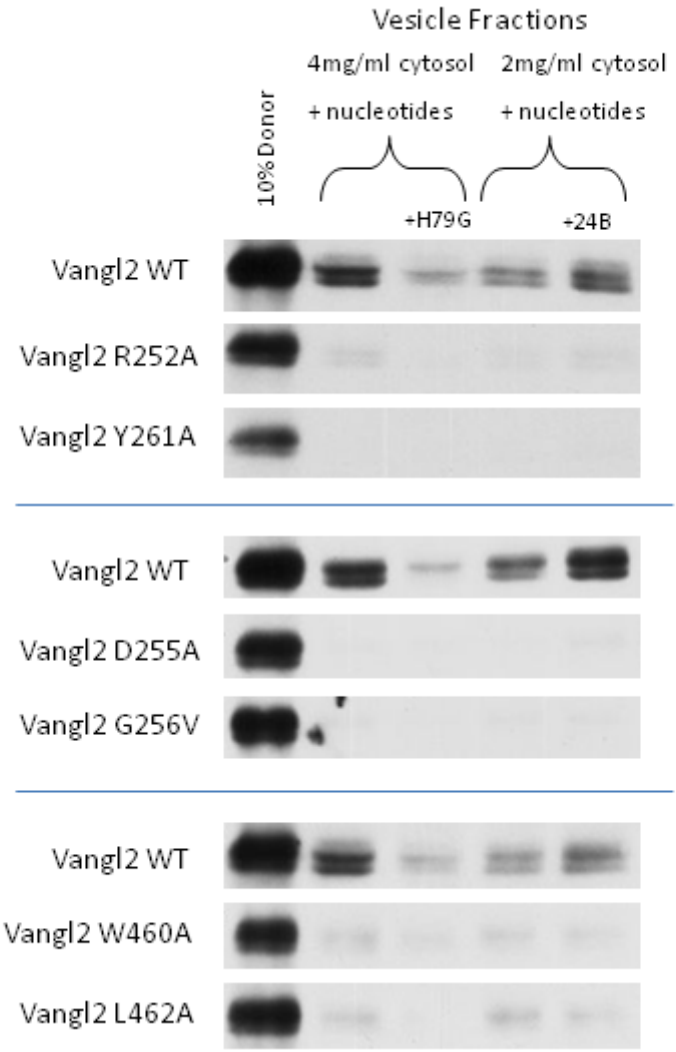

In vitro COPII budding reactions to compare the packaging of wild type Vangl2, against that of several Vangl2 looptail region mutants: R252A, Y261A, D255A, G256V, W460A, and L462A. In three experiments, each Vangl2 was separately translated and translocated into ER donor membranes, followed by a COPII budding reaction with different conditions as indicated. In all cases, positive control COPII cargo proteins from the same reaction were packaged normally (not shown).

Perhaps not surprisingly, each of the strongly defective amino acid residues are absolutely conserved among all the Vangl2 sequences tested from the *Drosophila melanogaster* homolog, Strabismus, to human Vangl2. Vangl1 also shows absolute conservation at the original looptail sites and at the new amino acid residues that contribute to transport. Cognate mutations of the original looptail residues have been shown to cause defective activity of the Vangl1 protein *in vivo* (Reynolds *et al.*, 2010). I would predict that the cognate mutations made in Vangl1 of these new residues would lead to similar trafficking defects in Vangl1 and reduced activity *in vivo*. I would also predict that mice with these new mutations in Vangl2 would show the same phenotype as the original looptail mice. Based on the strong conservation of these residues and what has been learned about the original looptail mutations in mice, it seems likely that mutations in residues important for Vangl2 transport could contribute to the pathology of neural tube disorders like spina bifidia or craniorachischisis in humans.

Attempts to detect a direct interaction between Vangl2 and Sec24B

Perhaps the simplest explanation of the trafficking defect seen in the Vangl2 looptail proteins is that they can no longer bind to machinery that selects and packages them into COPII vesicles. As was demonstrated in our paper, the COPII component Sec24B can strongly and specifically enhance the packaging of Vangl2 (Merte *et al.*, 2010). These results led me to hypothesize that Vangl2 binds directly to Sec24B and that the looptail mutations disrupt this interaction. Despite considerable effort, I have been unable to establish that such a direct interaction exists.

GST pull downs have been used in the past to show an interaction between the yeast Sec24p and cargo proteins (Springer and Schekman, 1998). Interactions between COPII proteins and cargo would probably have to be relatively weak compared to some other protein-protein interactions, since the COPII proteins must release the cargo after the vesicle has formed. This type of GST study is probably ideal for seeing a relatively weak interaction, since large amounts of protein can drive the equilibrium toward interaction. GST purification of the carboxyl-terminal cytosolic domain of Vangl2 proved to be very difficult, as nearly all of the protein was found in the pellet fraction of bacteria expressing the fusion protein. This is likely due to multiple intermolecular contacts causing large scale aggregation, since GST itself is known to dimerize, and as I demonstrate in the next section, Vangl2 itself can oligomerize. Numerous immunoprecipatations, both cell-based and cell-free, were performed without definitive results. My immunoprecipatation techniques have been successful in seeing interactions between other proteins, so I do not believe this to be a systematic problem. At this stage, it may still be possible that there is a direct interaction and that a new technique, like Tandem Affinity Purification (TAP)-tagging, would be successful in teasing it out. Additionally, I have also been working on the possibility that the interaction is not direct - that there may be an adaptor or chaperone that mediates Vangl2's interaction with Sec24B and the entry into COPII vesicles - which I will discuss later in this chapter.

Vangl2 forms oligomers, but oligomerization status of Vangl2 is not affected by the looptail mutations

One of the possible reasons that the looptail region mutations lead to Vangl2 becoming stuck in the ER is that they prevent oligomerization. A number of membrane proteins have been seen to require oligomerization before being competent to exit the ER, including ERGIC-53 (Nufer *et al.*, 2003). The formation of oligomers can mask retention motifs otherwise visible to the ER quality control machinery or it can provide a higher localized binding affinity for transport factors by nature of having several binding spots in close proximity. Shortly after embarking on a plan to determine if Vangl2 can form oligomers, I discovered evidence (tucked away in some supplemental material and not discussed in the main text) that Strabismus, the *Drosophila* homolog of Vangl2 forms oligomers (Bellaïche *et al.*, 2004).

In order to determine if Vangl2 forms oligomers like Strabismus, I expressed two differentially tagged versions of Vangl2 in cells to examine if one co-immunoprecipitated with the other. In addition to the existing 3xHA-tagged Vangl2 and eGFP-Vangl2 constructs, I constructed a 6xMyc-Vangl2. After co-transfecting HA-Vangl2 and eGFP-Vangl2 into Cos7 cells, I solubilized the cells with RIPA immunoprecipitation buffer and used HA antibody and protein A sepharose to immunoprecipitate the HA-Vangl2. An immunoblot analysis of the recovered material showed that along with the HA-Vangl2, significant amounts of eGFP-Vangl2 were also recovered (Figure 4.8A). In control pull downs where HA-Vangl2 was not expressed, eGFP-Vangl2 was not found – demonstrating that eGFP-Vangl2 was not precipitated by the Protein A Sepharose or HA antibody non-specifically. I confirmed this interaction by performing the same experiment using HA-Vangl2 along with Myc-Vangl2. Again, Myc-Vangl2 immunoprecipitated in the presence of HA-Vangl2 and the controls indicated specificity (Figure 4.8B). These experiments are the first to confirm that Vangl2 forms oligomers similar to the homolog *Drosophila* Strabismus.

The next step was to check whether the looptail mutations affected Vangl2 self-assembly. I performed the same immunoprecipitation experiment but expressed either the Lp255 or Lp464 version of HA-Vangl2 - with the wild type as a control. Using HA antibody, I found these mutant proteins bound equally well as wild type in the eGFP-tagged version of Vangl2 (Figure 4.8A). HA-tagged wild type with Myc-tagged looptail Vangl2 showed the same results. Furthermore, using the Myc- and HA- tagged Vangl2, I co-expressed looptail versions together – Lp255 with Lp255, or Lp464 with Lp464 – and found that the Myc-tagged Vangl2 interacted with the HA-tagged Vangl2 (Figure 4.8B). These experiments demonstrate that Vangl2 association is not sensitive to the looptail mutations. Thus, it appears that the state of oligomerization cannot explain the inhibition of ER export of the Vangl2 looptail mutant proteins.

Since the wild type version of Vangl2 bound to the looptail version of Vangl2, I reasoned that the wild type version may complement the looptail version to promote ER export of the mutant. This presumes that these two versions of Vangl2 are able to associate in the ER and that the recognition of the wild type protein for forward transport would override the looptail defect. The most sensitive way to test this was to

Figure 4.8 – Immunoprecipitation shows that Vangl2 can self-oligomerize

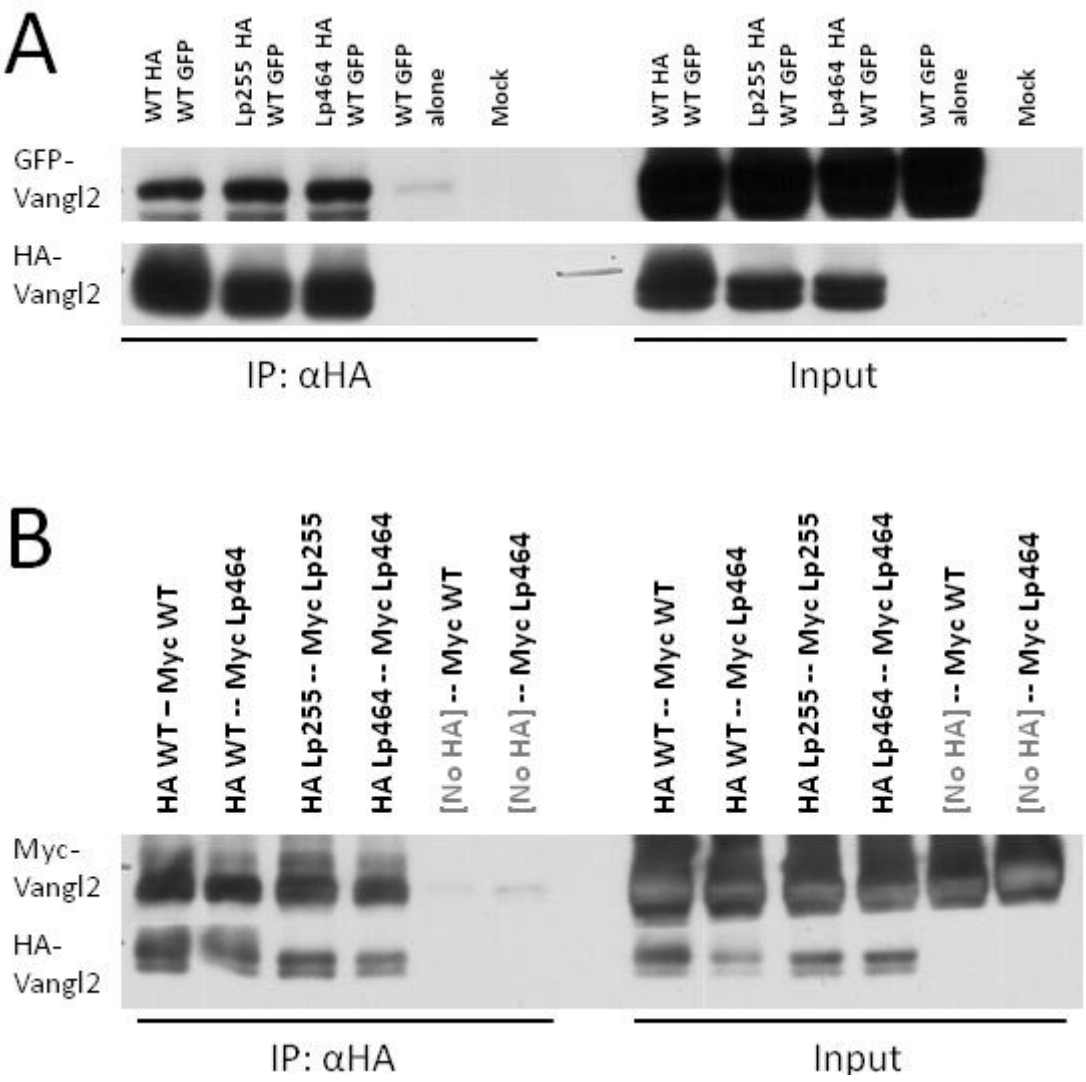

(A) and (B) Vangl2 can self-oligomerize. Cells were co-transiently transfected with (A) GFP- and HA-tagged Vangl2 or (B) Myc-and HA-tagged Vangl2. Cell lysates were used for immunoprecipitation with an anti-HA antibody, revealing the binding of both GFP- and Myc-tagged Vangl2. The looptail mutations had no effect on the ability to oligomerize, either in the context of wild type + looptail mutant or looptail mutant + looptail mutant combinations.

translate and translocate differentially tagged wild type and looptail versions of Vangl2 into the same donor membranes, followed by a COPII budding reaction to detect which proteins were packaged into vesicles. I first confirmed that the Myc-tagged Vangl2 acted the same way in the *in vitro* COPII budding reactions as did the HA-tagged Vangl2 (Figure 4.9). Myc-tagged protein was packaged well with 4mg/ml rat liver cytosol. Addition of the dominant negative Sar1A H79G inhibited packaging into vesicles. The packaging efficiency was lower in incubations containing 2mg/ml rat liver cytosol, but high levels of Vangl2 packaging into the vesicles was restored by addition of recombinant human Sec24B to the reaction. As a side note, the Myc-Vangl2 COPII packaging experiment provided a control to show that the packaging of Vangl2 and the sensitivity to the Sec24B recombinant protein was not due to the presence of the HA tag, with which the original experiments were done.

Now that I was sure that both HA- and Myc- Vangl2 behaved as expected, I performed the combined *in vitro* translation of Myc-Vangl2 wild type and HA-Vangl2 looptail 255 or looptail 464, followed by a COPII budding reaction. The results show that wild type Myc-Vangl2 trafficked normally, just like wild type Vangl2 expressed alone. Interestingly, the looptail HA-Vangl2 was completely excluded from the COPII vesicle fraction, this despite the fact that the wild type protein bound to the looptail protein in earlier experiments (Figure 4.10). These results may be an indication that the Vangl2 looptail proteins are actively retained at the ER by cytosolic factors -- otherwise at least some of the looptail proteins should be trafficking along with the wild type Vangl2, to which they can bind. A potential retention mechanism will be discussed in the conclusion of this chapter.

The functional implications of this oligomerization are unclear. For *Drosophila's* Strabismus, I found no literature of an attempt to characterize the oligomerization of Strabismus, i.e. the region of the protein responsible, the number of proteins in one complex, or whether Strabismus was functional as a monomer. A first attempt of mine at looking for the number of monomers in a complex using a blue native gel of cell lysate suggests that if Vangl2 is the only member of its complex, Vangl2 might exist as a tetramer, but this experiment will need to be repeated. I conclude that looptail protein retention at the ER is not due to oligomerization.

Vangl2 looptail proteins are structurally similar to the wild type protein

Another possible reason for the ER retention of Vangl2 looptail proteins is that they are misfolded or aggregated and become subject to engagement by the ER quality control machinery. One example of this problem is the protein Cystic Fibrosis Transmembrane Conductance Regulator (CFTR), where a common mutant form ΔF508, is misfolded, retained and then extracted from the ER, and finally degraded by the proteosome (Ward *et al.*, 1995; Sun *et al.*, 2006). One way to determine if a protein is misfolded, or at least folded differently, is to use limited proteolysis – which has been used to study the folding of CFTR (Kleizen *et al.*, 2005). Mutant and wild type protein

Figure 4.9 – Myc-Vangl2 is packaged the same way as HA-Vangl2 in the *in vitro* COPII budding reaction

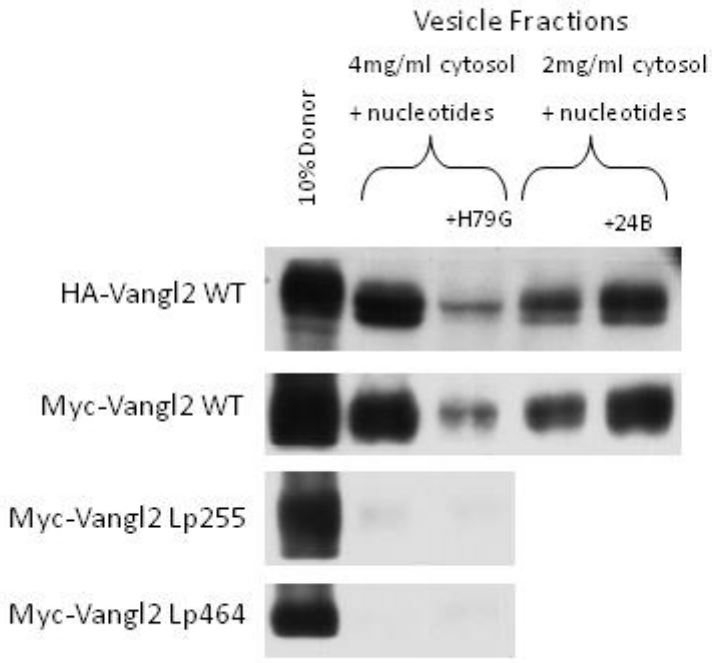

In vitro COPII budding reactions demonstrated that 6xMyc Vangl2 was packaged into vesicles just as 3xHA-Vangl2. As before, the packaging was inhibited by the dominant negative Sar1 H79G and enhanced by the addition of recombinant Sec24B. This result indicated that HA-Vangl2's entry into COPII vesicles and enhancement by Sec24B was not influenced by the HA tag. Like the HA-tagged versions, the Myc-tagged Vangl2 looptail mutants were not able to enter COPII vesicles.

Figure 4.10 – Co-translation of wild type and looptail Vangl2 shows that the wild type Vangl2 cannot enable transport of the looptail mutant

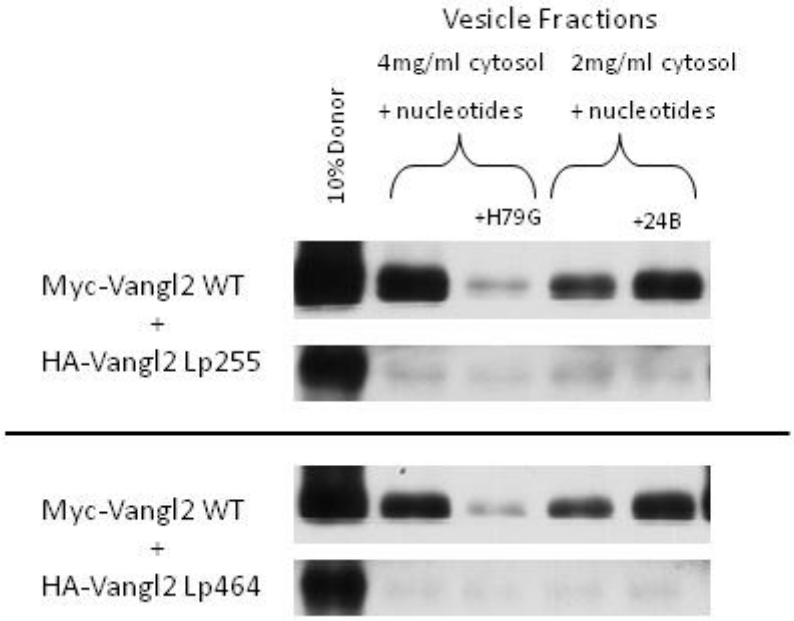

Wild type Myc-Vangl2 and HA-tagged looptail mutants D255E or S464N were *in vitro* translated into the same donor membranes and used in a COPII budding reaction. The wild type protein was packaged into COPII vesicles as normal, but despite the fact that the wild type protein can oligomerize with the looptail mutant, the looptail mutants were not included in the newly formed COPII vesicles.

embedded in the membrane may be compared by partial proteolytic mapping to detect differences in fragmentation on a SDS-page gel.

I analyzed the partial proteolysis of two different sources of Vangl2 wild type and looptail mutant proteins. First, I used a rabbit reticulocyte lysate to *in vitro* translate only the HA- tagged 283 amino acid cytosolic carboxyl-terminus of both the wild type and the looptail mutants. Then I measured the total protein concentration of the reticulocyte lysate + Vangl2 carboxy terminus, to adjust the appropriate trypsin concentration. After adding 1000 times less trypsin than the total concentration and keeping the tubes on ice, I removed aliquots at specific time points with respect to the addition of trypsin – 30 sec, 1 min, 3 min, 10 min, 30 min, and 60 min. Immunoblot of the HA tag showed that the protein was rapidly degraded, with most of it gone in 3 min for both the wild type and the looptail versions of the protein (Figure 4.11). If the looptail protein was grossly unfolded in comparison to the wild type, one might expect it to be degraded faster than the wild type, but no significant difference in degradation rate was observed. Also, if a protein is grossly unfolded compared to another, one might expect to see different sites of cleavage, leading to different size degradation products. A comparison of the smaller degradation products in these samples run on the gel did not reveal a difference in the size of degradation products, but there were not many bands seen, suggesting that the HA tag was cleaved off early (Figure 4.11).

I performed the limited proteolysis experiment in a different and perhaps more sensitive way, using transfected Vangl2 instead of *in vitro* translated Vangl2. This way I could test Vangl2 in its native integral membrane state, with enough material to blot with a (poor) polyclonal carboxyl-terminal anti-Vangl2 antibody, rather than looking at the more limited spectrum of peptides detected by the HA blot. First, I separately transfected wild type HA-Vangl2, and both of the looptail mutant Vangl2s into Cos7 cells. Then, I permeabilized the cells with digitonin to expose the cytoplasmic amino- and carboxyl-cytoplasmic tails of Vangl2. Finally, I treated the permeabilized cells with various concentrations of trypsin on ice for 10 min – control (no trypsin), 2µg/ml, 6µg/ml, 18µg/ml, and 50µg/ml. I processed the samples on SDS-PAGE and immunoblotted with both an HA antibody against the HA tag at the amino terminus and a Vangl2 polyclonal antibody that recognizes the carboxyl-terminus (Figure 4.12). As I had hoped, blotting with the polyclonal Vangl2 antibody yielded a greater diversity of degradation products, which allowed for a more sensitive determination of how the protein was cleaved. However, there were still no significant differences between wild type and looptail proteins seen in either the size of degradation products or the rate of degradation. This experiment indicates that the looptail proteins are not grossly misfolded or differently folded in comparison to wild type Vangl2. Thus, it seems that the reason for the looptail Vangl2 to be retained in the ER is not due to large changes in the folded state of the protein.

Figure 4.11 – Limited proteolysis of *in vitro* translated Vangl2 wild type and looptail mutants

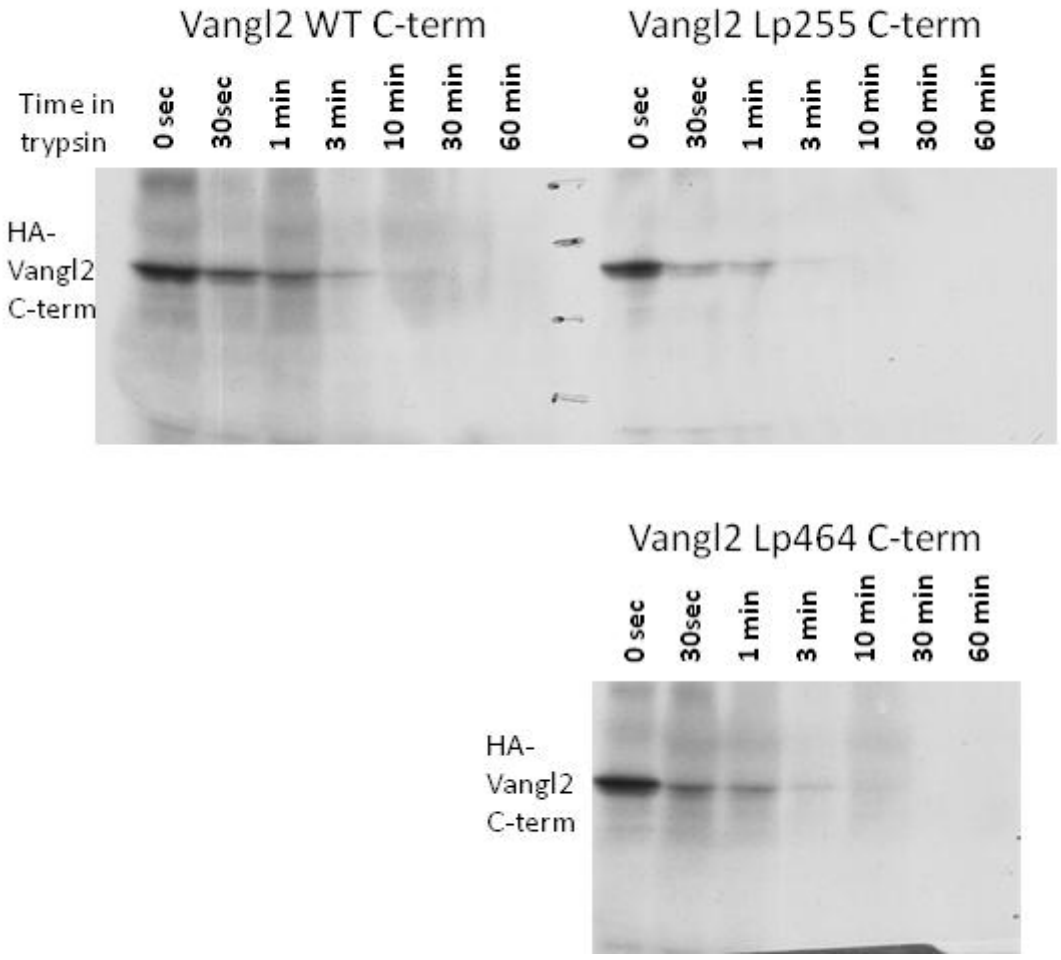

The wild type version of Vangl2's carboxyl-terminus, or that of the looptail mutants, was *in vitro* translated and then subjected to limited proteolysis using trypsin for the length of time indicated. All three are rapidly degraded with most of the protein removed in 3 min.

Figure 4.12 – Limited proteolysis of full length Vangl2 wild type and looptail mutants

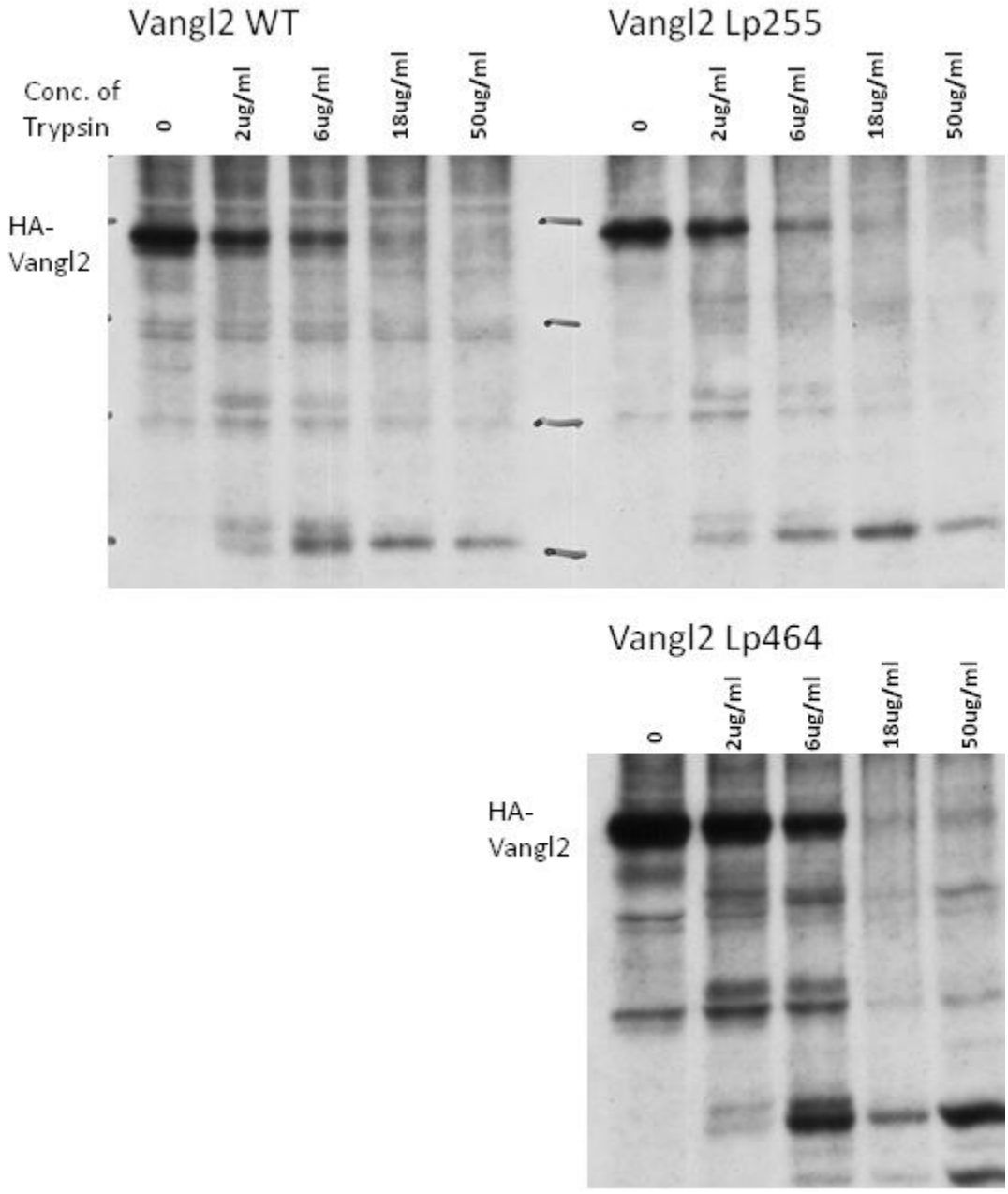

Wild type Vangl2 or the two looptail mutants were transfected into Cos7 cells. After 20 hours, the cells were permeabilized and subjected to limited proteolysis with the indicated amounts of trypsin for 10 min on ice. No significant difference was seen in either the degree of degradation or the pattern of degradation products.

Vangl2 predicted topology is likely correct, with 4 transmembrane domains and the amino- and carboxyl-termini facing the cytosol

In the initial characterization of Strabismus, 4 hydrophobic domains were detected, but only 2 were considered transmembrane domains (Wolff and Rubin, 1998). Later, when homologs of Strabismus were cloned in mice and *Xenopus laevis*, 4 potential transmembrane domains in Vangl2 were noted (Kibar *et al.*, 2001; Darken *et al.*, 2002). This is the prediction that remains in the databases today, which is based on hydrophobicity plots to indicate the transmembrane domains (Figure 4.13).

The matter of topology was confused perhaps by a recent publication in which it was claimed that cell surface Vangl2 could be biotinylated by a sulfo-NHS based biotin crosslinker (Devenport and Fuchs, 2008). However, according to the predicted topology, little of Vangl2 is exposed on the cell surface. The Sulfo-NHS moiety reacts with primary amines found in lysine residues or the primary amine at the amino-terminus of a protein. There are no lysine residues found in the two short 18 amino acid loops that are exposed extracellularly, and the amino-terminus is thought to be cytoplasmic. Thus, based on the predicted topology, sulfo-NHS biotin should not react with Vangl2 on intact cells. Furthermore, the same publication tested the biotinylation with the Vangl2 looptail mutations and reported labeling with the looptail mutants, concluding: "…the *Lp* mutation does not seem to compromise the relative stability and/or cell surface localization of Vangl2" (Devenport and Fuchs, 2008). This result would seem to be in direct conflict with our published results which show that the looptail mutant Vangl2 is strongly retained in the ER and is not at the cell surface.

I set out to try to reproduce their surface biotinylation results using the same reagents. Using Cos7 cells, I transfected separately wild type HA-Vangl2, looptail 255, and 464. Then, I treated the cells with the EZ-Link Sulfo-NHS-LC Biotin reagent in order to cross-link cells surface proteins to biotin. Next, I solubilized the cells with RIPA immunoprecipitation buffer and precipitated all the biotin-linked proteins using streptavidin Sepharose. To my surprise, I found that both Vangl2 wild type and the looptail versions were crosslinked to biotin (Figure 4.14). As a positive control, the transferrin receptor (TfR), a protein known to traffic to the cell surface, was also found biotinylated. As a negative control, ERGIC-53, a protein the cycles between the ER and the ERGIC compartments was not biotinylated. As another control, upon permeabilizing the plasma membrane with digitonin, all three, Vangl2, TfR, and ERGIC-53 were efficiently biotinylated. This was a puzzling result given the predicted topology, my previous results for the immunofluorescence localization of Vangl2, and the budding reactions that show that the looptail proteins are unable to leave the ER.

I examined the conditions of labeling in an effort to reconcile this discrepancy. The manufacturer's procedure for the biotinylation called for incubating the cells at pH8 for the duration of the crosslink incubation. At pH8, the crosslink reaction proceeds more efficiently than at a more physiological pH7. I wondered if this increase in pH could cause anomalous results, so I repeated the experiment, favoring a more physiological buffer at pH7 for the biotinylation reaction, rather than aim for the highest efficiency at pH8. The results at pH7 conformed to the predicted topology of Vangl2

Figure 4.13 – Predicted transmembrane domains of Vangl2 based on hydrophobicity

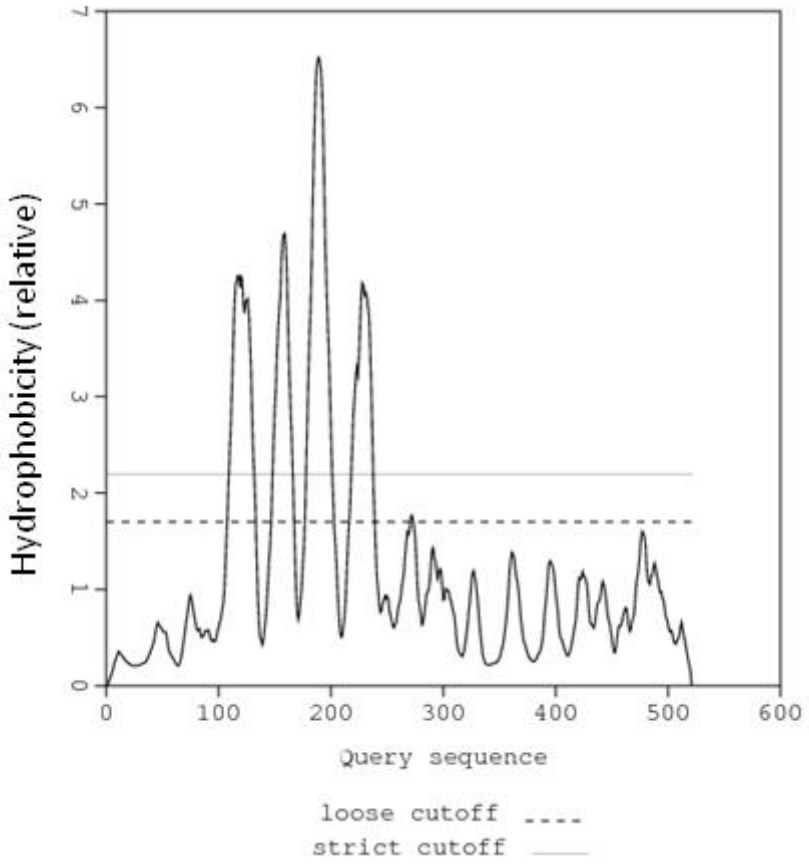

Hydrophobicity plot of mouse Vangl2 indicating likely transmembrane segments. Plot from the "DAS" - Transmembrane Prediction server (http://www.sbc.su.se/~miklos/DAS/)

Figure 4.14 – Surface Biotinylation of Vangl2 at pH8

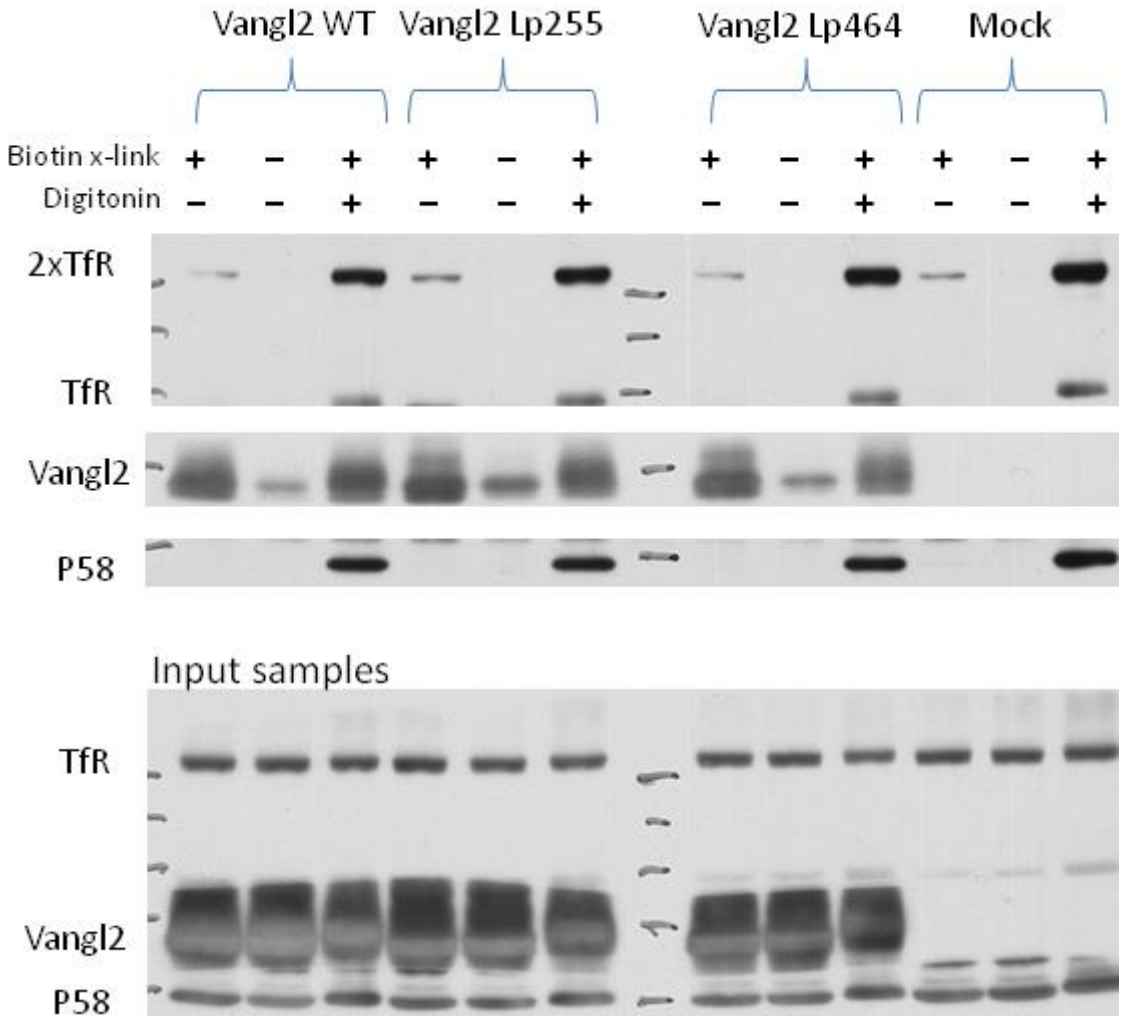

Cells expressing wild type or looptail mutant Vangl2 were treated with EZ-Link Sulfo-NHS-LC Biotin reagent in pH8 buffer, in order to cross-link cells surface proteins to biotin. Then, biotin-linked proteins were centrifuged using streptavidin Sepharose. Unexpectedly, both the wild type and looptail Vangl2 proteins appeared to be labeled. TfR is Transferrin Receptor, a positive control protein known to localize to the cell surface. P58 is a negative control that should not be at the cell surface. Digitonin control ensured that all 3 proteins were labeled.

and my previous results. At pH7, neither wild type nor looptail Vangl2 were biotinylated, the positive control protein, TfR was surface biotinylated (despite theoretical lower efficiency of crosslinking), and the negative control ERGIC-53 was not biotinylated (Figure 4.15). As before, disrupting the plasma membrane before biotinylation lead to efficient biotinylation of all three proteins. I conclude that pH8 creates conditions whereby some proteins inside the cell become accessible to labeling with the biotin reagent.

Cell surface proteolysis may also be used to probe membrane protein topology. Cleavage products may be used to assess the degree of integral protein exposure. Such an assay may also be used to assess the relative amounts of a protein found on the surface or in internal pools. In the case of Vangl2, with only two short loops of the protein predicted to be extracellular, it was unclear whether a surface protease would have access for cleavage in one or both loops.

I tested the ability of Vangl2 to be cleaved at the surface by two different proteases, trypsin and proteinase k. After transfecting HA-Vangl2 into HeLa cells, I separately treated cells with 4 different conditions: No protease control, Trypsin 50ug/ml, Proteinase K 50ug/ml, or Proteinase K 50ug/ml + digitonin 10ug/ml. The results show that Vangl2 was not cleaved by either protease on intact cells (Figure 4.16). A positive control surface protein, TfR was efficiently cleaved by both trypsin and proteinase K. As a control to show Vangl2 could be degraded, digitonin permealized cells were used with the result that proteinase k cleaved the Vangl2 protein. I interpret this result to mean that even though Vangl2 is at the cell surface, the two short loops are not long enough to be accessible to the protease.

The topology of Vangl2 is important as it may lead to insights into its function. Numerous proteins have been suggested to bind to Vangl2, including, Dishevelled, Prickle, Scribble, Rac1 and Frizzled, and determining the potential binding sites for these proteins will be informed by Vangl2's topology. One recent publication proposes that Vangl2 acts as a receptor, externally binding Frizzled on nearby cells and thereby contributes to the maintenance of polarity between neighboring cells (Wu and Mlodzik, 2008). This might be difficult to reconcile with the fact that little peptide is exposed extracellularly as judged by its protease inaccessibility. Nonetheless, my results are consistent with the predicted topology in which there are 4 transmembrane domains with the amino- and carboxyl-termini facing the cytoplasm. During preparation of this dissertation, Gravel and colleagues published an analysis of Vangl1 which further confirms this topology for the Vangl/Strabismus family (Gravel *et al.*, 2010).

Figure 4.15 – Surface Biotinylation of Vangl2 at pH7

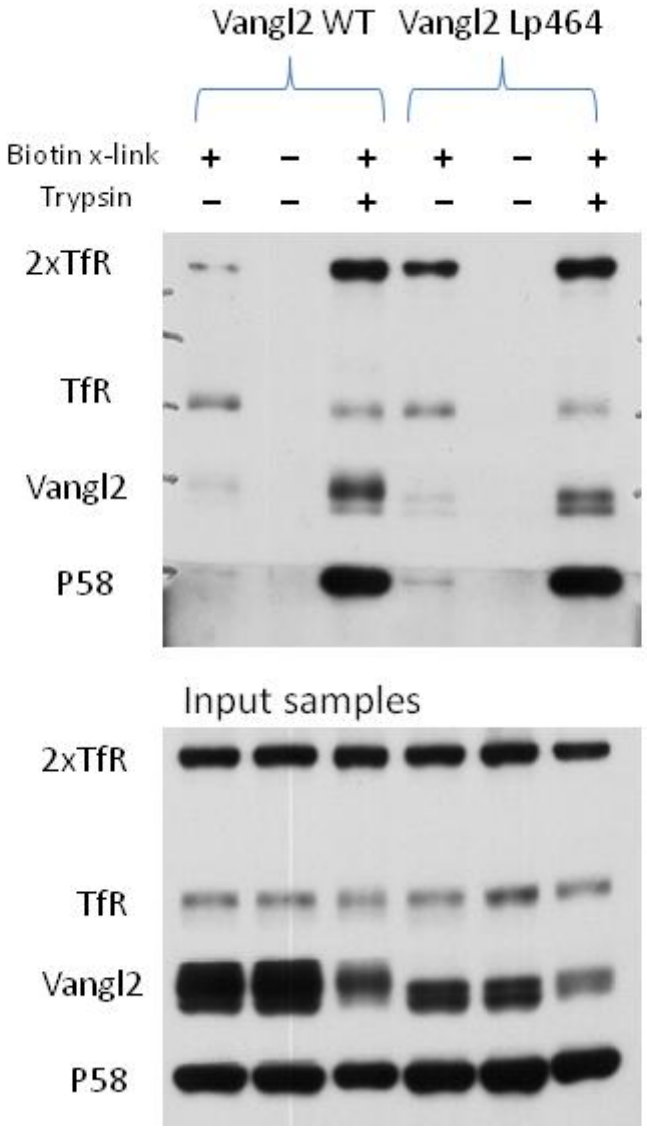

Similar to Figure 4.14 - Cells expressing wild type or looptail Vangl2 were treated with EZ-Link Sulfo-NHS-LC Biotin reagent, but a pH7 buffer instead of pH8 buffer was used. This gave the expected results in which neither wild type nor looptail Vangl2 are biotinylated, while the control TfR protein was biotinylated. Like the digitonin control in Figure 4.14, brief trypsinization and scraping the cells off the plate leads to a leaky plasma membrane, which showed that all proteins were biotinylated.

Figure 4.16 – Vangl2's extracellular loops are not accessible to surface protease

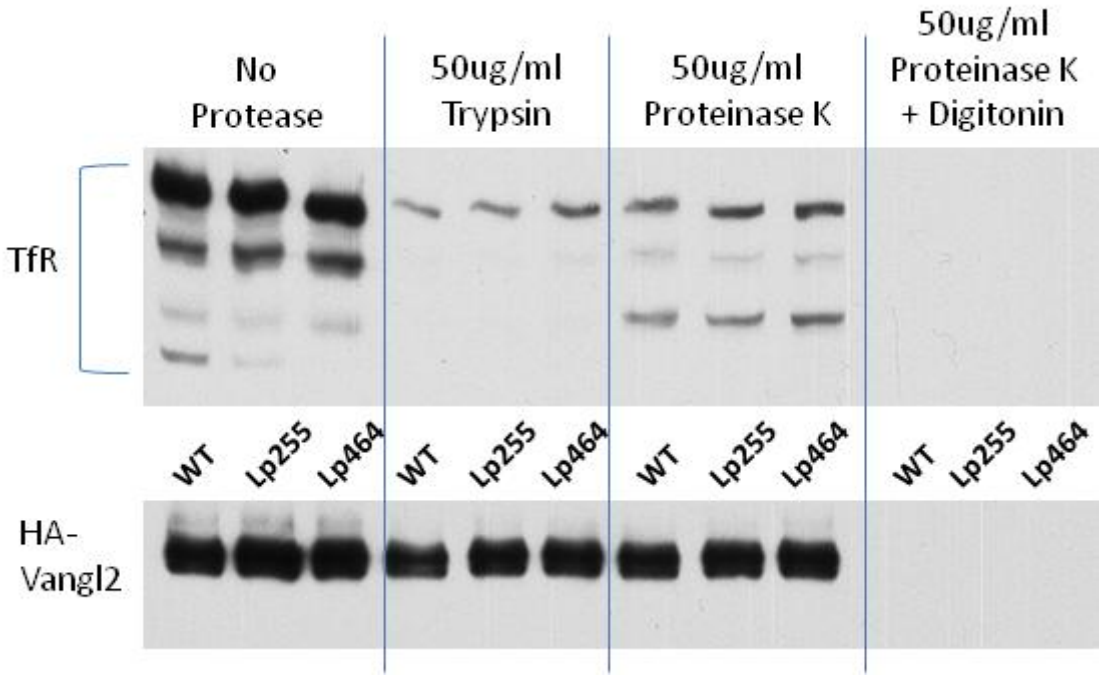

HeLa cells transfected with either wild type or looptail Vangl2 were treated with trypsin, proteinase K, or proteinase K + digitonin. In intact cells, Vangl2 was not accessible to tryspin or proteinase K alone, but addition of digitonin to permeabilize the plasma membrane showed that Vangl2 was cleaved by these proteases. Wild type Vangl2 should be at the cell surface, but its short extracellular loops do not allow cleavage. As a positive control, TfR can be cleaved by both trypsin and proteinase K.

Amino-terminal phosphorylation of Vangl2 is probably similar to Vangl1 and both are good candidates for the activity of casein kinase I.

Vangl2 in transfected cells appears as a doublet band on an immunoblot of a lysate fraction (Figure 4.17A) (Devenport and Fuchs, 2008). I investigated the possibility that Vangl2 is glycosylated, but none of the 3 potential sites for N-linked glycosylation (N-X-[S/T]) are predicted to face the lumen of the ER where N-glycosylation takes place. I also looked at the possibility of O-linked glycosylation, but a prediction of potential sites in Vangl2 did not turn up any good candidates. Vangl1 also displays a doublet on SDS-PAGE, which Kalabis *et al.* (2006) suggests is due to phosphorylation. Given the high degree of conservation between Vangl1 and Vangl2, it seems very likely that Vangl2 is similarly phosphorylated. To investigate the phosphorylation, Kalabis *et al.* used an antibody that is very specific for a particular type of serine/threonine phosphorylation – it only binds phosphorylated serine or threonine in the context of an upstream phenylalanine, tryptophan, or tyrosine or phosphorylated serine or threonine in the context of a downstream phenylalanine ([F/W/Y]-[S*/T*] or [S*/T*]-F) (anti-phospho-Ser/Thr (Phe) rabbit polyclonal, clone number 9631, Cell Signaling, Beverly, MA).

Despite this very specific phosphorylation motif, the authors did not investigate or identify regions of Vangl1 that contain potential sites of phosphorylation. Using this information and a collection of Vangl sequences from different species, I decided to see if I could narrow down which residues could be involved in this phosphorylation of Vangl1 and Vangl2. I assumed that the phosphorylated residues have been conserved because the same doublet bands are seen in immunoblots of human Vangl1 and mouse Vangl2. Compiling an alignment of 14 different Vangl1 and Vangl2 protein sequences from various species including those from human, mouse, zebrafish, and fruit fly, I determined that the likely phosphorylation site is near the extreme amino-terminus of these proteins (Figure 4.17B). In mouse Vangl2, at position 8 and position 11 there are conserved serine residues that are preceded upstream by conserved tyrosine residues. These are the only conserved phosphorylation sites found in both Vangl1 and Vangl2 that would be recognized by that specific anti-phospho-Ser/Thr (Phe) antibody. This does not mean, however, that these two are the only phosphorylation sites in Vangl1 and Vangl2, as there could be other sites of phosphorylation that are simply not detected by that specific antibody.

Intriguingly, these two identified serine residues are part of a larger section of conserved serine residues that are each separated by two other amino acids. There are no less than 6 well-conserved serines as part of 5 S-x-x-S motifs contiguous at the amino terminus of Vangl1 and Vangl2 (SxxSxxSxxSxxSxxS) (Figure 4.17B). The S-x-x-S motif has been previously identified as a site of casein kinase I mediated serine phosphorylation (Flotow *et al.*, 1990). The ability of casein kinase I to act on this S-x-x-S motif requires phosphorylation of the first serine and results in the phosphorylation of the second serine. Given this series of serine motifs, one can imagine a cascade of phosphorylation in which casein kinase I can processively phosphorylate each subsequent serine, as long as the first serine is phosphorylated. Indeed, this very idea

Figure 4.17 – Vangl2 doublet bands and a likely phosphorylation site

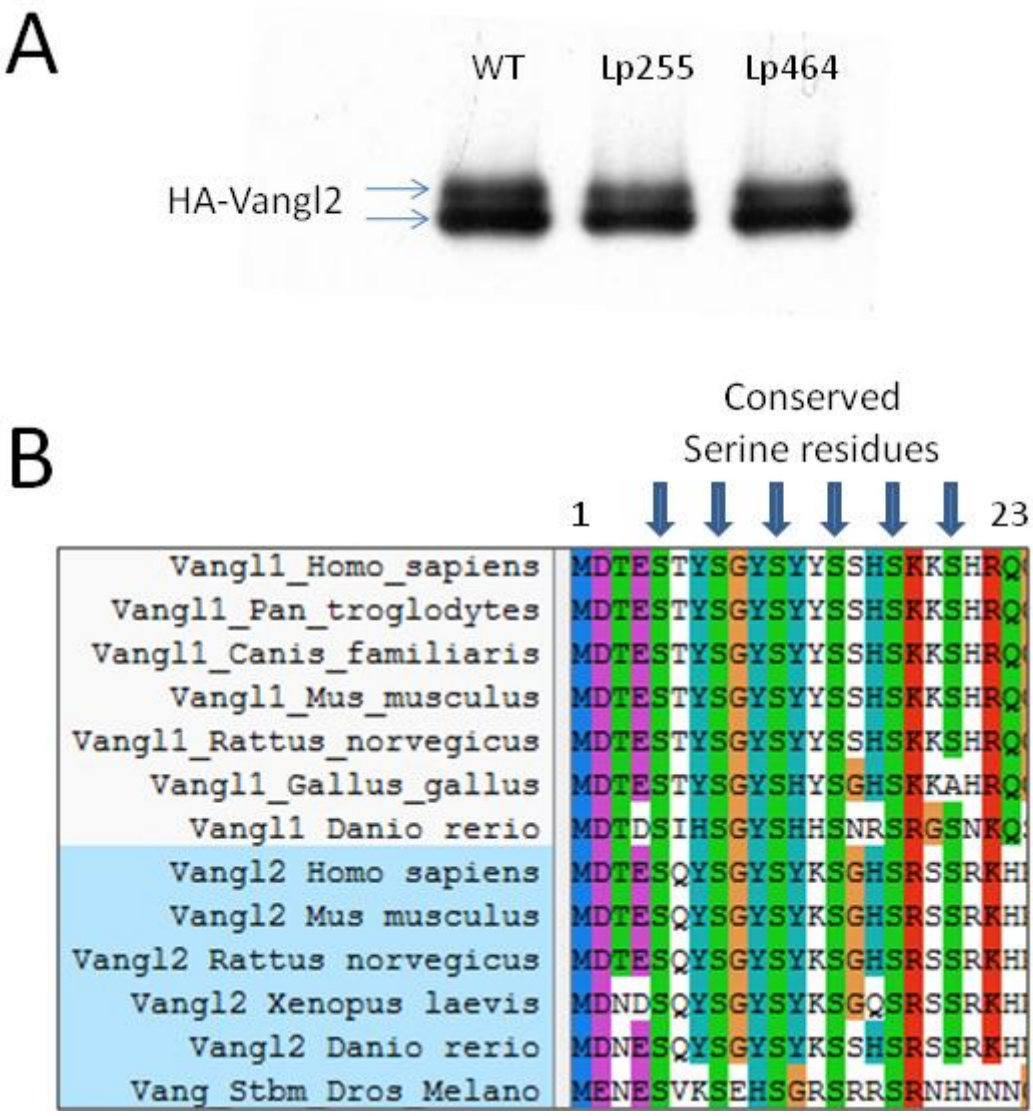

(A) Immunoblot of HA-Vangl2 wild type and looptail mutants, showing a doublet band – likely caused by phosphorylation.

(B) Protein sequence alignment of Vangl1 and Vangl2 from many different species. Conserved serine residues at the amino terminus are a likely phosphorylation site for casein kinase.

has been demonstrated *in vitro* with recombinant casein kinase I and a peptide from the protein Per2 which contains a very similar series of S-x-x-S motifs (Toh *et al.*, 2001). So how is the first serine residue phosphorylated? In the case of Per2, another kinase must initiate the phosphorylation cascade, but Vangl1 and Vangl2 appear to have a built in mechanism. Several cellular substrates for casein kinase I have acidic residues upstream of the target serine (Tuazon and Traugh, 1991). The negative charges on these motifs appear to substitute for a phosphorylated serine/threonine and while less efficient, still allow activity of casein kinase I. Vangl1 and Vangl2 have two conserved acidic amino acids, upstream of the initial serine at position 5 – an aspartic acid at position 2 and a glutamic acid at position 4.

Based on this information, I would predict that mutating the serine at position 5 in Vangl2 would lead to a loss of phosphorylation for all the subsequent serines and would likely result in the normally doublet Vangl2 being resolved into one band as visualized by immunoblot. The functional consequences of Vangl2 phosphorylation have not been investigated. In their paper on Vangl1 phosphorylation, Kalabis *et al.* suggested that treating cells with a peptide factor that leads to Vangl1 phosphorylation resulted in an altered subcellular localization for Vangl1, but the connection between the two events was not established (Kalabis *et al.*, 2006). A role for casein kinase in regulating Vangl2 is not unprecedented -- casein kinase I and II function during canonical and non-canonical WNT signaling, they are required for convergent extension in *Xenopus laevis*, and can phosphorylate Dishevelled (Bryja *et al.*, 2008). Additionally, as discussed in the previous section, when Wu and Mlodzik were testing for interaction between *Drosophila* Strabismus and Frizzled, they saw binding with only one of the two Strabismus bands (Wu and Mlodzik, 2008). They were apparently not aware of Strabismus' likely phosphorylation, suggesting that the second band represents some kind of processed form of Strabismus. Their experiments do not definitively establish this interaction, and to my knowledge this interaction has not been reported by others, but if true, this result suggests the binding of Strabismus to Frizzled is mediated by the phosphorylation state of Strabismus.

Vangl2 binds to Dishevelled and Prickle, Dishevelled binding is sensitive to the looptail mutations

As suggested earlier in this chapter, even though the packaging of Vangl2 is strongly enhanced by Sec24B, these proteins may not interact directly. Therefore, I sought to test other proteins that might act as a chaperone or adaptor for Vangl2. The first place I decided to start was to look at proteins that were already known to bind to Vangl2 or its homolog Strabismus. Among these are cytosolic proteins known to be involved in the process of planar cell polarity, namely Dishevelled, Prickle, and Scribble. If any of these proteins are involved in the ER export of Vangl2, then their binding to Vangl2 may be affected by the looptail mutations – which would explain why looptail mutant proteins are unable to leave the ER. From what I have determined in the literature, Dishevelled and Scribble are the only two proteins that have shown differential binding to Vangl2 in the context of the looptail point mutations. Scribble is

a cytosolic protein, first identified in *Drosophila*, involved in polarity signaling. In previous work, however, deletion of Scribble did not affect the localization of Strabismus, so it does not appear to be a good candidate to be involved in the ER export of Vangl2 (Courbard *et al.*, 2009). That left Dishevelled and Prickle, as known interactors with a potential for acting as adaptor proteins to help Vangl2 to leave the ER.

As discussed in chapter 1, Dishevelled (Dvl) is a cytosolic signal transduction protein that functions in both canonical and non-canonical WNT signaling. *Drosophila* Strabismus has demonstrated binding with *Drosophila* Dishevelled in several assays, although the functional implications for planar cell polarity are not clear (Park and Moon, 2002; Bastock et al., 2003). In mammals there are 3 paralogs: Dishevelled 1, 2, and 3. They have not been previously associated with COPII trafficking, but based on some earlier published work, I had an indication that they might be worth considering. Using a yeast two hybrid system, Torban and colleagues found that just like the *Drosophila* Strabismus binding to *Drosophila* Dishevelled, mammalian Vangl2 binds to mammalian Dishevelled. Importantly, however, both of the looptail point mutations in Vangl2 prevented the binding to all three of the Dishevelled paralogs (Torban et al., 2004).

I wanted to verify the mammalian Dishevelled's interaction with Vangl2 and test for myself the sensitivity of its binding to the looptail mutations. To do this I created Myc-tagged Dishevelled 1, 2 and 3 constructs and used these to produce RNA for each. I separately *in vitro* translated each Dishevelled paralog, as well as HA-tagged Vangl2 cytosolic carboxyl-terminal domains of wild type, looptail 255, and looptail 464. I mixed each Dishevelled paralog with each Vangl2 and then used the HA tag on the Vangl2 carboxyl-terminus to immunoprecipitate and probe for the presence of the Myc-tagged Dishevelled. I found that in agreement with prior results, the wild type cytosolic carboxyl-terminus of Vangl2 does bind to each Dishevelled 1, 2, and 3 (Figure 4.18). I also found, like Torban *et al.*, that there was less binding of Dishevelled to the Vangl2 looptail mutants, but there were interesting differences between the different Dishevelled paralogs (Figure 4.18). Dishevelled 3 was most strongly affected by the looptail mutations, with comparatively much less co-precipitating with the looptail Vangl2 than with the wild type. Dishevelled 1 was least affected by the looptail mutations showing nearly comparable levels co-precipitating with both the wild type and looptail. Dishevelled 2 binding to the looptail mutants was intermediate between Dishevelled 1 and 3.

Although my results and those of Torban *et al.* are broadly similar, that Dishevelled binds less avidly to the Vangl2 looptail mutants, there are some differences. According to their yeast two hybrid approach, all three Dishevelleds do not bind looptail mutant Vangl2 in the most stringent conditions, whereas in medium conditions of stringency, Dishevelled 2 and 3 bind, but Dishevelled 1 does not. Thus, Dishevelled 1 may be the most sensitive to the looptail mutations. This is in contrast to my immunoprecipitation results which show that Dishevelled 3 is most sensitive. Both of these approaches, yeast two hybrid and cell-free immunoprecipitation are somewhat

Figure 4.18 – Vangl2's carboxyl-terminus interacts with Dishevelled *in vitro* and looptail mutations affect the binding

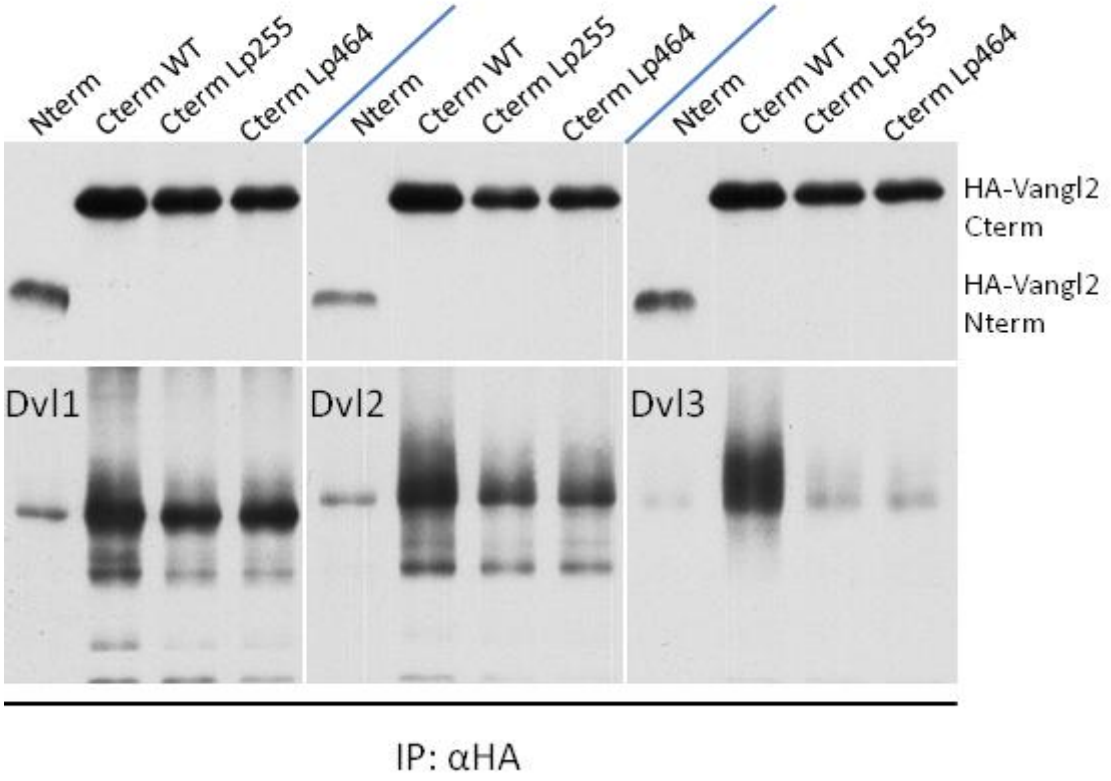

In vitro binding and immunoprecipitation of Vangl2 and Dishevelled. Each protein, HA-Vangl2 amino-terminus, carboxyl-terminus WT, Lp255, Lp464, and Myc-Dishevelled 1, 2, and 3 was *in vitro* translated with rabbit reticulocyte lysate. Then each pairwise combination was mixed and immunoprecipitated with the HA tag on Vangl2. Each Dishevelled binds to Vangl2's carboxyl-terminus, but each is affected differently by the looptail mutations, with Dishevelled 3 most severely affected.

artificial, so I sought to confirm my results in cells, relying on endogenous Dishevelled. Using either Cos7 cells or HeLa cells, I separately expressed full length wild type Vangl2 or the two looptail mutant Vangl2s, then preformed an immunoprecipitation and probed an immunoblot for the presence of endogenous Dishevelled 1, 2, and 3. I found that Cos7 and HeLa cells do not express much Dishevelled 1 or 2, but they do express Dishevelled 3. As in the cell-free immunoprecipitation, there was much less Dishevelled 3 co-immunoprecipitated with the looptail mutants than with the wild type Vangl2 (Figure 4.19).

Prickle is also a cytoplasmic protein that is involved in planar cell polarity and at least in *Drosophila*, is known to bind to Vangl2 (Bastock et al., 2003). In mammals, there are 4 prickle paralogs, but most of the research that has been done on the Prickle genes focuses on the Prickle 1 and 2. I acquired Prickle 1 and 2 cDNA and made Myc-tagged plasmids in a mammalian expression vector. Using these constructs, I performed the cell-free translation and immunoprecipitation with Vangl2 in the same way that I did with the Dishevelled constructs. I observed a good interaction between Vangl2 and Prickle 1 and 2, but this interaction was only partly sensitive to the looptail mutations (Figure 4.20). To my knowledge, this is the first demonstration that mammalian Prickle binds to Vangl2 similarly to the *Drosophila* proteins, which demonstrates the high degree of conservation in the planar cell polarity pathway between fly and mammal.

Since the Prickle proteins did not show a big difference in binding to Vangl2 wild type or looptail, I set them aside and have been focusing on the potential role of Dishevelled in the ER export of Vangl2. To that end, I have been able to knockdown Dishevelled 3 in HeLa cells and will be testing the localization of Vangl2, and the ability of Vangl2 to be packaged into vesicles in the absence of Dishevelled. If it turns out that the export of Vangl2 does depend on Dishevelled, I should be able to determine if Dishevelled is acting as an adaptor between Vangl2 and COPII, or if it has another role, for instance as a chaperone that binds and masks ER retention motifs.

Figure 4.19 – Immunoprecipitation of Vangl2 can pull out endogenous Dishevelled 3 and this interaction is affected by the looptail mutations

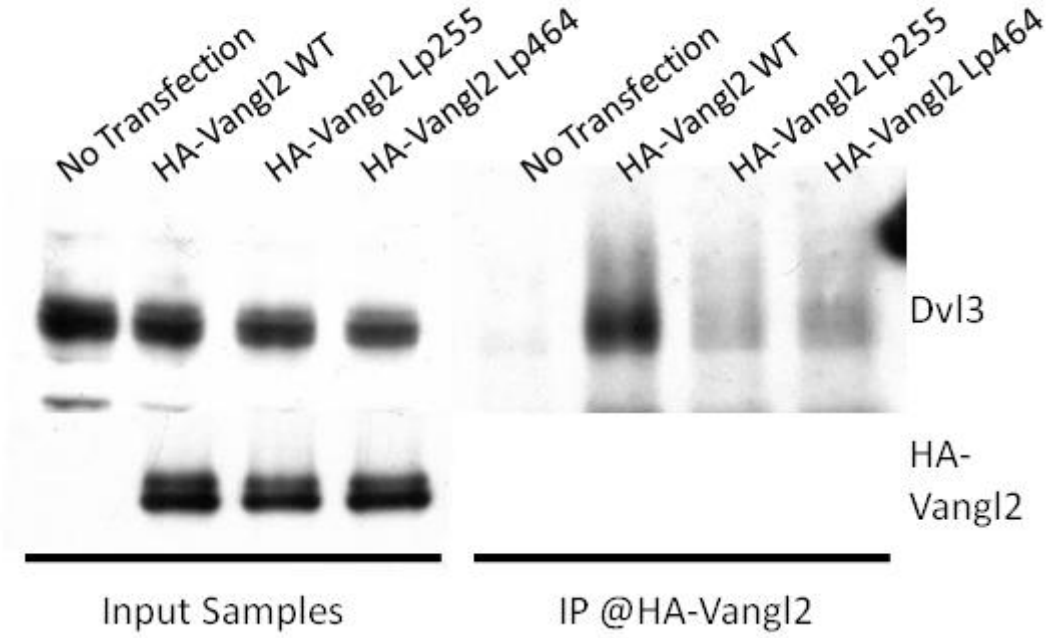

HeLa cells were transiently transfected with HA-Vangl2 wild type or the looptail mutants. Then, 20h later, cells were lysed and an immunoprecipitation was performed with an anti-HA antibody. Endogenous Dishevelled 3 was detected in the immunoprecipitation with wild type Vangl2 but there was much less in the immunoprecipitation with the looptail mutants.

Figure 4.20 – Vangl2's carboxyl-terminus interacts with Prickle *in vitro* and the looptail mutations do not strongly affect the binding

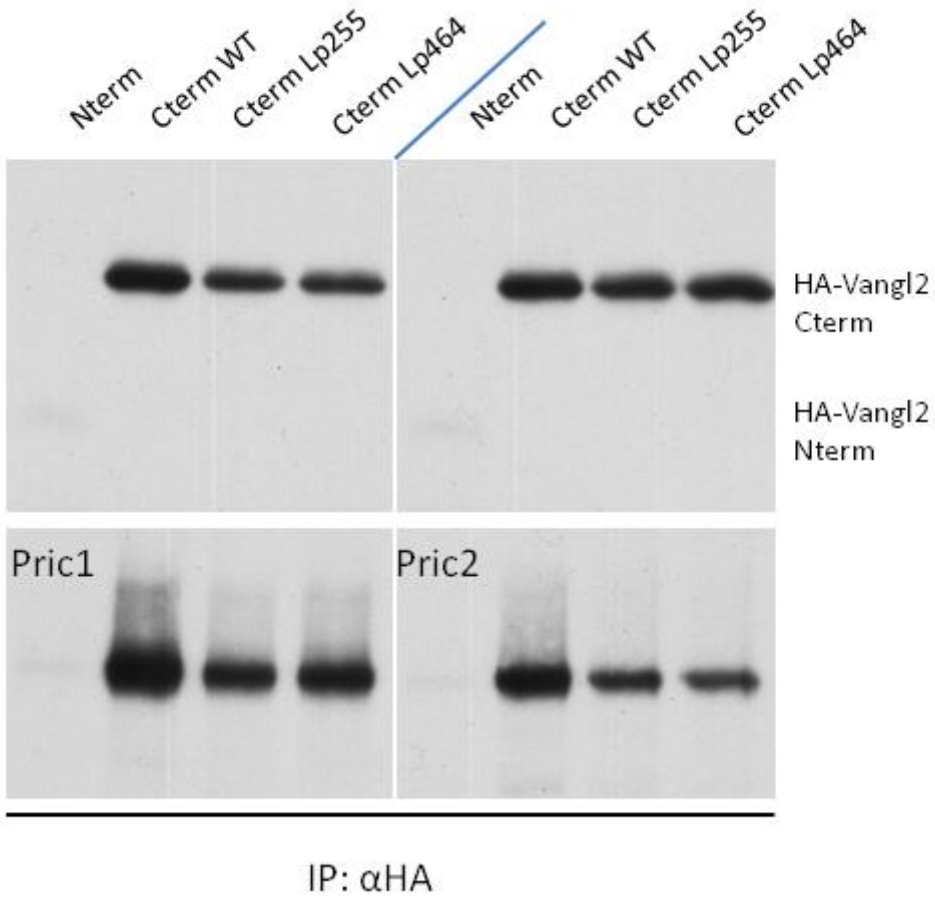

In vitro binding and immunoprecipitation of Vangl2 and Prickle. Each protein, HA-Vangl2 amino-terminus, carboxyl-terminus WT, Lp255, Lp464, and Myc-Prickle 1 and 2 was translated in a rabbit reticulocyte lysate. Then each pairwise combination was mixed and immunoprecipitated with the HA tag on Vangl2. Each Prickle binds to Vangl2's carboxyl-terminus, and each can still bind to the Vangl2 looptail mutants though with lower efficiency.

Discussion

I believe the work in this chapter represents considerable progress in the understanding of the molecular mechanisms governing the intracellular localization of Vangl2. Vangl2 plays a central and essential role in establishing planar cell polarity in a wide range of metazoans, and defects in the traffic or activity of this signaling receptor have a role in human embryonic development.

Although others have tested Vangl2's extreme carboxyl-terminus for its potential role in binding to planar cell polarity effectors like Dishevelled, this is the first study to show that the extreme carboxyl-terminus is important for efficient ER export of Vangl2. The fact that some cell surface staining was seen in the V521G mutant may distinguish the role of the very carboxyl-terminus of Vangl2 from the domain defined by the looptail mutations. In contrast to V521G, immunofluorescence images of both Vangl2 looptail proteins show very stringent reticular ER staining, and no surface staining. The small amount of Vangl2 V521G at the cell surface could arise from a defect in concentrative sorting of Vangl2, where inefficient transport may continue by a default bulk flow process.

This study is also the first scanning point mutation analysis of the looptail regions of Vangl2 or its homologs, and it revealed a number of important residues surrounding the original looptail positions. Together with the original looptail residues, these mutations comprise the amino acid sequences RxxDGxxxxY and WxLxS for the looptail sites 255 and 464, respectively. Much effort was spent on trying to determine exactly why the looptail mutations prevent the ER export of Vangl2. Although the matter is not resolved, I have made progress in narrowing down the probable cause. The looptail mutations do not have any effect on the oligomerization status of Vangl2, nor do they cause any large scale folding changes that I could detect using proteolysis assays.

I believe that either Vangl2 looptail mutants cannot bind an adaptor/chaperone protein or that folding has been perturbed subtly. A great candidate for the potential adaptor/chaperone is Dishevelled. A next step will be to examine the new Vangl2 point mutants to see if they impair Dishevelled binding in proportion to their traffic defect. Attempts at discovering other proteins in a cell lysate that bind differentially to the Vangl2 wild type or looptail proteins were not successful. This adaptor/chaperone would not necessarily interact with COPII and drive forward transport. Another possibility is that this binding protein may mask retention motifs that otherwise keep Vangl2 in the ER. The strong reticular staining seen in the looptail mutants is suggestive of an active retention mechanism. I recently identified conserved potential ER retention motifs in Vangl2, positioned roughly halfway in between the two looptail sites (Figure 4.21). This area contains 9 arginine residues that are configured in 4 separate R-x-R motifs, a strong ER retention signal (Zerangue *et al.*, 1999). Perhaps Dishevelled or another chaperone protein enables Vangl2 ER export by masking these arginine residues, thus preventing engagement with the ER retention machinery. It has been suggested by others that the R-x-R motifs are recognized by the COPI coat retrograde machinery and that is the mechanism which leads to ER retention (Yuan *et*

Figure 4.21 – Arginine motifs in Vangl2 may represent an ER retention signal

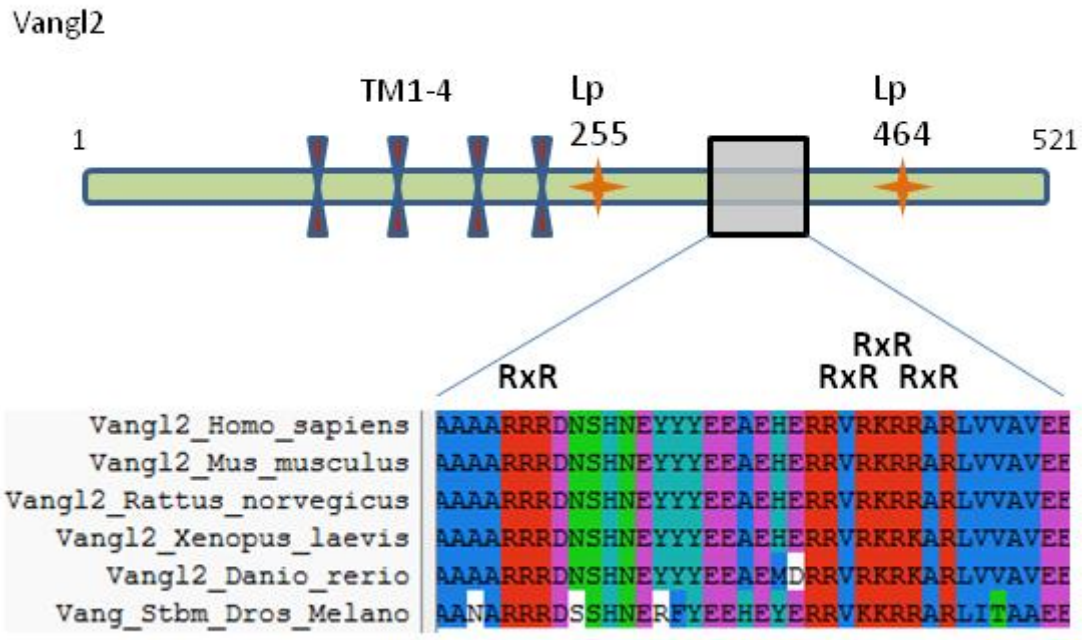

Schematic diagram and protein sequence alignment for the region of Vangl2 from amino acid 328-365, indicating the location of arginine motifs that could be involved in the ER retention of the Vangl2 looptail mutants.

al., 2003). This retrograde transport explanation could not explain my observation that Vangl2 looptail mutant protein can not be packaged into COPII vesicles. Alternatively, these arginine motifs could directly engage cytosolic ER-associated degradation (ERAD) machinery. An ATPase involved in ERAD, VCP/p97, recognizes an R-K-R-R motif on another protein called Ataxin-3 (Boeddrich *et al.*, 2006). This same R-K-R-R motif is found in the arginine rich region of Vangl2 and appears in a similar context.

If the looptail mutations are leading to active ER retention, what then about forward COPII transport and the activity of Sec24B in improving Vangl2 vesicle packaging? The forward transport signal in Vangl2 may be the carboxyl-terminal valine. An extreme carboxyl-terminal valine has been considered an ER export motif in other proteins (Nufer *et al.*, 2002). Nufer *et al.* found that carboxyl-terminal valine cargo proteins interact with Sec23 and Sec24, but it is not clear if these COPII proteins are interacting directly or indirectly with the carboxyl-terminal valine. Another PDZ protein called GRASP65 may act as an adaptor protein to recognize the carboxyl-terminal valine of cargo proteins and enable efficient ER export (D'Angelo *et al.*, 2009). One of the cargo proteins they tested is Frizzled 4, which besides being part of WNT signaling pathways like Vangl2, also has a very similar carboxyl-terminus: -SETVV and -SETSV for Frizzled 4 and Vangl2, respectively. Additionally, a yeast homolog of GRASP65 called Grh1p has previously been found to bind to Sec23 / Sec24 (Behnia *et al.*, 2007).

Based on all that I have learned about Vangl2 and including some of these new ideas about the potential roles of Dishevelled and GRASP65, I propose a model of Vangl2 ER export as illustrated in Figure 4.22. Dishevelled binding masks the arginine motifs and prevents ER retention. GRASP65 binds to the carboxyl-terminal valine residue and promotes forward transport via an interaction with COPII – potentially a specific interaction with Sec24B. There remains some work to determine if this model holds true, but this work is well on its way to a comprehensive understanding of the mechanisms and regulation of the ER export of Vangl2.

Figure 4.22 – Proposed model for ER export of Vangl2

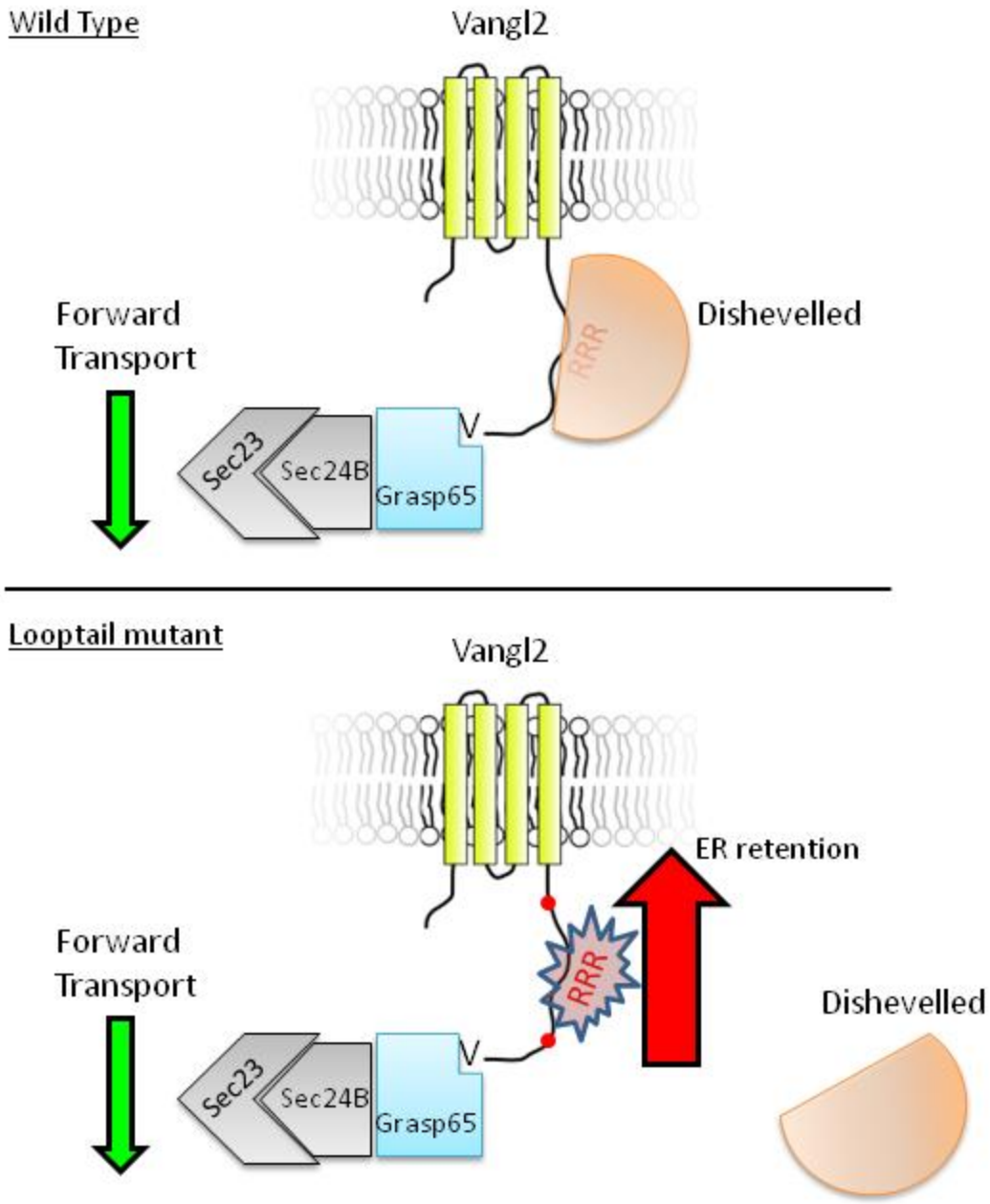

Multiple mechanisms enable the COPII transport of Vangl2. Vangl2 can traffic when its ER retention motifs are masked, potentially by Dishevelled. GRASP65 or another chaperone can bind to the extreme carboxyl-terminus and promote forward transport. The looptail mutations expose the arginine retention motifs, preventing transport.

Methods

Immunofluorescence – As described in chapter 3

In vitro COPII budding, in vitro translation/translocation – As described in chapter 3

Immunoprecipitation – As described in Chapter 3

Limited proteolysis – First method: Cytoplasmic carboxyl-terminus of HA-Vangl2 WT, Lp255, and Lp464 were *in vitro* translated in rabbit reticulocyte lysate. Then the protein concentration of the lysate was assessed. Trypsin was added to each at a concentration of $1/1000^{th}$ of the total protein concentration. At each time point, 0sec, 30sec, 1min, 3min, 10min, 30min, and 60min, a 10µl aliquot was removed from the main tube. For these aliquots, 20µg soybean trypsin inhibitor was added, and allowed to incubate on ice for 5 min. Then, 28µl of 90°C hot Buffer C + 5x Dye (pre-mixed) was added to make a total of 40µl. Then the sample was incubated 90°C for 10min. (Buffer C is as described in chapter 3)

Second method: Cos7 cells were transfected overnight with HA-Vangl2 WT, Lp255, or Lp464. Cells were washed and scraped in PBS. After centrifugation and resuspension in PBS, cells were treated with digitonin to permeabilize the plasma membrane. Protein concentration was measured and cells were centrifuged and resuspended to 5mg/ml for each of three types, WT, Lp255, and Lp464. Equal amounts of cells were aliquoted into different tubes and trypsin was added to a final concentration of 0µg/ml, 2µg/ml, 6µg/ml, 18µg/ml, 50µg/ml. Tubes were incubated at 4°C for 15min. Then, 2µl of 10µg/µl Soybean Trypsin Inhibitor was added, mixed and incubated for 3 min on ice. An aliquot of 90°C hot Buffer C + 5x Dye (pre-mixed) was added for 50µl total volume. Tubes were incubated at 90°C for 10min and then frozen.

Surface biotinylation – Cos7 cells were transfected with HA-Vangl2 WT, Lp255, or Lp464 in a six well plate overnight. Then next day, cells were washed with PBS, keeping the cells in wells. EZ-Link Sulfo-NHS-LC Biotin was dissolved 4.7 mg in 4ml PBS pH7 or pH8. PBS control or PBS with EZ-Link Biotin was added to the wells and incubated for 30min on ice. After incubation, cells were washed with 3 times with PBS with 200mM glycine. Then, cells were solubilized in 200µl RIPA buffer + protease inhibitors, scraped, and put into tubes. The tubes were centrifuged at 15000g x 10min to sediment debris. The supernatant was moved to a new tube, keeping a separate aliquot for the "Input" sample. To the remaining supernatant, 40µl of 50% slurry of Streptavidin Sepharose (20µl beads) was added and samples were rotated at 4°C for 2 h. Beads were centrifuged and washed 4x in RIPA buffer. The beads were resuspended in 48µl buffer C + 32µl 5x dye (2x dye final in 80µl).

References

Bastock R, Strutt H, Strutt D. (2003). Strabismus is asymmetrically localised and binds to Prickle and Dishevelled during Drosophila planar polarity patterning. *Development*. 130(13):3007-14.

Behnia R, Barr FA, Flanagan JJ, Barlowe C, Munro S. (2007). The yeast orthologue of GRASP65 forms a complex with a coiled-coil protein that contributes to ER to Golgi traffic. *J Cell Biol*. 176(3):255-61.

Bellaïche Y, Beaudoin-Massiani O, Stuttem I, Schweisguth F. (2004). The planar cell polarity protein Strabismus promotes Pins anterior localization during asymmetric division of sensory organ precursor cells in Drosophila. *Development*. 131(2):469-78.

Boeddrich A, Gaumer S, Haacke A, Tzvetkov N, Albrecht M, Evert BO, Müller EC, Lurz R, Breuer P, Schugardt N, Plassmann S, Xu K, Warrick JM, Suopanki J, Wüllner U, Frank R, Hartl UF, Bonini NM, Wanker EE. (2006). An arginine/lysine-rich motif is crucial for VCP/p97-mediated modulation of ataxin-3 fibrillogenesis. *EMBO J*. 25(7):1547-58.

Bryja V, Schambony A, Cajánek L, Dominguez I, Arenas E, Schulte G. (2008). Beta-arrestin and casein kinase 1/2 define distinct branches of non-canonical WNT signalling pathways. *EMBO Rep*. 9(12):1244-50.

Courbard JR, Djiane A, Wu J, Mlodzik M. (2009). The apical/basal-polarity determinant Scribble cooperates with the PCP core factor Stbm/Vang and functions as one of its effectors. *Dev Biol*. 333(1):67-77.

D'Angelo G, Prencipe L, Iodice L, Beznoussenko G, Savarese M, Marra P, Di Tullio G, Martire G, De Matteis MA, Bonatti S. (2009). GRASP65 and GRASP55 sequentially promote the transport of C-terminal valine-bearing cargos to and through the Golgi complex. *J Biol Chem*. 284(50):34849-60.

Darken RS, Scola AM, Rakeman AS, Das G, Mlodzik M, Wilson PA. (2002). The planar polarity gene strabismus regulates convergent extension movements in Xenopus. *EMBO J*. 21(5):976-85.

Devenport D, Fuchs E. (2008). Planar polarization in embryonic epidermis orchestrates global asymmetric morphogenesis of hair follicles. *Nat Cell Biol*. 10(11):1257-68.

Fernández-Larrea J, Merlos-Suárez A, Ureña JM, Baselga J, Arribas J. (1999). A role for a PDZ protein in the early secretory pathway for the targeting of proTGF-alpha to the cell surface. *Mol Cell*. 3(4):423-33.

Flotow H, Graves PR, Wang AQ, Fiol CJ, Roeske RW, Roach PJ. (1990). Phosphate groups as substrate determinants for casein kinase I action. *J Biol Chem*. 265(24):14264-9.

Gravel M, Iliescu A, Horth C, Apuzzo S, Gros P. (2010). Molecular and Cellular Mechanisms Underlying Neural Tube Defects in the Loop-tail Mutant Mouse. *Biochemistry*. Apr 2. [Epub ahead of print]

Jessen JR and Solnica-Krezel L. (2004). Identification and developmental expression pattern of van gogh-like 1, a second zebrafish strabismus homologue. *Gene Expr Patterns*. 4(3):339-44.

Kalabis J, Rosenberg I, Podolsky DK. (2006). Vangl1 protein acts as a downstream effector of intestinal trefoil factor (ITF)/TFF3 signaling and regulates wound healing of intestinal epithelium. *J Biol Chem*. 281(10):6434-41.

Kay BK, Kehoe JW. (2004). PDZ domains and their ligands. *Chem Biol*. 11(4):423-5.

Kibar Z, Underhill DA, Canonne-Hergaux F, Gauthier S, Justice MJ, Gros P. (2001). Identification of a new chemically induced allele (Lp(m1Jus)) at the loop-tail locus: morphology, histology, and genetic mapping. *Genomics*. 72(3):331-7.

Kibar Z, Vogan KJ, Groulx N, Justice MJ, Underhill DA, Gros P. (2001). Ltap, a mammalian homolog of Drosophila Strabismus/Van Gogh, is altered in the mouse neural tube mutant Loop-tail. *Nat Genet*. 28(3):251-5.

Kibar Z, Torban E, McDearmid JR, Reynolds A, Berghout J, Mathieu M, Kirillova I, De Marco P, Merello E, Hayes JM, Wallingford JB, Drapeau P, Capra V, Gros P. (2007). Mutations in VANGL1 Associated with Neural-Tube Defects. *N Engl J Med*. 356(14):1432-7.

Kibar Z, Bosoi CM, Kooistra M, Salem S, Finnell RH, De Marco P, Merello E, Bassuk AG, Capra V, Gros P. (2009). Novel mutations in VANGL1 in neural tube defects. *Hum Mutat*. 30(7):E706-15.

Kleizen B, van Vlijmen T, de Jonge HR, Braakman I. (2005). Folding of CFTR is predominantly cotranslational. *Mol Cell*. 20(2):277-87.

Merte J, Jensen D, Wright K, Sarsfield S, Wang Y, Schekman R, Ginty DD. (2010). Sec24b selectively sorts Vangl2 to regulate planar cell polarity during neural tube closure. *Nat Cell Biol*. 12(1):41-6

Murdoch JN, Doudney K, Paternotte C, Copp AJ, Stanier P. (2001). Severe neural tube defects in the loop-tail mouse result from mutation of Lpp1, a novel gene involved in floor plate specification. *Hum Mol Genet*. 10(22):2593-601.

Nufer O, Guldbrandsen S, Degen M, Kappeler F, Paccaud JP, Tani K, Hauri HP. (2002). Role of cytoplasmic C-terminal amino acids of membrane proteins in ER export. *J Cell Sci*. 115(Pt 3):619-28.

Nufer O, Kappeler F, Guldbrandsen S, Hauri HP. (2003). ER export of ERGIC-53 is controlled by cooperation of targeting determinants in all three of its domains. *J Cell Sci*. 116(Pt 21):4429-40.

Park M, Moon RT. (2002). The planar cell-polarity gene stbm regulates cell behaviour and cell fate in vertebrate embryos. *Nat Cell Biol*. 4(1):20-5.

Reynolds A, McDearmid JR, Lachance S, Marco PD, Merello E, Capra V, Gros P, Drapeau P, Kibar Z. (2010) VANGL1 rare variants associated with neural tube defects affect convergent extension in zebrafish. *Mech Dev*. [Epub ahead of print]

Springer S, Schekman R. (1998). Nucleation of COPII vesicular coat complex by endoplasmic reticulum to Golgi vesicle SNAREs. *Science*. 281(5377):698-700.

Strong LC and Hollander WF. (1949). Hereditary loop-tail in the house mouse. *Jour.Hered.* 40:329-334.

Sun F, Zhang R, Gong X, Geng X, Drain PF, Frizzell RA. (2006). Derlin-1 promotes the efficient degradation of the cystic fibrosis transmembrane conductance regulator (CFTR) and CFTR folding mutants. *J Biol Chem*. 281(48):36856-63.

Toh KL, Jones CR, He Y, Eide EJ, Hinz WA, Virshup DM, Ptácek LJ, Fu YH. (2001). An hPer2 phosphorylation site mutation in familial advanced sleep phase syndrome. *Science*. 291(5506):1040-3.

Torban E, Wang HJ, Groulx N, Gros P. (2004). Independent mutations in mouse Vangl2 that cause neural tube defects in looptail mice impair interaction with members of the Dishevelled family. *J Biol Chem*. 279(50):52703-13.

Tuazon PT, Traugh JA. (1991). Casein kinase I and II--multipotential serine protein kinases: structure, function, and regulation. *Adv Second Messenger Phosphoprotein Res*. 23:123-64.

Wallingford J, Fraser S, Harland R. (2002). Convergent Extension: The Molecular Control of Polarized Cell Movement during Embryonic Development. *Developmental Cell*, 2(6):695-706.

Ward CL, Omura S, Kopito RR. (1995). Degradation of CFTR by the ubiquitin-proteasome pathway. *Cell*. 83(1):121-7.

Wolff T, Rubin GM. (1998). Strabismus, a novel gene that regulates tissue polarity and cell fate decisions in Drosophila. *Development*. 125(6):1149-59.

Wu J, Mlodzik M. (2008). The frizzled extracellular domain is a ligand for Van Gogh/Stbm during nonautonomous planar cell polarity signaling. *Dev Cell*. 15(3):462-9.

Yuan H, Michelsen K, Schwappach B. (2003). 14-3-3 dimers probe the assembly status of multimeric membrane proteins. *Curr Biol*. 13(8):638-46.

Zerangue N, Schwappach B, Jan YN, Jan LY. (1999). A new ER trafficking signal regulates the subunit stoichiometry of plasma membrane K(ATP) channels. *Neuron*. 22(3):537-48.

Chapter Five:

Conclusion, Preliminary Data,

and Future Directions

Conclusion

I have been able to use the principles and methods of biochemistry and cell biology to discover some important aspects of protein trafficking in mammalian cells. COPII transport is an essential activity in every eukaryotic organism, ranging from yeast to humans. Each and every active cell in these organisms uses COPII anterograde transport as a crucial first step for the proper localization of thousands of membrane and luminal proteins. Many of the original discoveries about COPII and indeed the entire secretory system were first described in yeast. This single-celled model organism has proved invaluable in deciphering the basic functions of the subunits that make up the COPII coat. With this knowledge in hand, the field is able to tackle the more complex mammalian system, where a wider diversity of cargo molecules is matched by a wider diversity of COPII coat paralogs. This work is a characterization of the one of those COPII paralogs, Sec24B, and the unique protein that it transports, Vangl2.

The published article in chapter 3 was the first report of a phenotype for a mutation in a mammalian Sec24. We found that mice with defective Sec24B have major neural tube defects and other phenotypes such as misaligned cochlear cells. At this point, it is not certain whether mutations in Sec24B could be a causative agent for the development of neural tube defects in humans, but I think there is a good chance that such an association will be found in the future. Human mutations that lead to neural tube defects have been difficult for the scientific community to identify thus far, but Sec24B is a fresh angle on neural tube closure based on the activity of the planar cell polarity pathway. I also expect that different phenotypes for the other Sec24 paralogs will be published in the future, as mouse models for these have already been created (David Ginsburg, personal communication). Sec24 is the COPII subunit most critical for binding and selecting cargo proteins for inclusion into vesicles. Given the numerous cargo molecules in mammalian cells, it is not surprising to find 4 different paralogs of Sec24.

It is interesting that mice with null mutations in Sec24B had such a specific phenotype that resembled planar cell polarity defects. One might have expected more defects found in other tissues due to the lack of transport of various other cargo proteins, but except for the tissues known to be affected by planar cell polarity, the mice appeared normal (Janna Merte, personal communication). My interpretation is that very few essential proteins are specifically transported by Sec24B and that other essential cargos are able to traffic through the action of the other Sec24 paralogs. Vangl2 is one of the proteins that is specific for Sec24B. An *in vitro* reconstitution of Vangl2 ER export into COPII vesicles showed that Sec24B can enhance the packaging Vangl2, but the other Sec24s do not have this effect. Based on the strong phenotypes seen in different organisms with Vangl2 defects, I think it is plausible that Vangl2, and perhaps its paralog Vangl1, are the only planar cell polarity proteins that need the activity of Sec24B for efficient transport during development. Vangl2 is dosage sensitive, as seen in mice with the looptail mutations.

Vangl2 is a critical protein in the planar cell polarity pathway, used to organize tissue during development. Vangl2 has numerous functional interactions with other

components of the pathway. The genetic study of planar cell polarity has been aided by the discovery of "looptail" mutant mice that have point mutations in Vangl2 and lead to a null phenotype. Despite the 60+ years since the first looptail mouse was found, no one had previously determined the basic defect in looptail Vangl2 traffic. In chapter 3, I demonstrate that Vangl2 looptail mutant proteins are retained in the ER and unable to package into COPII vesicles.

In chapter 4, I went on to further characterize the Vangl2 protein and its looptail mutant forms. I show that the looptail point mutations are part of a larger motif, a series of neighboring amino acids, mutations in which lead to ER transport defects. As demonstrated, these looptail regions are important for the binding of Dishevelled and likely form a conformational binding site. I also show that the extreme carboxyl-terminus of Vangl2 is important for its efficient ER export. In dissecting the molecular nature of Vangl2, I have confirmed several features of *Drosophila* Strabismus that also apply to mammalian Vangl2. Among these conserved features are that Vangl2 can oligomerize and that Vangl2 binds to Dishevelled and Prickle proteins. In addition, I have tested the topology and folding status of wild type and mutant Vangl2 proteins. Through careful inspection of protein sequence conservation, I have proposed several features of Vangl2 that have not yet been described, including a phosphorylation site, and a possible site that controls the ER retention of Vangl2.

I believe these findings and those listed below represent significant progress in our understanding of both mammalian COPII transport and the molecular nature of proteins involved in planar cell polarity. These pursuits are surely worthwhile as we consider the widespread utilization of COPII transport among the kingdoms of life and the implications of the planar cell polarity pathway on human health and disease.

Preliminary Data and Future Directions

In vitro translation and COPII budding

In vitro reconstitution is a powerful technique that allows fine control in dissecting the details of a cellular pathway. In using this approach, I have refined the very effective procedure of combining *in vitro* translation and *in vitro* COPII budding reactions. Combining these experiments allows one to study the ER export of proteins that would normally be found at other places in the cell, such as Vangl2 at the cell surface. The Vangl2 mutant budding data in this dissertation is perhaps the most extensive use of this technique yet. I also adapted and extended this technique to show that *in vitro* translation and COPII budding could be performed on cells that are still attached to their growth substrate. In permeabilized cells that are still attached to their original substrate, I observed that the microtubule network remains largely intact. This new modified technique could be very useful for reconstituting and studying the movement of COPII-derived vesicles along microtubules. Also, because the Golgi compartment is associated with the microtubule organizing center, I expect that the Golgi membrane will be largely intact in these attached, permeabilized cells. This may

allow an *in vitro* reconstitution of Golgi trafficking and budding without the difficult step of first purifying Golgi membrane-containing cell fractions.

COPII budding of other planar cell polarity membrane proteins

As shown in Figure 1.2, there are other membrane proteins involved in the planar cell polarity pathway. I was successful in detecting the COPII packaging of PTK7 using the combined *in vitro* translation and budding system. Unlike Vangl2, PTK7 packaging did not appear to be enhanced by Sec24B. This result was too late for inclusion in the published work that comprises chapter 3. The other membrane proteins, Frizzled and Celsr, proved to be technically challenging to test in the same way as Vangl2. These two proteins did not *in vitro* translate efficiently and did not translocate into the ER donor membrane. Celsr is a very large protein, with most of its sequence extracellular. In order to study its trafficking, one could truncate parts of the extracellular domain and keep the cytosolic domain intact.

Characterizing what makes Sec24B unique

As demonstrated in chapter 3, Sec24B alone appears able to enhance the COPII packaging of Vangl2. So how is Sec24B able to do this whereas the other Sec24s can not? In looking at an alignment of mammalian Sec24 protein sequences, it is clear that they are highly conserved in roughly the latter two-thirds of the protein. The amino terminus among the different Sec24s is most divergent, including that of Sec24B, which is longer than all the other Sec24s. These divergent amino termini may provide differentiation for binding to particular cargo proteins that the other Sec24s cannot. I hypothesize that the amino terminus of Sec24B be essential for the packaging of Vangl2. I created truncations of Sec24B that should allow one to determine if this amino terminus is important for Vangl2 trafficking. These truncations were put into plasmids for insect cell baculovirus expression, and purified protein was produced. There are 4 truncations which remove the first 103, 216, 292, and 460 amino acids from Sec24B.

COPII expression in differentiating neural cells

In collaboration with Phung Gip from Carolyn Bertozzi's lab here at Berkeley, I along with an undergraduate student, Carolyn Haunschild, looked into the COPII proteins in human embryonic stem cells differentiating into neural cells. Using antibodies specific for each different COPII paralog, we analyzed COPII protein expression in cell lysates from different time points along a course of differentiation. The main conclusion from these samples was that the expression of Sec24D was much increased in differentiating neural spheres compared to undifferentiated cells. The other COPII proteins we tested, including other Sec24, Sec23, and Sar1 proteins, did not vary or were not expressed very much. The finding that Sec24D is important for these very

early stages of embryo development would correlate well with the observation that mice embryos are not viable without Sec24D (David Ginsburg, personal communication).

COPII packaging of proinsulin

Proinsulin and its cleavage product, insulin, are essential parts of glucose metabolism in mammals. In beta cells of the pancreas, proinsulin is translated and translocated into the ER lumen where it travels through the secretory pathway. It is unclear if proinsulin enters COPII vesicles through an active recruitment mechanism or if it is included simply by bulk flow. To differentiate these possibilities, I set out to establish a proinsulin COPII budding reaction, using rat INS-1 cells that are known to produce insulin. At one point it appeared that that the reaction was working but the antibody I was using to detect proinsulin was discontinued, and a few attempts with other antibodies did not uncover a suitable replacement. I expect that with a good antibody, or using the *in vitro* translation system, a robust proinsulin COPII budding reaction could be established.

Appendix I :

List of plasmids created

Plasmid Full Name	Plasmid Insert	Vector Name	Epitope Tag	Restriction Sites (5'/3')	Antibotic Res.	Species
3xHA Vangl2 Lp D255E	Vangl2 Lp D255E	pCS2+	3xHA	FseI / AscI	amp	Mouse
3xHA Vangl2 Lp S464N	Vangl2 Lp S464N	pCS2+	3xHA	FseI / AscI	amp	Mouse
3xHA Vangl2 V251A	Vangl2 V251A	pCS2+	3xHA	FseI / AscI	amp	Mouse
3xHA Vangl2 R252A	Vangl2 R252A	pCS2+	3xHA	FseI / AscI	amp	Mouse
3xHA Vangl2 S253A	Vangl2 S253A	pCS2+	3xHA	FseI / AscI	amp	Mouse
3xHA Vangl2 T254A	Vangl2 T254A	pCS2+	3xHA	FseI / AscI	amp	Mouse
3xHA Vangl2 D255A	Vangl2 D255A	pCS2+	3xHA	FseI / AscI	amp	Mouse
3xHA Vangl2 G256R	Vangl2 G256R	pCS2+	3xHA	FseI / AscI	amp	Mouse
3xHA Vangl2 G256V	Vangl2 G256V	pCS2+	3xHA	FseI / AscI	amp	Mouse
3xHA Vangl2 G256N	Vangl2 G256N	pCS2+	3xHA	FseI / AscI	amp	Mouse
3xHA Vangl2 S258A	Vangl2 S258A	pCS2+	3xHA	FseI / AscI	amp	Mouse
3xHA Vangl2 R259A	Vangl2 R259A	pCS2+	3xHA	FseI / AscI	amp	Mouse
3xHA Vangl2 F260A	Vangl2 F260A	pCS2+	3xHA	FseI / AscI	amp	Mouse
3xHA Vangl2 Y261A	Vangl2 Y261A	pCS2+	3xHA	FseI / AscI	amp	Mouse
3xHA Vangl2 K458A	Vangl2 K458A	pCS2+	3xHA	FseI / AscI	amp	Mouse
3xHA Vangl2 Q459A	Vangl2 Q459A	pCS2+	3xHA	FseI / AscI	amp	Mouse
3xHA Vangl2 W460A	Vangl2 W460A	pCS2+	3xHA	FseI / AscI	amp	Mouse
3xHA Vangl2 T461A	Vangl2 T461A	pCS2+	3xHA	FseI / AscI	amp	Mouse
3xHA Vangl2 L462A	Vangl2 L462A	pCS2+	3xHA	FseI / AscI	amp	Mouse
3xHA Vangl2 V463A	Vangl2 V463A	pCS2+	3xHA	FseI / AscI	amp	Mouse
3xHA Vangl2 S464A	Vangl2 S464A	pCS2+	3xHA	FseI / AscI	amp	Mouse
3xHA Vangl2 E465A	Vangl2 E465A	pCS2+	3xHA	FseI / AscI	amp	Mouse
3xHA Vangl2 E465A+E466A	Vangl2 E465A+E466A	pCS2+	3xHA	FseI / AscI	amp	Mouse
3xHA Vangl2 P467A	Vangl2 P467A	pCS2+	3xHA	FseI / AscI	amp	Mouse
3xHA Vangl2 V468A	Vangl2 V468A	pCS2+	3xHA	FseI / AscI	amp	Mouse
3xHA Vangl2 T469A	Vangl2 T469A	pCS2+	3xHA	FseI / AscI	amp	Mouse
3xHA Vangl2 R514A	Vangl2 R514A	pCS2+	3xHA	FseI / AscI	amp	Mouse
3xHA Vangl2 L515A	Vangl2 L515A	pCS2+	3xHA	FseI / AscI	amp	Mouse
3xHA Vangl2 Q516A	Vangl2 Q516A	pCS2+	3xHA	FseI / AscI	amp	Mouse
3xHA Vangl2 S517A	Vangl2 S517A	pCS2+	3xHA	FseI / AscI	amp	Mouse

Plasmid Full Name	Plasmid Insert	Vector Name	Epitope Tag	Restriction Sites (5'/3')	Antibotic Res.	Species
3xHA Vangl2 E518A	Vangl2 E518A	pCS2+	3xHA	FseI / AscI	amp	Mouse
3xHA Vangl2 T519A	Vangl2 T519A	pCS2+	3xHA	FseI / AscI	amp	Mouse
3xHA Vangl2 S520A	Vangl2 S520A	pCS2+	3xHA	FseI / AscI	amp	Mouse
3xHA Vangl2 V521G	Vangl2 V521G	pCS2+	3xHA	FseI / AscI	amp	Mouse
6xMyc Vangl2 WT	Vangl2 WT	pCS2+	6xMyc	FseI / AscI	amp	Mouse
6xMyc Vangl2 Lp D255E	Vangl2 Lp D255E	pCS2+	6xMyc	FseI / AscI	amp	Mouse
6xMyc Vangl2 Lp S464N	Vangl2 Lp S464N	pCS2+	6xMyc	FseI / AscI	amp	Mouse
3xHA Vangl2 Nterm (1-108)	Vangl2 Nterm (1-108)	pCS2+	3xHA	FseI / AscI	amp	Mouse
3xHA Vangl2 Cterm (238-521)	Vangl2 Cterm (238-521)	pCS2+	3xHA	FseI / AscI	amp	Mouse
3xHA Vangl2 Cterm (238-521) LpD255E	Vangl2 Cterm (238-521) LpD255E	pCS2+	3xHA	FseI / AscI	amp	Mouse
3xHA Vangl2 Cterm (238-521) LpS464N	Vangl2 Cterm (238-521) LpS464N	pCS2+	3xHA	FseI / AscI	amp	Mouse
6xMyc Vangl2 Nterm (1-108)	Vangl2 Nterm (1-108)	pCS2+	6xMyc	FseI / AscI	amp	Mouse
6xMyc Vangl2 Cterm (238-521)	Vangl2 Cterm (238-521)	pCS2+	6xMyc	FseI / AscI	amp	Mouse
6xMyc Vangl2 Cterm (238-521) LpD255E	Vangl2 Cterm (238-521) LpD255E	pCS2+	6xMyc	FseI / AscI	amp	Mouse
6xMyc Vangl2 Cterm (238-521) LpS464N	Vangl2 Cterm (238-521) LpS464N	pCS2+	6xMyc	FseI / AscI	amp	Mouse
3xHA Vangl2 WT	Vangl2 WT	pCDNA3.1	3xHA	XbaI / EcoRI	amp / Neo	Mouse
3xHA Vangl2 WT	Vangl2 WT	pIRES-Hyg	3xHA	BsrG1 / NheI	amp / Hyg	Mouse
GST Vangl2 Nterm (1-107)	Vangl2 Nterm (1-107)	pGex2T	GST	BanHI / EcoRI	amp	Mouse
GST Vangl2 Cterm (241-521)	Vangl2 Cterm (241-521)	pGex6p2	GST	EcoRI / XhoI	amp	Mouse
GST Vangl2 Cterm (241-521) LpD255E	Vangl2 Cterm (241-521) LpD255E	pGex6p2	GST	EcoRI / XhoI	amp	Mouse
GST Vangl2 Cterm (241-521) LpS464N	Vangl2 Cterm (241-521) LpS464N	pGex6p2	GST	EcoRI / XhoI	amp	Mouse
GST Vangl2 Cterm (241-521) T519A	Vangl2 Cterm (241-521) T519A	pGex6p2	GST	EcoRI / XhoI	amp	Mouse
GST Vangl2 Cterm (241-521) V521G	Vangl2 Cterm (241-521) V521G	pGex6p2	GST	EcoRI / XhoI	amp	Mouse
GST Vangl2 Cterm (378-521)	Vangl2 Cterm (378-521)	pGex6p2	GST	EcoRI / XhoI	amp	Mouse
GST Vangl2 Cterm (430-521)	Vangl2 Cterm (430-521)	pGex6p2	GST	EcoRI / XhoI	amp	Mouse
GST Vangl2 Cterm (451-521)	Vangl2 Cterm (451-521)	pGex6p2	GST	EcoRI / XhoI	amp	Mouse
GST Vangl2 Cterm (378-475)	Vangl2 Cterm (378-475)	pGex6p2	GST	EcoRI / XhoI	amp	Mouse
GST Vangl2 Cterm (430-475)	Vangl2 Cterm (430-475)	pGex6p2	GST	EcoRI / XhoI	amp	Mouse
GST Vangl2 Cterm (451-475)	Vangl2 Cterm (451-475)	pGex6p2	GST	EcoRI / XhoI	amp	Mouse

Plasmid Full Name	Plasmid Insert	Vector Name	Epitope Tag	Restriction Sites (5'/3')	Antibotic Res.	Species
3xHA Sec24A	Sec24A	pCS2+	3xHA	FseI / AscI	amp	Human
3xHA Sec24B	Sec24B	pCS2+	3xHA	FseI / AscI	amp	Human
3xHA Sec24C	Sec24C	pCS2+	3xHA	FseI / AscI	amp	Human
3xHA Sec24D	Sec24D	pCS2+	3xHA	FseI / AscI	amp	Human
6xMyc Sec24A	Sec24A	pCS2+	6xMyc	FseI / AscI	amp	Human
6xMyc Sec24B	Sec24B	pCS2+	6xMyc	FseI / AscI	amp	Human
6xMyc Sec24C	Sec24C	pCS2+	6xMyc	FseI / AscI	amp	Human
6xMyc Sec24D	Sec24D	pCS2+	6xMyc	FseI / AscI	amp	Human
Flag Sec23A	Sec23A	pCS2+	Flag	BamHI / AscI	amp	Human
Flag Sec23B	Sec23B	pCS2+	Flag	BamHI / AscI	amp	Human
3xHA Frizzled 3	Frizzled 3	pCDNA3.1 ver.A (-)	3xHA	NheI / AscI / NotI / EcoRI	amp / Neo	Mouse
3xHA Frizzled 6	Frizzled 6	pCDNA3.1 ver.A (-)	3xHA	NheI / AscI / NotI / EcoRI	amp / Neo	Mouse
3xHA Frizzled 3	Frizzled 3	pCS2+	3xHA	NheI / AscI / NotI / EcoRI	amp	Mouse
3xHA Frizzled 6	Frizzled 6	pCS2+	3xHA	NheI / AscI / NotI / EcoRI	amp	Mouse
3xHA Dishevelled 1	Dishevelled 1	pCS2+	3xHA	FseI / AscI	amp	Mouse
3xHA Dishevelled 2	Dishevelled 2	pCS2+	3xHA	FseI / AscI	amp	Mouse
3xHA Dishevelled 3	Dishevelled 3	pCS2+	3xHA	FseI / AscI	amp	Human
6xMyc Dishevelled 1	Dishevelled 1	pCS2+	6xMyc	FseI / AscI	amp	Mouse
6xMyc Dishevelled 2	Dishevelled 2	pCS2+	6xMyc	FseI / AscI	amp	Mouse
6xMyc Dishevelled 3	Dishevelled 3	pCS2+	6xMyc	FseI / AscI	amp	Human
3xHA Prickle 1	Prickle 1	pCS2+	3xHA	FseI / AscI	amp	Mouse
3xHA Prickle 2	Prickle 2	pCS2+	3xHA	FseI / AscI	amp	Mouse
6xMyc Prickle 1	Prickle 1	pCS2+	6xMyc	FseI / AscI	amp	Mouse
6xMyc Prickle 2	Prickle 2	pCS2+	6xMyc	FseI / AscI	amp	Mouse
His Sec24B Δ103 (103-1268)	Sec24B Δ103 (103-1268)	pFastBac	His	NcoI / SpeI	amp	Human
His Sec24B Δ218 (218-1268)	Sec24B Δ218 (218-1268)	pFastBac	His	NcoI / SpeI	amp	Human
His Sec24B Δ292 (292-1268)	Sec24B Δ292 (292-1268)	pFastBac	His	NcoI / SpeI	amp	Human
His Sec24B Δ460 (460-1268)	Sec24B Δ460 (460-1268)	pFastBac	His	NcoI / SpeI	amp	Human